

Dissertation zur Erlangung des Doktorgrades  
der Fakultät für Chemie und Pharmazie  
der Ludwig-Maximilians-Universität München



**Identification of MKP-1 as a central mediator of  
cytoprotective effects in human endothelial cells:  
pathways of induction**

**Robert Fürst**

aus Temeschburg

2005



### Erklärung

Diese Dissertation wurde im Sinne von § 13 Abs. 3 bzw. 4 der Promotionsordnung vom 29. Januar 1998 von Frau PD Dr. Alexandra K. Kiemer und Frau Prof. Dr. Angelika M. Vollmar betreut.

### Ehrenwörtliche Versicherung

Diese Dissertation wurde selbstständig, ohne unerlaubte Hilfe erarbeitet.

München, 03.12.2004

---

(Robert Fürst)

Dissertation eingereicht am: 03.12.2004

1. Gutachter: Frau Prof. Dr. Angelika M. Vollmar

2. Gutachter: Herr Prof. Dr. Ernst Wagner

Mündliche Prüfung am: 03.02.2005



***deeply grateful and with love***

---

***dedicated to my family***



## **Contents**





---

<b>1</b>	<b>INTRODUCTION</b>	<b>1</b>
<b>1.1</b>	<b>The endothelium</b>	<b>3</b>
1.1.1	Endothelial cell characteristics	3
1.1.2	Atherosclerosis, inflammation, and endothelial cell activation	4
<b>1.2</b>	<b>Aim of the study</b>	<b>6</b>
<b>1.3</b>	<b>MAP kinases and MAP kinase phosphatases</b>	<b>7</b>
<b>1.4</b>	<b>Atrial natriuretic peptide</b>	<b>10</b>
<b>1.5</b>	<b>ROS and NAD(P)H oxidase</b>	<b>13</b>
<b>1.6</b>	<b>Glucocorticoids</b>	<b>15</b>
<b>2</b>	<b>MATERIALS AND METHODS</b>	<b>19</b>
<b>2.1</b>	<b>Materials</b>	<b>21</b>
<b>2.2</b>	<b>Cell culture</b>	<b>22</b>
2.2.1	Solutions	22
2.2.2	Culture of HUVEC and HMEC	22
2.2.3	Passaging	23
2.2.4	Long time storage	23
2.2.5	Starvation	23
<b>2.3</b>	<b>Western blot analysis</b>	<b>24</b>
2.3.1	Solutions	24
2.3.2	<i>In vivo</i> samples	25
2.3.3	<i>In vitro</i> samples	25
2.3.4	Stripping, reprobing, and coomassie staining	26
<b>2.4</b>	<b>RT-PCR</b>	<b>26</b>
2.4.1	Isolation and characterization of total RNA	26
2.4.2	Reverse transcription	27
2.4.3	Polymerase chain reaction	27

---

<b>2.5</b>	<b>ROS measurement in cultured endothelial cells</b>	<b>28</b>
<b>2.6</b>	<b>ROS measurement in the endothelium of intact rat lung vessels</b>	<b>31</b>
2.6.1	Animals	31
2.6.2	Isolated-perfused rat lung preparation	31
2.6.3	<i>In situ</i> fluorescence microscopy	32
<b>2.7</b>	<b>Electrophoretic mobility shift assay (EMSA)</b>	<b>33</b>
2.7.1	Extraction of nuclear protein	33
2.7.2	Radioactive labeling of consensus oligonucleotides	33
2.7.3	Binding reaction and electrophoretic separation	34
<b>2.8</b>	<b>Transfection experiments</b>	<b>35</b>
2.8.1	Rac1 mutants	35
2.8.2	Antisense oligodesoxynucleotides	35
2.8.3	AP-1 decoy	36
<b>2.9</b>	<b>Rac pull-down assay</b>	<b>36</b>
2.9.1	Principle of the assay	36
2.9.2	Preparation of the GST-PBD sepharose beads	37
2.9.3	Pull-down assay	38
<b>2.10</b>	<b>Immunocytochemistry and confocal microscopy</b>	<b>39</b>
<b>2.11</b>	<b>Flow cytometry (FACS)</b>	<b>39</b>
<b>2.12</b>	<b>Statistical analysis</b>	<b>40</b>
<b>3</b>	<b>RESULTS</b>	<b>41</b>
<b>3.1</b>	<b>ANP and MKP-1</b>	<b>43</b>
3.1.1	MKP-1 induction by ANP	43
3.1.1.1	Time and concentration course of MKP-1 induction	43
3.1.1.2	Influence of cycloheximide on MKP-1 induction	44
3.1.1.3	MKP-1 induction depends on cGMP/NPR-A	44
3.1.1.4	PKG I is not expressed in HUVEC	45

---

3.1.2	ANP induces endothelial ROS production	45
3.1.2.1	Time and concentration course of ROS generation	45
3.1.2.2	ROS generation depends on cGMP/NPR-A	46
3.1.3	ROS mediate the induction of MKP-1 by ANP	47
3.1.3.1	Antioxidants abrogate ANP-induced MKP-1 expression	47
3.1.3.2	Hydrogen peroxide induces MKP-1	47
3.1.4	Involvement of NAD(P)H oxidase	48
3.1.4.1	Influence of PEG-SOD and SOD on ANP-induced ROS generation	48
3.1.4.2	Influence of PEG-catalase and catalase on ANP-induced ROS generation	49
3.1.4.3	Influence of DPI and gp91ds- <i>tat</i> on ANP-induced ROS generation	49
3.1.4.4	Influence of PEG-SOD and SOD on ANP-induced MKP-1 expression	50
3.1.4.5	Influence of PEG-catalase and catalase on ANP-induced MKP-1 expression	51
3.1.4.6	Influence of DPI and apocynin on ANP-induced MKP-1 expression	51
3.1.4.7	Expression of Nox homologues' transcripts in HUVEC and HMEC	52
3.1.4.8	Influence of Nox2 and Nox4 antisense on ANP-induced ROS generation	52
3.1.4.9	Influence of Nox2 and Nox4 antisense on ANP-induced MKP-1 expression	53
3.1.5	Involvement of Rac1	53
3.1.5.1	ANP activates Rac1	53
3.1.5.2	ANP induces Rac1 translocation	54
3.1.5.3	Rac1 is crucially involved in ANP-induced ROS generation and MKP-1 expression	55
3.1.6	MKP-1 induction is not mediated by PKC, ERK, or p38 MAPK	55
3.1.7	Role of JNK and AP-1	56
3.1.7.1	JNK mediates the induction of MKP-1 by ANP	56
3.1.7.2	ANP rapidly activates JNK	57
3.1.7.3	Superoxide is involved in the activation of JNK by ANP	57
3.1.7.4	ANP activates AP-1 <i>via</i> JNK	58
3.1.7.5	AP-1 is crucially involved in the upregulation of MKP-1 by ANP	58
3.1.8	ROS generation in intact blood vessels	59

---

<b>3.2</b>	<b>Dexamethasone and MKP-1</b>	<b>62</b>
3.2.1	Dex reduces TNF- $\alpha$ -induced E-selectin expression	62
3.2.2	Dex at low concentrations does not influence NF- $\kappa$ B	62
3.2.3	p38 MAPK is involved in TNF- $\alpha$ -induced E-selectin expression	63
3.2.4	Influence of Dex on TNF- $\alpha$ -activated p38 MAPK	64
3.2.5	Vanadate abrogates the influence of Dex on p38 MAPK	65
3.2.6	MKP-1 induction by Dex	65
3.2.7	Dex induces MKP-1 <i>via</i> glucocorticoid receptor	66
3.2.8	MKP-1 antisense restores p38 MAPK activation	66
3.2.9	MKP-1 antisense restores E-selectin expression	67
<b>4</b>	<b>DISCUSSION</b>	<b>69</b>
<b>4.1</b>	<b>ANP and MKP-1</b>	<b>71</b>
4.1.1	Beneficial actions of MKP-1	71
4.1.2	ANP induces MKP-1	72
4.1.3	Generation of ROS by ANP	73
4.1.4	Involvement of NAD(P)H oxidase	74
4.1.5	The role of Rac1	76
4.1.6	Involvement of the JNK/AP-1 pathway	77
4.1.7	General comments	78
<b>4.2</b>	<b>Dexamethasone and MKP-1</b>	<b>79</b>
4.2.1	Dex reduces E-selectin expression independent of NF- $\kappa$ B	79
4.2.2	The role of p38 MAPK in TNF- $\alpha$ -induced E-selectin expression	79
4.2.3	Dex reduces p38 MAPK activity <i>via</i> induction of MKP-1	80
4.2.4	MKP-1 is critical for the inhibition of p38 MAPK activity and E-selectin induction	81
4.2.5	The functional role of MKP-1 induction by Dex	81

---

<b>5</b>	<b>SUMMARY</b>	<b>83</b>
5.1	MKP-1 and ANP	85
5.2	MKP-1 and Dex	85
5.3	MKP-1 as a central protective mediator of the endothelium	86
<b>6</b>	<b>REFERENCES</b>	<b>89</b>
<b>7</b>	<b>APPENDIX</b>	<b>107</b>
7.1	Abbreviations	109
7.2	Alphabetical list of companies	111
7.3	Publications	113
7.3.1	Original publications	113
7.3.2	Reviews	113
7.3.3	Oral presentations	114
7.3.4	Poster presentations	115
7.3.5	Awards	115
7.4	Curriculum vitae	116
7.5	Acknowledgements	117



# 1 Introduction





## 1.1 The endothelium

### 1.1.1 Endothelial cell characteristics

The endothelium is a monolayer of cells which line the lumen of all blood vessels, thereby serving as a barrier between blood and tissue. In the past, the endothelium has been described as a non-reactive, inert vessel “wall paper”. During the last decades, it became clear that endothelial cells (ECs) actively participate in many physiological processes. The endothelium is now regarded as a disseminated organ with important metabolic, synthetic, secretory, and immunological functions, exerting influence on smooth muscle cells, platelets, and leukocytes *via* autocrine and paracrine mechanisms.<sup>1</sup>

(i) The endothelium has important transport functions: ECs tightly control the passage of molecules and cells from the blood to the underlying interstitium by different mechanisms, such as active transport (e.g. for glucose, amino acids), transcytosis (e.g. by caveolae), or paracellular transport (e.g. through tight junctions). These mechanisms are of great importance in order to meet the metabolic needs of the underlying tissue.<sup>1,2</sup>

(ii) The endothelium controls the vascular tone and is important for blood pressure regulation. ECs produce many substances which act as vasodilators or vasoconstrictors. These substances are released in response to humoral and mechanical stimuli and affect the adjacent smooth muscle cells. Prominent vasodilators are nitric oxide (NO) and prostacyclin (PGI<sub>2</sub>). Endothelin-1 (ET-1) and the platelet-activating factor (PAF) represent important vasoconstricting factors.<sup>1,2</sup>

(iii) The endothelium regulates coagulation. On their surface, ECs express a variety of molecules that regulate hemostasis. Resting ECs provide an anti-thrombotic surface by expressing anti-thrombotic factors (e.g. glycosaminoglycans, thrombomodulin) and by secreting anti-thrombotic autacoids (NO, PGI<sub>2</sub>, adenosine), thus facilitating blood flow and inhibiting platelet adhesion and coagulation. Vascular

injury induces tissue factor (TF) expression and the endothelium gets transformed to a pro-coagulant state.<sup>1,2</sup>

(iv) The endothelium plays a key role in the body's host defense and in inflammation: ECs are strategically well positioned at the tissue-blood barrier. In general, the immune response depends on the communication between cells by different mediators, such as cytokines. ECs are able to produce and react to a variety of these mediator substances, thereby interfering with inflammatory processes.<sup>1,2</sup> An initiating step in inflammatory events is the recruitment of circulating leukocytes towards sites of inflammation. These leukocytes have to transmigrate across the endothelium (diapedesis), a process which is tightly controlled by ECs. Moreover, ECs are able to directly react to infections: different cytokines, adhesion molecules, and enzymes (such as matrix metalloproteinases or NO synthase) are upregulated in the endothelium in response to a variety of microbial mediators.<sup>3,4</sup>

In the recent years, not only the important physiological functions of ECs have been investigated. The endothelium has also increasingly been recognized to be involved in different pathophysiological states: a disturbed endothelial function plays a crucial role in a variety of diseases, such as atherosclerosis, sepsis, hypertension, diabetes, thrombotic disorders, and cancer metastasis.<sup>2</sup> Thus, influencing different endothelial processes by affecting the underlying molecular signaling mechanisms has become an important approach for drug discovery in order to defeat these severe disorders.

### **1.1.2 Atherosclerosis, inflammation, and endothelial cell activation**

Atherosclerosis is the most important contributor to cardiovascular disease (CVD). CVD currently represents the major reason for premature deaths in industrial countries.<sup>5</sup> Therefore, understanding and influencing the pathogenesis of atherosclerosis is of utmost importance in order to discover new approaches for drug therapy. Atherosclerosis is a chronic disorder, which is characterized by the formation of plaques in arterial blood vessels. These atheromatous plaques can occlude the vessel leading to a damage of the surrounding tissue due to a strongly impaired oxygen supply. From a classical view, the major cause for atherosclerosis is the accumulation of fatty deposits (oxidized

lipoproteins) and fibrous elements in the vessel lumen. In the past, scientists focused their research on the involvement of lipoproteins and smooth muscle cell proliferation. In recent years, however, atherosclerosis has increasingly been recognized as a predominantly inflammatory disease.<sup>5-7</sup> In addition to the involvement of inflammatory cells (T-lymphocytes, monocytes/macrophages), many pro-inflammatory mediators (cytokines, mainly interleukins and tumor necrosis factor- $\alpha$  [TNF- $\alpha$ ]) initiate different responses that promote atherosclerosis.<sup>8</sup> These substances switch ECs from a resting to an activated status, which is characterized by an induction of adhesion molecules, increased oxidative stress, and reduced nitric oxide generation.<sup>3,4,9</sup>

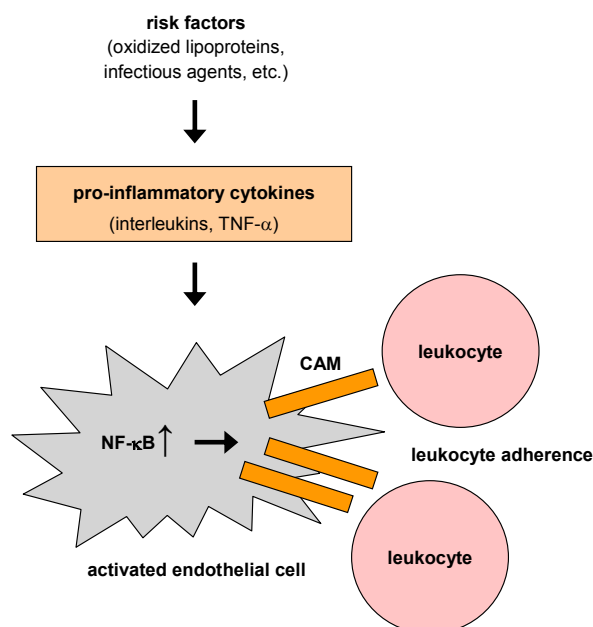


**Figure 1:** The attachment of circulating leukocytes to activated endothelial cells is widely regulated by cellular adhesion molecules (CAMs) and the transcription factor nuclear factor- $\kappa$ B (NF- $\kappa$ B).

An increased recruitment and attachment of circulating leukocytes to the endothelium was found to be an early step in the development of atherosclerosis.<sup>7,10,11</sup> The adherence of leukocytes to ECs (figure 1) and their subsequent migration across the endothelium (diapedesis) depends on a cascade of events mediated by a family of cell adhesion molecules (CAMs) expressed on the endothelial surface. Vascular cell adhesion molecule-1 (VCAM-1), intercellular adhesion molecule-1 (ICAM-1), and E-selectin represent important CAMs, which are involved in the pathogenesis of atherosclerosis.<sup>6</sup> Interleukins and TNF- $\alpha$  are known to strongly induce CAM expression. The induction of CAMs seems

to be largely regulated by the transcription factor nuclear factor- $\kappa$ B (NF- $\kappa$ B, figure 1), a central mediator of the innate immune response, which controls a great variety of inflammatory events.<sup>12,13</sup>

## 1.2 Aim of the study

In recent years, MKP-1, the mitogen-activated protein kinase phosphatase-1, has increasingly been recognized as an important mediator responsible for the transduction of anti-inflammatory and cytoprotective effects in different cell-types. MKP-1 predominantly acts as a negative regulator of different members of the family of mitogen-activated protein kinases (MAPKs), which take part in the control of diverse cellular functions. Thus, MKP-1 is able to affect important physiological and pathophysiological events. Interestingly, the role of MKP-1 in the endothelium has as yet been only poorly investigated.

Aim of the present study was to characterize the role of MKP-1 in endothelial cells. A precise definition of both the functions of MKP-1 and the mechanisms of its induction is of special interest considering this phosphatase to be a valuable drug target. For this purpose, two different projects were pursued:

(i) Characterization of the pathway by which ANP induces MKP-1 expression:

In the model of endothelial inflammation, i.e. in TNF- $\alpha$ -activated endothelial cells, the cardiovascular hormone atrial natriuretic peptide (ANP) was shown to exert significant protective, anti-inflammatory actions: ANP reduces stress fiber formation, macromolecular permeability, and the attraction of leukocytes.<sup>14,15</sup> Since the ANP-induced induction of MKP-1 is critical for all of these effects, we wanted to elucidate the underlying molecular signaling mechanisms leading to an upregulation of MKP-1 by ANP, thereby focusing on an involvement of protein kinases and reactive oxygen species (ROS).

(ii) Characterization of the function of glucocorticoid-induced MKP-1 expression:

MKP-1 has been introduced as a potential mediator of the anti-inflammatory effects of glucocorticoids in different cell types. However, nothing has as yet been known about the role of MKP-1 in the signaling of glucocorticoids in endothelial cells. We aimed to clarify whether MKP-1 is upregulated in

endothelial cells by the synthetic glucocorticoid dexamethasone (Dex). Moreover, we also wanted to reveal the functional significance of MKP-1 induction: in a model of endothelial inflammation (ECs activated by  $\text{TNF-}\alpha$ ), we aimed to elucidate the effect of MKP-1 on the expression of the CAM E-selectin. Since E-selectin is largely regulated by  $\text{NF-}\kappa\text{B}$ , a discrimination between MKP-1 and  $\text{NF-}\kappa\text{B}$  as targets of the anti-inflammatory actions of Dex was required.

### 1.3 MAP kinases and MAP kinase phosphatases

Cells must permanently be responsive to biochemical and biophysical signals. Most stimuli to which cells react are sensed by receptors on the cytoplasmic membrane. These receptors generate signals which have to be transmitted to the respective cellular target by intracellular signal transduction pathways. The phosphorylation and dephosphorylation of proteins – exerted by the enzyme families of protein kinases and phosphatases, respectively – is the most important step by which a signal is intracellularly relayed. A major group of signal transducers in eukaryotes is the family of mitogen-activated protein kinases (MAPKs). MAPKs not only relay, but also amplify and integrate diverse signals in order to coordinate the cellular response. They participate in a huge variety of physiological and pathological processes.<sup>16,17</sup>

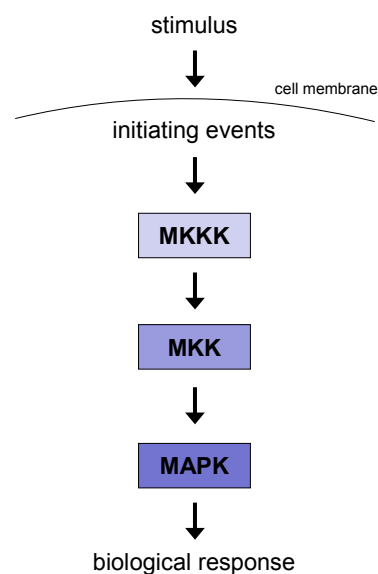


**Figure 2:** MAPK signaling pathway. Upon an extracellular stimulus, a kinase cascade is initiated leading to distinct biological responses, like an altered gene expression or an activation of further kinases. Abbreviations: MAPK kinase kinase (MKKK), MAPK kinase (MKK). Adapted from Herlaar *et al.*<sup>18</sup>

MAPKs belong to different signaling cascades composed of different protein kinases in series, termed MAPK kinase kinase (MKKK) and MAPK kinase (MKK), that lead to a final activation of an effector MAPK, which is in turn able to influence multiple cellular targets. Mostly, MAPKs alter gene expression or activate further kinases.<sup>18</sup>

Three major MAPK families are known: (i) extracellular-regulated protein kinases (ERK), (ii) c-Jun N-terminal kinases (JNK), and (iii) p38 MAPKs. Each MAPK family comprises of different isoforms. The ERK pathway plays a prominent role in processes like cell proliferation and differentiation. JNK and p38 MAPK are predominantly involved in apoptosis, stress response, and in inflammatory events.<sup>19-21</sup> All MAPKs are activated by the same biochemical way (figure 2): MKKK phosphorylates the dual specificity serine/threonine kinase MKK, which phosphorylates both the threonine (Thr) and tyrosine (Tyr) residue in the activation loop of MAPK. Both residues have to be phosphorylated for activation of the MAP kinases. All MAPKs share the sequence Thr-X-Tyr. X differs depending on the MAPK family: glutamic acid for ERK, proline for JNK, and glycine for p38 MAPK.<sup>18,19</sup>

The mechanisms of MAPK activation have been extensively studied in the last decades. The pathways of their deactivation, however, have as yet been investigated to a much lesser extent, although MAPK inactivation has increasingly been recognized as a crucial event in the cellular signal transduction network. The dephosphorylation of one critical amino acid (Thr or Tyr) is sufficient to inactivate MAPKs. Three types of phosphatases can be involved in the process of MAPK deactivation: protein tyrosine phosphatases (PTPs) and serine/threonine-specific phosphatases, which remove one phosphate, or dual-specificity phosphatases (DUSPs), which remove both phosphates (figure 3).<sup>22,23</sup>

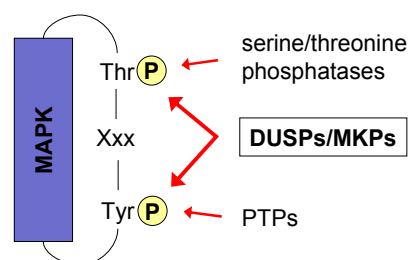


**Figure 3:** Inactivation of MAPKs. Three classes of phosphatases are able to inactivate MAPKs: serine/threonine phosphatases, protein tyrosine phosphatases (PTPs), and dual-specificity phosphatases (DUSPs)/MAPK phosphatases (MKPs).

DUSPs are regarded as key players for the inactivation of different MAPK families and have therefore also been termed MAPK phosphatases (MKPs). Ten genes coding for members of the MKP family are known so far. Due to structural similarities, MKPs can be divided into three subgroups. MKP-1 (DUSP1, hVH1, CL100, 3CH134) and MKP-2 (DUSP4, hVH2, TYP1) are two important members of the subgroup I. They both show a nuclear localization (for MKP-1 see figure 4). MKP-3 (DUSP6, rVH6, PYST1) is the prototypical member of subgroup II, which shows a cytosolic localization. Subgroup III consists of MKP-7 (DUSP16, MKP-M, localized in the cytosol) and vVH5 (DUSP8, M3/6, localized in the nucleus and the cytosol, shuttle protein).<sup>24</sup>

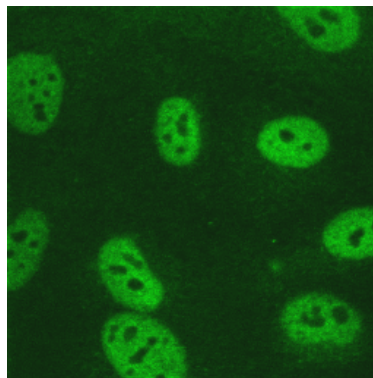


**Figure 4:** MKP-1 is localized in the nucleus. Human umbilical vein endothelial cells (HUVECs) were stained for MKP-1 and confocal microscopy was performed as described in section 2.10.

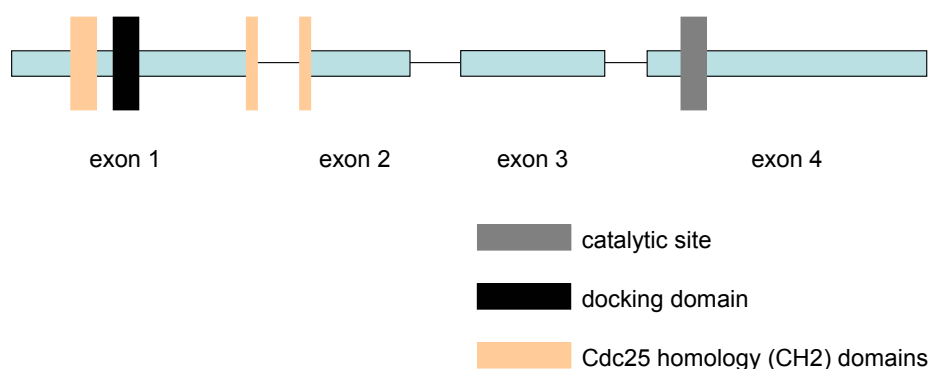


**Figure 5:** Structure of subgroup I MKPs (e.g. MKP-1). Adapted from Theodosiou *et al.*<sup>24</sup>

The structure of subgroup I of MKPs is schematically depicted in figure 5. The catalytic site of MKPs is known to exist in a low-activity state. Upon binding of the substrate (activated MAPKs), the critical active-site residues are rearranged and adopt a catalytically active conformation. MKPs contain two

regions with similarity to the Cdc25 phosphatase and one docking site for MAPKs, which is able to bind to the common docking domain (CD) of MAPKs.<sup>24</sup>

MKP-1 is able to bind all three major types of MAPKs, i.e. ERK, JNK, and p38 MAPK.<sup>23</sup> Binding of MAPKs was shown to result in phosphorylation of MKP-1, which does not influence its catalytical activity, but seems to stabilize MKP-1 by reducing its catabolism.<sup>24</sup> MKP-1 is known to be rapidly degraded (half live approx. 45 min) by the ubiquitin/proteasome-pathway.<sup>25</sup> MKP-1 is constitutively expressed at low levels and underlies – as an immediate early gene product<sup>26</sup> – a tight and rapid transcriptional upregulation by different stimuli, predominantly by agents which induce MAPKs, which means that MKP-1 takes part in a negative feedback loop controlling the activity of MAPKs.<sup>22</sup>

As mentioned in chapter 1.2, we aimed to elucidate the underlying signaling mechanisms leading to an upregulation of MKP-1 in human endothelial cells by the cardiovascular hormone atrial natriuretic peptide. Interestingly, only little is known about the signaling events leading to an induction of MKP-1 in endothelial cells. Based on the knowledge of an involvement of reactive oxygen species (ROS)<sup>27,28</sup> and different kinases (MAPKs, protein kinase C),<sup>29-32</sup> we hypothesized that ROS initiate a signaling cascade leading to an activation of kinases, which results in an increased expression of MKP-1.

## 1.4 Atrial natriuretic peptide

In 1981 de Bold *et al.* observed that an infusion of atrial tissue extracts into rats causes a strong natriuresis.<sup>33</sup> This study was the initial point for the discovery of the natriuretic peptide (NP) family, a family of cardiovascular hormones. The first discovered member, atrial natriuretic peptide (ANP), was described as a natriuretic, diuretic, and vasorelaxant agent. Later on, two other NPs were discovered: brain natriuretic peptide (BNP) and C-type natriuretic peptide (CNP).<sup>34</sup> Recently, dendroaspis natriuretic peptide (DNP), originally found in the green mamba snake, was revealed to be present in humans.<sup>35</sup>



ANP is primarily produced in the cardiac atria. The most important stimulus for its release is an increased atrial wall tension. ANP is a circular, disulfide bond-containing peptide composed of 28 amino acids (figure 6), which is generated by cleavage of the precursor hormone pro-ANP.<sup>36</sup>

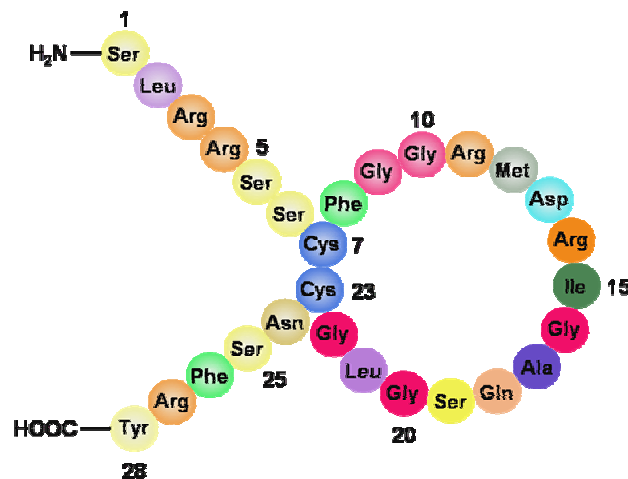


**Figure 6:** Structure of human atrial natriuretic peptide (ANP).

BNP was initially discovered in brain homogenates, but the predominant sites of its synthesis and release are ventricular myocardial cells. Both ANP and BNP exert natriuretic, diuretic, and vasorelaxant effects and play an important role as regulators of blood pressure and volume homeostasis by counterbalancing the renin-angiotensin-aldosterone system. Target organs predominantly represent the kidneys for ANP and BNP, and the vasculature for CNP, which is mainly expressed in the brain and seems to be an important neuroendocrine regulator. Moreover, relevant amounts of CNP are produced by the endothelium and CNP is suggested as an autocrine/paracrine vasoregulator.<sup>34,37</sup>

Natriuretic peptides exert their various effects by binding to three different types of transmembrane NP receptors (NPRs).<sup>38-40</sup> Their structure is schematically depicted in figure 7. NPR-A and NPR-B are particulate guanylyl cyclases. Most of the biological actions of NPs are mediated by these receptors. Their activation results in an increase of intracellular cyclic guanosine monophosphate (cGMP) levels. NPR-A predominantly binds ANP and BNP, whereas NPR-B shows the strongest affinity to CNP. The third receptor, NPR-C, binds all NPs and mainly acts as a clearance receptor and plays an important

role in the elimination of NPs. Besides this action, NPR-C has also been shown to mediate an inhibition of adenylyl cyclase and an activation of phospholipase C *via* inhibitory G proteins.<sup>41</sup>

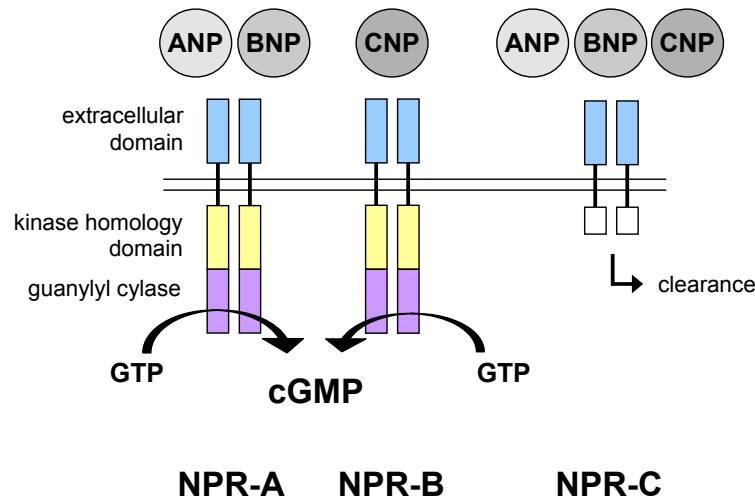


**Figure 7:** Structure of the natriuretic peptide receptors (NPRs).

NPs not only affect the body's volume homeostasis, but also seem to play a fundamental role in cardiovascular remodeling and have functions as diagnostic parameters for cardiovascular conditions.<sup>42</sup> ANP and BNP have also proven a therapeutic potency: for a few years they have been available as drugs for the treatment of acutely decompensated heart failure. Besides the administration of exogenous NP, increasing endogenous NP levels by inhibition of their degradation is suggested as a potentially valuable therapeutic strategy for cardiovascular disease.<sup>43</sup>

Besides its prominent role in regulating volume homeostasis and cardiac function, ANP has been shown to be vasoprotective: ANP exerts proliferative effects on the endothelium and has, therefore, beneficial actions in vascular regeneration. ANP also possesses the potency to maintain endothelial barrier function, i.e. ANP can protect against endothelial hyper-permeability. Moreover, ANP was shown to largely inhibit the attraction and adhesion of leukocytes and to induce cytoprotective proteins, such as heme oxygenase-1.<sup>37</sup>

## 1.5 ROS and NAD(P)H oxidase

In the 1950s, the appearance of free radicals in biological materials was discovered.<sup>44</sup> Two major types of free radicals exist: reactive oxygen species (ROS) with superoxide as most relevant member, and reactive nitrogen species (RNS) with nitric oxide (NO) as major representative (figure 8). The superoxide anion is formed by the univalent reduction of oxygen. This process is mediated by enzymes such as nicotinamide adenine dinucleotide phosphate (NADPH) oxidase (Nox), xanthine oxidase, or by components of the mitochondrial electron transport chain. As a highly reactive radical, superoxide is rapidly converted into the nonradical hydrogen peroxide (H<sub>2</sub>O<sub>2</sub>), a process which is catalyzed by the enzyme superoxide dismutase (SOD). In the presence of transition metals, such as ferrous ions, superoxide can be converted into the highly reactive hydroxyl radical. The relatively stable oxidant hydrogen peroxide is mainly degraded by the enzymes catalase and glutathione peroxidase (GPx). NO is generated enzymatically by NO synthase (NOS) and is able to rapidly react with superoxide, leading to the formation of peroxynitrite.<sup>45,46</sup>

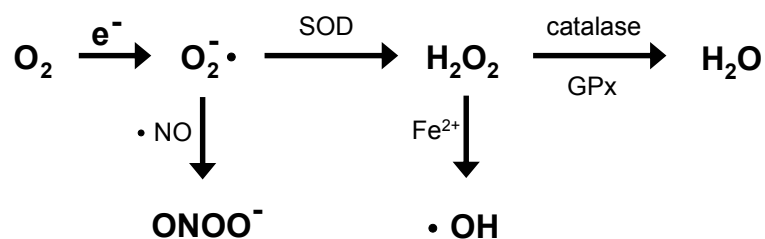


**Figure 8:** Pathways of reactive oxygen species (ROS) formation and degradation.

For several decades, ROS were considered as toxic by-products of metabolic processes being able to badly damage cellular components. Many pathological states have been linked to elevated ROS levels (oxidative stress), such as cancer, atherosclerosis, hypertension, diabetes mellitus, rheumatoid arthritis, chronic heart failure, and ischemia reperfusion injury.<sup>45,47</sup> In the last years, more and more studies revealed that radicals not only take part in pathophysiological processes, but also participate in cell signaling and regulation of cell functions, and therefore can be regarded as second messenger molecules.<sup>48-50</sup> Numerous physiological actions are regulated by ROS, mainly involving the controlled production of NO by NOS or superoxide by Nox. Prominent examples are the regulation of vascular

tone, cell adhesion, immune response, and programmed cell death.<sup>45,47</sup> A particularly active field of research deals with the role of ROS in the cardiovascular system. ROS seem to have distinct functions on each cell type in the vasculature, especially on vascular smooth muscle and endothelial cells. Both are able to produce ROS mainly by the NAD(P)H oxidase enzyme family.<sup>47,51</sup>

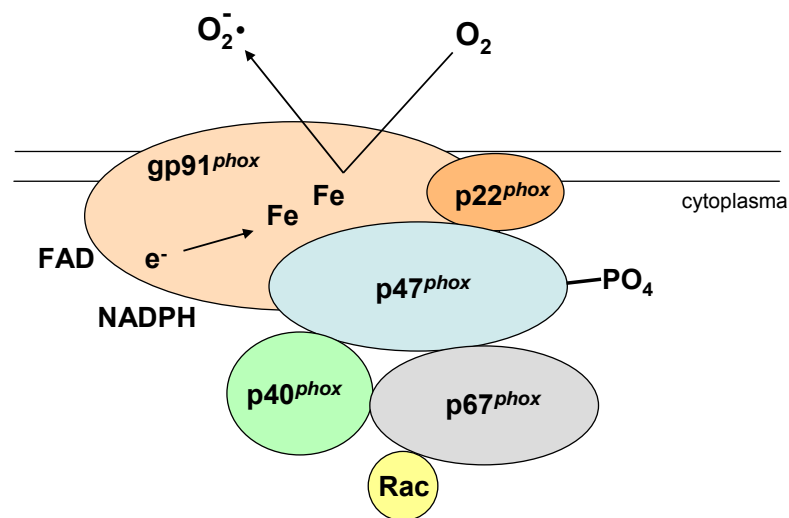


**Figure 9:** Structure of the phagocyte NAD(P)H oxidase (phox) in its active form. Abbreviations: flavin adenine dinucleotide (FAD), nicotinamide adenine dinucleotide phosphate (NADPH).

NAD(P)H oxidase was discovered in phagocytic leukocytes, such as neutrophils, eosinophils, and monocytes/macrophages, which play a highly important role in the innate immune response. A crucial component of this response is the ability of phagocytes to generate high amounts of ROS *via* Nox. The prototypical phagocyte-type NAD(P)H is a multi-component, flavin-heme enzyme which transfers electrons across the plasma membrane to oxygen (figure 9). The univalent reduction of molecular oxygen results in the formation of a superoxide anion. Superoxide is released into the extracellular milieu as well as into phagocytic vacuoles. The phagocyte Nox is composed of membrane-bound and soluble cytosolic subunits. The membrane-bound cytochrome  $b_{558}$  complex consists of the two subunits gp91<sup>phox</sup> and p22<sup>phox</sup>. The cytosolic components are p47<sup>phox</sup>, p67<sup>phox</sup>, p40<sup>phox</sup> and the small Rho-GTPase Rac1/2. p47<sup>phox</sup>, p67<sup>phox</sup>, and p40<sup>phox</sup> exist as a cytosolic macromolecular complex. Upon different stimuli (e.g. phagocytosis), NAD(P)H oxidase assembles in a complex process involving phosphorylation of p47<sup>phox</sup>, Rac activation, and cytoskeleton-dependent translocation of the cytosolic components to the plasma membrane. Only the fully assembled complex expresses catalytic activity.<sup>52-54</sup> Recent evidence shows that all NAD(P)H oxidase subunits are present and functional in

human endothelial cells. In contrast to phagocyte Nox, the oxidase is constitutively active at a very low level even in resting cells.<sup>55</sup> Accordingly, endothelial Nox was suggested to exist preassembled in association with membranes of the endoplasmatic reticulum.<sup>56-61</sup>

With the increase of information concerning the human genome, several novel gp91<sup>phox</sup> homologues have been discovered, suggesting that enzymes similar to the phagocytic oxidase function in a variety of tissues. The physiological functions of these novel NAD(P)H oxidases (Nox1, Nox2  $\equiv$  gp91<sup>phox</sup>, Nox3, Nox4, and Nox5) are widely unknown and currently under intensive investigation. In endothelial cells, besides Nox2/gp91<sup>phox</sup>, Nox4 has been found as a catalytically active Nox homologue.<sup>62</sup>

Concerning the involvement of the small Rho-GTPase Rac, it is known that both isoforms, Rac1 and Rac2, are able to activate Nox<sup>53</sup>. The family of Rho-GTPases consists of Rho, Rac, and Cdc42. The Rho family is part of the Ras superfamily of GTP-binding proteins. GTPases act as a molecular switch, cycling between an active GTP-bound and an inactive GDP-bound state. In the active state, Rho-GTPases are able to interact with a variety of target molecules to initiate a downstream response, while the intrinsic GTPase activity returns the proteins to the inactive GDP-bound state.<sup>63</sup> Besides its crucial role as an activating subunit of NAD(P)H oxidases in phagocytes, Rac is also of great importance for cytoskeletal reorganization processes.<sup>64,65</sup>

## 1.6 Glucocorticoids

In 1950, Hench, Kendall, and Reichstein won the Nobel Prize in Medicine and Physiology for the discovery of the adrenal cortex hormones, their structures, and biological effects.<sup>66</sup> Glucocorticoids (GCs), predominantly cortisol (hydrocortisone), are produced by the cortex of adrenal glands using cholesterol as starting substance. Their production is regulated by the adrenocorticotrophic hormone (ACTH) from the anterior pituitary. ACTH, in turn, is controlled by the corticotropin-releasing hormone (CRH) from the hypothalamus. GCs are essential for normal development and exert influence on different metabolic processes. Their name derives from the effect of raising blood glucose levels due to stress situations by stimulating gluconeogenesis in the liver, which involves catabolic processes like

proteolysis and lipolysis. Moreover, GCs affect the immune system by exerting anti-inflammatory actions: GC inhibit the release of proteolytic enzymes, leukocyte diapedesis, the arachidonic acid cascade, histamine release, and synthesis of different pro-inflammatory cytokines.<sup>67</sup>

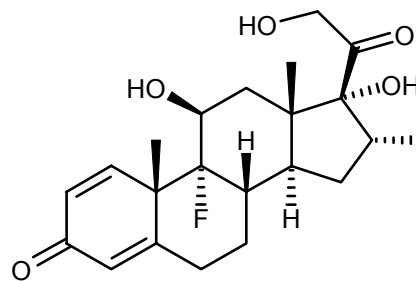


**Figure 10:** Structure of the synthetic glucocorticoid dexamethasone (Dex).

Synthetic glucocorticoids, such as dexamethasone (Dex) (figure 10), are well established and widely used immunosuppressive, anti-inflammatory drugs. GCs have been proven to exert beneficial effects in different autoimmune diseases and in a plethora of disorders with an inflammatory component, e.g. chronic allergic diseases, asthma, rheumatoid arthritis, Crohn's disease, or chronic ulcerative colitis.<sup>67</sup>

Principally, GC act by binding to their intracellular glucocorticoid receptor (GR). Subsequently to its ligand-dependent activation, the receptor translocates to the nucleus and acts (i) as a transcription factor upon binding to glucocorticoid responsive elements (GRE) of distinct gene promoters or (ii) as a direct inhibitor of transcription factors like signal transducers and activators of transcription (STATs), activator protein-1 (AP-1), or NF- $\kappa$ B<sup>68</sup> – a protein-protein interaction known as transrepression (figure 11). Metabolic effects, which represent most side effects of GCs, are mainly ascribed to the transcriptional activity of GR, whereas the anti-inflammatory actions are thought to be predominantly mediated *via* the mechanism of transrepression.<sup>69,70</sup> The development of “dissociative glucocorticoids” which solely activate transrepression without affecting metabolic processes is thought to solve the problem of deleterious side effects in the long-term treatment with GC.<sup>71</sup>

Since some of the GC actions, like acute anti-anaphylactic or cardiovascular protective effects, are known to be very rapid, a new concept of “non-transcriptional” GR effects emerged in the last years:

the activated GR initiates a signaling cascade without a direct action on gene transcription (figure 11). However, an indirect, subsequent downstream transcriptional activation mediated by the initiated signaling pathway is not excluded.<sup>72</sup>

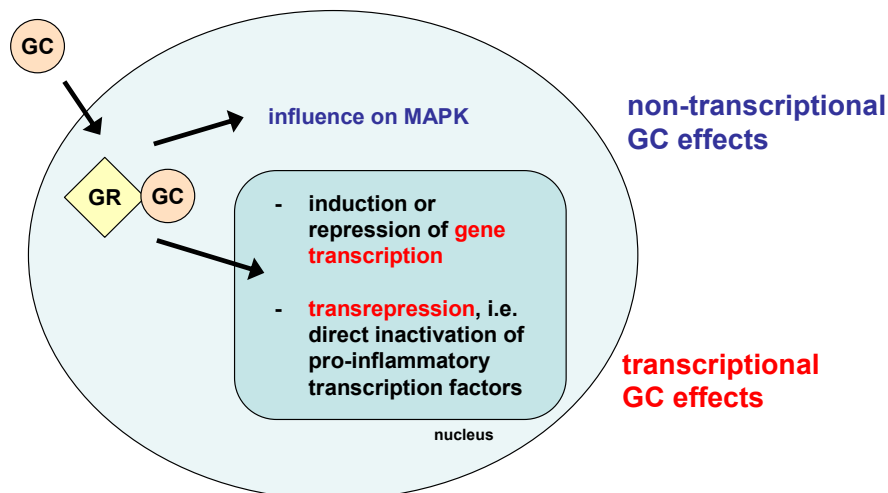


**Figure 11:** Transcriptional and non-transcriptional effects of glucocorticoids (GC). GC readily cross the cytoplasmic membrane and activate the cytosolic glucocorticoid receptor (GR), which either exerts direct effects on signaling cascades (such as MAPKs) or translocates to the nucleus and regulates gene transcription *via* acting as a transcription factor or *via* the mechanism of transrepression.

In the context of non-transcriptional GR effects, a crosstalk between GC and MAPK pathways has increasingly been investigated.<sup>73</sup> GC have been shown to induce MKP-1 in different cell-types.<sup>74</sup> The induction seems to be mediated *via* GR and to depend on ongoing transcription. An involvement of MKP-1 in the anti-inflammatory effects of GCs in the endothelium has as yet not been investigated. Therefore, we aimed to clarify whether Dex is able to induce MKP-1 in endothelial cells. We also wanted to reveal a functional relevance of the Dex-induced increase of MKP-1 protein: in a model of endothelial inflammation, i.e. in TNF- $\alpha$ -activated endothelial cells, we investigated the involvement of MKP-1 in Dex-induced reduction of p38 MAPK activity and E-selectin expression. As mentioned in chapter 1.1.2, E-selectin is known to be largely regulated by NF- $\kappa$ B, a discrimination between p38 MAPK and NF- $\kappa$ B as targets of the anti-inflammatory actions of Dex was mandatory.





## **2 Materials and methods**



## 2.1 Materials

Medium 199, glutamine, penicillin, streptomycin, and amphotericin B were from PAN Biotech (Aidenbach, Germany). Fetal bovine serum (FBS) was from Biochrom (Berlin, Germany). DMEM was from Cambrex (Verviers, Belgium). Endothelial cell growth medium (ECGM) was from Promocell (Heidelberg, Germany). Atrial natriuretic factor (1-28, rat) (ANP) was from Calbiochem (Schwalbach, Germany) or from Bachem (Heidelberg, Germany), and cANF from Saxon Biochemicals (Hannover, Germany). 8-Br-cGMP, SB203580, calphostin C, PD98059, phorbol-12-myristate-13-acetate (PMA), and SP600125 were from Calbiochem (Schwalbach, Germany). Endothelial medium supplement, tumor necrosis factor- $\alpha$  (TNF- $\alpha$ ), dexamethasone (Dex), cycloheximide, tiron, diphenyleioidonium chloride (DPI), *N*-acetyl-*L*-cysteine (NAC), ebselen, superoxide dismutase (SOD), pegylated superoxide dismutase (PEG-SOD), catalase, pegylated catalase (PEG-catalase), isopropyl- $\beta$ -D-thiogalactopyranoside (IPTG), and apocynin were from Sigma-Aldrich (Taufkirchen, Germany). N<sup>G</sup>-nitro-*L*-arginine (L-NNA) was from Alexis (Grünberg, Germany). Complete<sup>®</sup>, collagenase A, and GTP $\gamma$ S were from Roche (Mannheim, Germany). N-cyclohexyl-3-aminopropanesulfonic acid (CAPS) was from USB (Cleveland, USA). LB broth base (Lennox LB broth base) was from Gibco/Invitrogen (Karlsruhe, Germany). Anti-gp91<sup>phox</sup>/Nox2, anti-p47<sup>phox</sup>, anti-Nox4, and anti-MKP-1 antibody were from Santa Cruz (Heidelberg, Germany). Anti-JNK and anti-phospho-JNK were from Cell Signaling/New England Biolabs (Frankfurt am Main, Germany), and anti-Rac from Upstate/Biomol (Hamburg, Germany). AlexaFluor488 goat anti-mouse, dihydrofluorescein diacetate (H<sub>2</sub>FDA), and dihydrodichlorofluorescein diacetate (H<sub>2</sub>DCFDA) were from Molecular Probes/Invitrogen (Karlsruhe, Germany). Phycoerythrin (PE)-labeled anti-E-selectin (CD62E) was from Leinco/Biotrend (Cologne, Germany). Horseradish peroxidase (HRP)-conjugated goat anti-rabbit was from Dianova (Hamburg, Germany) and HRP-conjugated goat anti-mouse from Biozol (Eching, Germany) or Cell Signaling/New England Biolabs (Frankfurt am Main, Germany). AP-1 decoy and scrambled decoy, i.e. phosphorothioate-modified oligodesoxynucleotides, and primers for MKP-1 and Nox1-5 were from MWG Biotech (Ebersberg, Germany). MKP-1, gp91<sup>phox</sup>/Nox2, and Nox4 sense and antisense oligodesoxynucleotides were from biomers.net (Ulm, Germany). All other chemical agents (analytical

grade) were from Sigma-Aldrich (Taufkirchen, Germany), from Roth (Karlsruhe, Germany), or from Merck (Darmstadt, Germany).

## **2.2 Cell culture**

### **2.2.1 Solutions**

Phosphate buffered saline (PBS) pH 7.4 is composed of NaCl 123.2 mM,  $\text{KH}_2\text{PO}_4$  3.16 mM, and  $\text{Na}_2\text{HPO}_4$  10.4 mM. Phosphate buffered saline pH 7.4 with magnesium and calcium (PBS+) consists of NaCl 137 mM, KCl 2.68 mM,  $\text{Na}_2\text{HPO}_4$  8.10 mM,  $\text{KH}_2\text{PO}_4$  1.47 mM,  $\text{MgCl}_2$  0.5 mM, and  $\text{CaCl}_2$  0.68 mM.

### **2.2.2 Culture of HUVEC and HMEC**

Human umbilical vein endothelial cells (HUVEC) were prepared by digestion of umbilical veins with 0.1 g/l collagenase A (37°C, 45 min).<sup>75</sup> For experiments investigating the induction of MKP-1 by ANP, HUVEC were cultured in Medium 199 supplemented with 20 % heat-inactivated fetal bovine serum (FBS), 2 % endothelial medium supplement, 2 mM glutamine, 100 U/ml penicillin, 100 µg/ml streptomycin, and 2.5 µg/ml amphotericin B. For experiments regarding the investigation of the induction of MKP-1 by dexamethasone, HUVEC were cultured in endothelial cell growth medium supplemented with 100 U/ml penicillin and 100 µg/ml streptomycin.

CDC/EU.HMEC-1 (human microvascular endothelial cells, HMEC) were obtained from the CDC (Atlanta, USA). HMEC are an immortalized cell line (human dermal microvascular endothelial cells transfected with a plasmid coding for the transforming SV40 large T-antigen) that has been shown to retain endothelial morphologic, phenotypic, and functional characteristics.<sup>76</sup> HMEC were cultured in endothelial cell growth medium supplemented with 100 U/ml penicillin and 100 µg/ml streptomycin.

The cells were cultured in an incubator (Heraeus, Hanau, Germany) in a humidified atmosphere at 5 % CO<sub>2</sub> and 37°C. Both HUVEC and HMEC were routinely tested for mycoplasma contamination with the PCR detection kit VenorGeM (Minerva Biolabs, Berlin, Germany).

### **2.2.3 Passaging**

For passaging, cells were washed twice with PBS and detached by treating with a trypsin/ethylene diamine tetraacetic acid (EDTA) (T/E) solution containing trypsin 0.05 % and EDTA 0.02 % in PBS for 1-2 min at 37°C. The digestion was stopped with Medium 199 containing 10 % heat-inactivated FBS, 100 U/ml penicillin, 100 µg/ml streptomycin, and 2.5 µg/ml amphotericin B. Generally, cells were subcultured to a ratio of 1:3 (related to area) in cell culture flasks or plates (TPP, Trasadingen, Switzerland) and grown until confluence. HUVEC of passage no. 3 were used for all experiments.

### **2.2.4 Long-time storage**

For long-time storage confluent cells were trypsinized, centrifuged, and resuspended in freezing medium, which consists of cell culture medium supplemented with 10 % dimethylsulfoxide (DMSO, cryoprotectant). The cell suspension was transferred to cryovials and gradually frozen at -20°C for one day, at -80°C for one week, and then stored at -196°C in liquid nitrogen. For thawing, cells were rapidly warmed to 37°C, centrifuged, and resuspended in cell culture medium.

### **2.2.5 Starvation**

In general, cells were starved for 4 h in pure Medium 199 before performing experiments. For experiments performed with dexamethasone, cells were additionally starved overnight in a glucocorticoid-free starvation medium (DMEM containing 20 % heat-inactivated charcoal-stripped FBS, 2 mM glutamine, 100 U/ml penicillin, 100 µg/ml streptomycin, 2.5 µg/ml amphotericin B, and 10 ng/ml basic fibroblast growth factor). Since fetal bovine serum (FBS) contains significant amounts

of different steroids, such as glucocorticoids, cells are permanently exposed to glucocorticoids during cell growth. To eliminate an influence of the medium on the glucocorticoid system, steroids were removed by charcoal-treatment: FBS was gently swirled with activated charcoal overnight at 4°C and afterwards cleaned from charcoal by repeated centrifugation.

## 2.3 Western blot analysis

### 2.3.1 Solutions

Cell lysis buffer contained tris(hydroxymethyl)aminomethane-HCl (Tris-HCl) pH 7.4 50 mM, sodium dodecyl sulfate (SDS) 0.1 %, nonidet P-40 (NP-40/Igepal CA 630) 1 %, sodium deoxycholate 0.25 %, NaCl 150 mM, Complete<sup>®</sup> (protease inhibitor cocktail) 4 %, phenylmethylsulfonyl fluoride (PMSF, protease inhibitor) 1 mM. For the protection of phosphorylated proteins the buffer additionally contained the phosphatase inhibitors NaF 1 mM and activated Na<sub>3</sub>VO<sub>4</sub> 1 mM. 3x Laemmli sample buffer was composed of Tris-HCl pH 8.8 187.5 mM, SDS 6 %, glycerol 30 %, β-mercaptoethanol 12.5 %, and bromphenolblue 0.015 %. The resolving gel (10 %) contained an acrylamide 30 %-bisacrylamide 0.8 %-solution (rotiphorese<sup>®</sup> Gel 30) 40 %, Tris pH 8.8 375 mM, SDS 0.1 %, N,N,N',N'-tetramethylethylenediamine (TEMED) 0.1 %, and ammonium peroxodisulfate (APS) 0.5 %. The stacking gel contained rotiphorese<sup>®</sup> Gel 30 17 %, Tris pH 6.8 125 mM, SDS 0.1 %, TEMED 0.2 %, and APS 1 %. The electrophoresis buffer consisted of Tris 0.3 %, glycine 1.44 %, and SDS 0.1 %. The anode buffer contained Tris 12 mM, N-cyclohexyl-3-aminopropanesulfonic acid (CAPS) 8 mM, and methanol 15 %, and the cathode buffer Tris 12 mM, CAPS 8 mM, and SDS 0.1 %. Tris-buffered saline solution with tween (TBS-T) pH 8.0 is composed of Tris 0.3 %, NaCl 1.1 %, and tween 20 0.2 %.

### 2.3.2 *In vivo* samples

Lung samples were kindly provided by Renate Noske-Reimers and Prof. Dr. Wolfgang Kübler (Charité, Institute of Physiology, Berlin, Germany). In anesthetized Sprague-Dawley rats ( $268 \pm 6$  g body weight), a bolus of ANP or an equivalent volume of NaCl were injected *via* a central venous catheter. ANP dosage was calculated to reach a blood concentration of  $1 \mu\text{M}$  under the assumption of a rat blood volume of  $64 \text{ ml/kg}$  body weight.<sup>77</sup> 1 h after bolus administration lungs were excised and cryopreserved in liquid nitrogen. Lung tissue was cryocut and protein was extracted. Protein concentrations were measured by the method of Bradford.<sup>78</sup> Western blot analysis was performed as described under 2.3.3.

### 2.3.3 *In vitro* samples

Cells were cultured in 6- or 12-well plates, grown until confluence, and treated as indicated in the respective figure legends. Cells were washed twice with ice-cold PBS, lysed in modified RIPA buffer and centrifuged. For adjusting the samples to the same protein content, protein concentration of the supernatant was determined by the bicinchoninic acid method (BC assay reagents, Interdim, Montluçon, France) (Ref). Laemmli sample buffer was added and the samples were heated at  $95^\circ\text{C}$  for 5 min. Subsequently, a denaturing discontinuous polyacrylamide gel electrophoresis (SDS-Disc-PAGE) (Mini-Protean 3, Bio-Rad, Munich, Germany) was performed for separation of proteins. Proteins were blotted onto a polyvinylidene fluoride (PVDF) membrane (Immobilon-P, Millipore, Schwalbach, Germany) by semi-dry electro-blotting (1 h,  $1.56 \text{ mA/cm}^2$ ) (Bio-Rad, Munich, Germany). The membrane was dried for 30 min at  $80^\circ\text{C}$  and afterwards saturated (blocked) in 5 % non-fat dry milk (Bio-Rad, Munich, Germany) in TBS-T for 2 h. Incubation with the primary antibody was performed overnight at  $4^\circ\text{C}$  by gently shaking the membrane in the antibody dilution. Subsequently, the membrane was washed three times with TBS-T and incubated with horseradish peroxidase (HRP)-conjugated secondary antibody for 2 h at room temperature. The membrane was again washed three times with TBS-T. For visualization of bands, an enhanced chemoluminescence detection kit (ECL plus, Amersham, Freiburg, Germany) was used and membranes were applied to a medical x-ray

film (Super RX, Fuji, Düsseldorf, Germany) or to an image station (Kodak Image Station 440cf, Kodak, Rocester, USA). Films were developed with an AGFA Curix 60 (AGFA, Cologne, Germany) and scanned for subsequent digital analysis.

### **2.3.4 Stripping, reprobing, and coomassie staining**

For removing antibodies from the membrane (stripping), blots were incubated for 30 min at 50°C in a stripping buffer consisting of Tris-HCl 62.5 mM, SDS 2 %, and  $\beta$ -mercaptoethanol 0.8 %. The membrane was extensively washed with TBS-T and blocked for 2 h in non-fat dry milk (5 % in TBS-T). Subsequently, the membrane was incubated with new antibodies (reprobing) according to section 2.3.3. To check the uniformity of protein loading and transfer, gels were stained by a protein dyeing solution containing coomassie brilliant blue 3 %, acetic acid 10 %, and ethanol 45 %.

## **2.4 RT-PCR**

### **2.4.1 Isolation and characterization of total RNA**

Cells were grown in 25 cm<sup>2</sup> cell culture flasks or in 60 mm dishes until confluence. Total RNA was prepared using the RNA isolation RNeasy Mini Kit (Qiagen, Hilden, Germany). The cells were lysed and homogenized in a buffer containing  $\beta$ -mercaptoethanol and the chaotropic denaturing salt guanidine isothiocyanate. RNases are immediately inactivated by the buffer. Ethanol was added for creating appropriate binding conditions of RNA to the silica-gel-based membranes of the microspin columns. All other cellular component were removed by different washing procedures. Subsequently, the purified RNA was eluated under low salt conditions from the column. RNA molecules longer than 200 nucleotides are predominantly isolated, which provides an enrichment of mRNA. The size distribution of the isolated RNA is comparable to that obtained by the classical RNA isolation method of centrifugation through a CsCl cushion.



The obtained amount of RNA was quantified photometrically (Lambda Bio 20 Photometer, PerkinElmer, Überlingen, Germany). Absorption was measured at 260 nm ( $A_{260}$ ) and 280 nm ( $A_{280}$ ). The RNA concentration was calculated from the  $A_{260}$  value. The ratio  $A_{260}/A_{280}$  was used for characterizing the purity of RNA (optimum: 1.8-2.0). Strong absorption at 280 nm indicates protein contaminations.

The integrity of the isolated RNA was checked by agarose gel (1.2 %) (SeaKem LE Agarose, BioWhittaker, Rockland, USA) electrophoresis (Owl Separation Systems, Portsmouth, USA). TAE consisting of Tris 40 mM, EDTA 1 mM, and acetic acid 1.1 % was used as electrophoresis buffer. Ethidium bromide was directly added to the agarose gel solution (final concentration 0.5 µg/ml). For sample loading 6x blue/orange loading dye (Promega, Heidelberg, Germany) was used. Bands were visualized under UV-light (254 nm) on an image station (Kodak Image Station 440cf, Kodak, Rochester, USA). The intensity ratio of the two major bands (ribosomal 28S and 18S RNA) was used to estimate RNA integrity.

## 2.4.2 Reverse transcription

Reverse transcription was performed using a reverse transcription system kit (Promega, Heidelberg, Germany). This kit uses the reverse transcriptase from the avian myoblastosis virus (AMV-RT). Samples were incubated at 42°C for 25 min. The reaction was stopped by incubation at 99°C for 5 min.

## 2.4.3 Polymerase chain reaction

MKP-1 PCR was performed with Taq DNA polymerase from *Thermophilus aquaticus* (Promega, Heidelberg, Germany). MKP-1 primers: 5'-GCTGTGCAGCAACAGTC-3' and 5'-TACCTTATGAGGAC-TAATCG-3'. GAPDH primers: 5'-TCACTCAAGATTGTCAGCAA-3' and 5'-AGATCCACGACGGACAC-ATT-3'. PCR conditions for MKP-1: 94°C 5:00 min; (94°C 1:00 min, 57°C 2:00 min, 72°C 1:00 min) 35 cycles; 72°C 5:00 min. PCR conditions for GAPDH: 93°C 1:06 min; (93°C 0:24 min, 55°C

0:30 min, 73°C 1:00 min) 30 cycles; 73°C 10:00 min. Nox1-5 RT-PCR was performed using the Access RT-PCR System (Promega, Heidelberg, Germany). This one-tube two-enzyme system uses AMV-RT and Tfl DNA polymerase from *Thermus flavus*. Reverse transcription was performed at 48°C for 45 min. Reaction was stopped by incubation at 94°C for 2 min. Nox1 primers: 5'-TGGCTAAATCCCATCCAGTC-3' and 5'-AGTGGGAGTCACGATCATCC-3'. Nox2 primers: 5'-TGG-ATAGTGGGTCCCATGTT-3' and 5'-GCTTATCACAGCCACAAGCA-3'. Nox3 primers: 5'-CCAGGGC-AGTACATCTTGGT-3' and 5'-CTGTGCCTCACTGCATTTGT-3'. Nox4 primers: 5'-TGTTGGATGACTGGAAACCA-3' and 5'-TGGGTCCACAACAGAAACA-3'. Nox5: 5'-CTACGTGGTAGTGGGGC-TGT-3' and 5'-AACAAGATTCCAGGCACCAG-3'. PCR conditions: (94°C 0:30 min; 60°C 1:00 min, 68°C 2:00 min) 40 cycles; 68°C 7:00 min. The PCR products were separated by agarose gel electrophoresis as described under 2.4.1.

## 2.5 ROS measurement in cultured endothelial cells

Dihydrofluorescein diacetate (H<sub>2</sub>FDA) was used to assess the generation of intracellular reactive oxygen species (ROS).<sup>79</sup> H<sub>2</sub>FDA easily penetrates the cell membrane. Cleavage of its ester groups by intracellular esterases leads to the formation of the negatively charged, intracellular-trapped ROS-sensitive dye dihydrofluorescein. Oxidation of dihydrofluorescein results in highly fluorescent derivatives of fluorescein. The absorption and emission spectrum of fluorescein is depicted in figure 12. Fluorescence was measured with a SpectraFluor Plus microplate reader (Tecan, Crailsheim, Germany) using an excitation and emission wavelength of 485 nm and 535 nm, respectively.

Cells were grown until confluence in 24- or 96-well plates and treated as indicated in the respective figures. After treatment, cells were washed twice with HBSS pH 7.4 consisting of NaCl 142 mM, KCl 5.4 mM, Na<sub>2</sub>HPO<sub>4</sub> 0.28 mM, KH<sub>2</sub>PO<sub>4</sub> 0.37 mM, CaCl<sub>2</sub> 1.22 mM, MgSO<sub>4</sub> 0.81 mM, glucose 5.6 mM, and HEPES 20 mM. Subsequently, cells were loaded with 20 μM H<sub>2</sub>FDA (in HBSS) by incubation for 20 min at 37°C in the dark, and washed again. All experiments were taken 30 min after treatment (except for time courses).

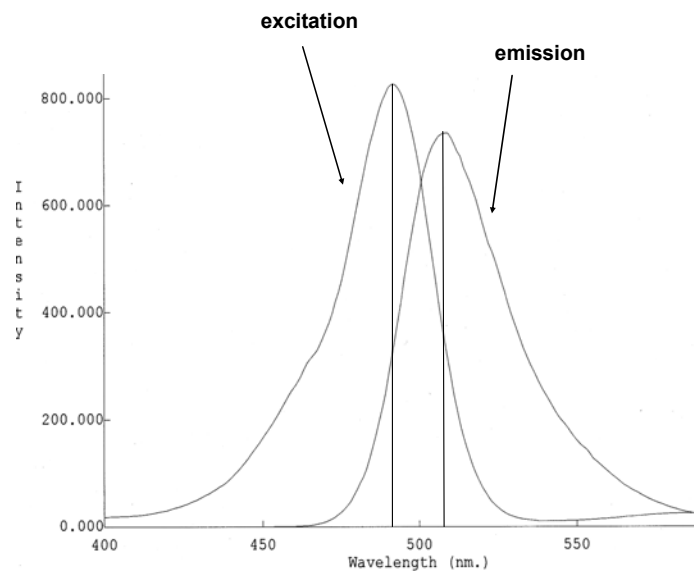


**Figure 12:** Absorption and emission spectrum of fluorescein.

The validity of the ROS assay was tested by two ways: (i) Freshly isolated pig granulocytes – known for their ROS-producing capacity – were loaded with  $H_2FDA$  as described above and treated with the phorbol ester PMA, a known inducer of ROS generation in phagocytes, for the indicated times (figure 13A). (ii) HUVEC were treated with the oxidant hydrogen peroxide (figure 13B). The fluorescence signal clearly rose in both settings.

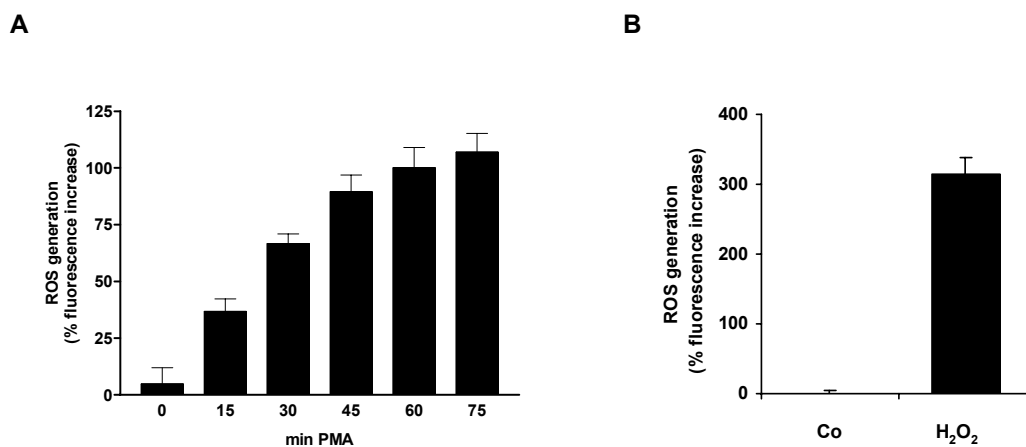


**Figure 13:** Validity of the ROS assay. **A:** Freshly isolated pig granulocytes were incubated with  $20 \mu M H_2FDA$  for 20 min. Cells were treated with phorbol-12-myristate-13-acetate (PMA,  $100 nM$ ) for the indicated times. **B:** HUVEC were loaded with  $20 \mu M H_2FDA$  for 20 min. Hydrogen peroxide ( $H_2O_2$ ,  $100 \mu M$ ) was added to the cells for 30 min.

Dihydrofluorescein is known to react with a variety of oxidants including superoxide, hydrogen peroxide, and peroxynitrite.<sup>79</sup> Peroxynitrite is the reaction product of superoxide and nitrogen oxide (NO). To figure out whether peroxynitrite/NO is involved in the increase of the fluorescence signal generated by ANP, we applied the endothelial NO synthase (NOS) inhibitor N<sup>G</sup>-nitro-L-arginine (L-NNA). As shown in figure 14A, L-NNA only slightly decreased the ANP-induced ROS generation, pointing to an only marginal involvement of peroxynitrite/NO. Since the question raised whether ANP influences the generation of NO, an arginine/citrullin conversion assay was kindly performed by Thomas Räthel. Figure 14B shows that ANP does not induce endothelial NO generation. These results clearly indicate that peroxynitrite is not or only to an extremely low degree involved in the ANP-induced fluorescence signal increase and, moreover, that NO needed for the generation of peroxynitrite does not arise from ANP-treatment, since treatment with L-NNA alone decreased the fluorescence signal, it much more seems to result from the basal endothelial NO pool.

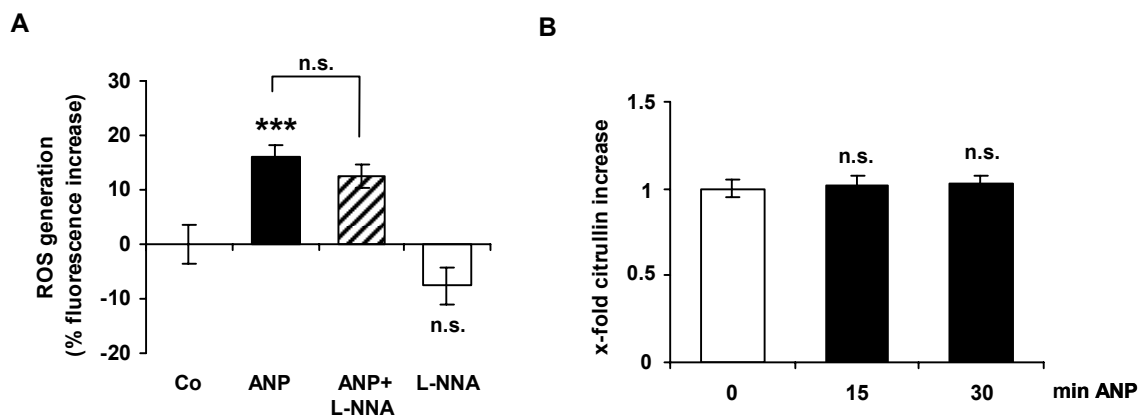


**Figure 14:** **A:** ROS generation. HUVEC were either left untreated (Co), treated with ANP (1  $\mu$ M) or L-NNA (125  $\mu$ M, 60 min) alone, or pre-treated with L-NNA (125  $\mu$ M, 60 min) before ANP (1  $\mu$ M). **B:** Arginine/citrullin conversion assay. HUVEC were treated with ANP (1  $\mu$ M) for the indicated times. \*\*\*  $P \leq 0.001$  vs. Co.

## 2.6 ROS measurement in the endothelium of intact rat lung vessels

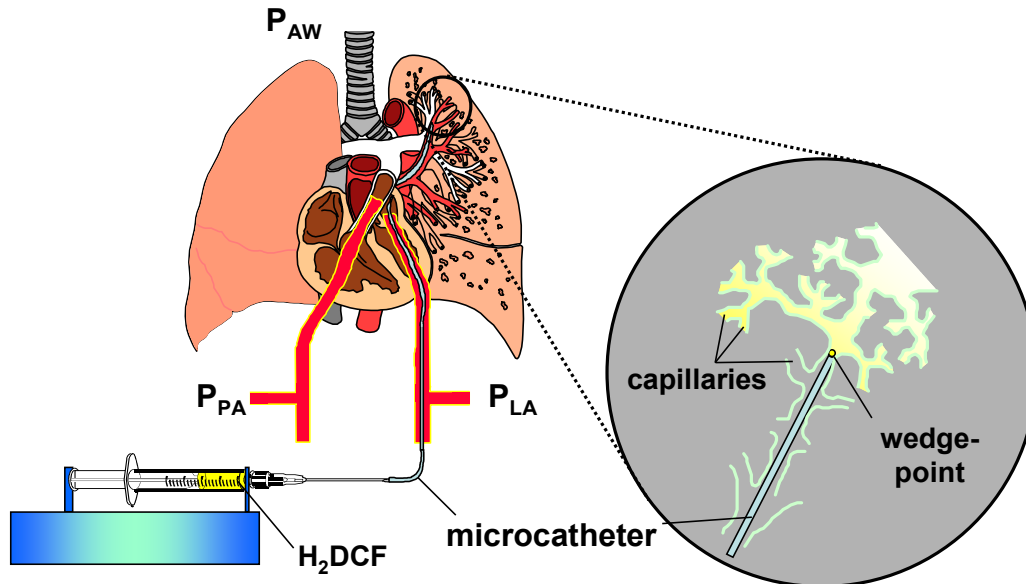


**Figure 15:** Fluorescence measurement of ROS in the endothelium of isolated-perfused rat lung vessels.

The experiments described in this section were kindly performed by Corinna Brückl (Institute for Surgical Research, University of Munich, Germany) and Dr. Wolfgang Kübler (Institute of Physiology, Charité – Medical School of the Berlin Universities, Campus Benjamin Franklin, Germany).

### 2.6.1 Animals

Male Sprague-Dawley rats ( $487 \pm 20$  g body weight) were obtained from the local breeding facilities of the academical institution. All animals received care in accordance with the "Guide for the Care and Use of Laboratory Animals" (NIH publication no. 85-23, rev. 1985), and the study was approved by the animal care and use committees of the local government authorities.

### 2.6.2 Isolated-perfused rat lung preparation

Lungs excised from anesthetized Sprague-Dawley rats were continuously perfused with 14 ml/min autologous rat blood at 37°C. Lungs were constantly inflated at positive airway pressure of 5 cmH<sub>2</sub>O

with a gas mixture of 21 % O<sub>2</sub>, 5 % CO<sub>2</sub>, and 74 % N<sub>2</sub>, that maintained blood PO<sub>2</sub> (140 mmHg), PCO<sub>2</sub> (35 mmHg), and pH (7.4) (Chiron Diagnostics, Fernwald, Germany). Left atrial pressure was adjusted to 5 cmH<sub>2</sub>O, yielding pulmonary artery pressures of 10 ± 1 cmH<sub>2</sub>O. P<sub>PA</sub> and P<sub>LA</sub> were continuously monitored (Servomed SMS 308; Hellige, Freiburg, Germany) and displayed on a multichannel recorder (Oscilloreg, Siemens, Erlangen, Germany). Lungs were positioned on a custom-built vibration-free table and superfused with normal saline at 37°C to prevent drying. For local delivery of fluorescent probes and drugs to pulmonary microvessels *in situ*, a microcatheter (Ref. 800/110/100, SIMS Portex Ltd., Kent, UK) was advanced through the left atrium and wedged in a pulmonary vein draining a capillary area on the lung surface.<sup>80,81</sup> For a schematic overview of the experimental setting see figure 15.

### 2.6.3 *In situ* fluorescence microscopy

In isolated-perfused rat lungs, ROS production was determined by digital fluorescence imaging of lung capillary endothelial cells loaded with the ROS-sensitive dye H<sub>2</sub>DCF.<sup>82</sup> Membrane-permeable H<sub>2</sub>DCF diacetate (2 μM), which de-esterifies intracellularly to cell-impermeable H<sub>2</sub>DCF, was infused into pulmonary venular capillaries using the venous microcatheter. Endothelial H<sub>2</sub>DCF fluorescence was excited by near monochromatic illumination from a galvanometric scanner (Polychrome II, TILL Photonics, Martinsried, Germany) at 488 nm. The excitation light was directed through an Olympus BX50 upright microscope equipped with appropriate dichroic and emission filters (Olympus Optical Co., Hamburg, Germany). Fluorescence emission was collected through an apochromat objective (UAPO 40x W2/340, Olympus Optical Co.) by a CCD camera (Imago, TILL Photonics), stored on a personal computer and subjected to digital image analysis (TILLvision 4.0, TILL Photonics). Fluorescence images of single subpleural capillaries were obtained in 5 s intervals, and exposure time for a single image was limited to 7 milliseconds. Off-line, images were corrected for background as determined over alveolar spaces. Throughout experiments, the fluorescence background remained unchanged. Single venular capillaries were viewed at a focal plane corresponding to their maximum diameter (12-25 μm). Although the only cell type in the vascular wall of these capillaries are endothelial cells,<sup>83</sup> fluorescent dyes may leak across the endothelial layer to enter adjacent cells such

as epithelial cells of juxtaposed alveoli or enter blood cells such as leukocytes or platelets. To avoid these potential pitfalls, we maintained absorptive conditions within the capillary and cleared the capillary of blood before dye infusion.<sup>84</sup>

## 2.7 Electrophoretic mobility shift assay (EMSA)

### 2.7.1 Extraction of nuclear protein

HUVEC were grown in 6-well plates until confluence and were treated as indicated in the respective figures. Nuclear extracts were prepared according to the method of Schreiber *et al.*<sup>85</sup> as follows: after treatment, cells were washed twice with ice-cold PBS, scraped off in PBS with a rubber cell scraper, centrifuged, and resuspended in an ice-cold buffer containing N-(2-hydroxyethyl)piperazine-N'-(2-ethanesulfonic acid) (HEPES) pH 7.9 10 mM, KCl 10 mM, EDTA 0.1 mM, ethylene glycol-O,O'-bis-(2-amino-ethyl)-N,N,N',N'-tetraacetic acid (EGTA) 0.1 mM, dithio-1,4-threitol (DTT) 1 mM, PMSF 0.5 mM, and Complete<sup>®</sup> 1 %. Cells were incubated on ice for 15 min. Nonidet P-40 was added to the cells and after vigorous vortexing the homogenate was centrifuged. The nuclear pellet was resuspended by vigorous rocking for 15 min at 4°C in a buffer containing HEPES pH 7.9 20 mM, NaCl 400 mM, EDTA 1 mM, EGTA 0.5 mM, glycerol 25 %, DTT 1 mM, PMSF 1 mM, and Complete<sup>®</sup> 2 %. The nuclear extract was centrifuged and the supernatant containing nuclear proteins was frozen at -80°C. The protein concentrations were determined by the method of Bradford.<sup>78</sup>

### 2.7.2 Radioactive labeling of consensus oligonucleotides

Double-stranded oligonucleotide probes containing the consensus sequence either for AP-1 (5'-CGCTTGATGAGTCAGCCGGAA-3') or for NF- $\kappa$ B (5'-AGTTGAGGGGACTTTCCAGGC -3') (both from Promega, Mannheim, Germany) were 5'-end-labeled with adenosine 5'-[ $\gamma$ -<sup>32</sup>P]triphosphate (3,000 Ci/mmol) (Amersham, Freiburg, Germany) by using the T4 polynucleotide kinase (PNK) (USB,

Cleveland, USA), which catalyzes the transfer of the terminal phosphate of ATP to the 5'-hydroxyl termini of DNA. The oligonucleotides were incubated with T4 PNK for 10 min at 37°C and the reaction was stopped by adding EDTA-solution (0.5 M). The radiolabeled DNA was separated from unlabeled remnants by using NucTrap probe purification columns (Stratagene, La Jolla, USA). Radiolabeled DNA was eluted from the column by STE buffer pH 7.5 containing Tris-HCl 10 mM, NaCl 100 mM, and EDTA 1 mM and frozen at -20°C.

### **2.7.3 Binding reaction and electrophoretic separation**

5x binding buffer pH 7.5 is composed of glycerol 20 %, MgCl<sub>2</sub> 5 mM, EDTA 2.5 mM, NaCl 250 mM, and Tris-HCl 50 mM. Gel loading buffer pH 7.5 consists of Tris-HCl 250 mM, bromphenolblue 0.2 %, and glycerol 40 %. The reaction buffer contains DTT 2.6 mM, 5x binding buffer 90%, and gel loading buffer 10 %. 10x TBE pH 8.3 is composed of Tris 0.89 M, boric acid 0.89 M, and EDTA 0.02 M.

Equal amounts of nuclear protein (approx. 2 µg) were incubated for 5 min at room temperature in a total volume of 14 µl containing poly(dIdC) 2 µg and reaction buffer 3 µl. Subsequently, 1 µl of the radiolabeled oligonucleotide probe (approx. 300,000 cpm) was added. After incubation for 30 min at room temperature, the nucleoprotein-oligonucleotide complexes were resolved by electrophoresis (Mini-Protean 3, Bio-Rad, Munich, Germany) on non-denaturing polyacrylamide gels (4.5 %) containing 10x TBE 5.3 %, acrylamide 30 %-bisacrylamide 0.8 %-solution (rotiphorese Gel 30) 15.8 %, glycerol 2.6 %, TEMED 0.05 %, and APS 0.08 %. TBE was used as electrophoresis buffer. Bands were visualized by applying the gels to Cyclone Storage Phosphor Screens (Canberra-Packard, Dreieich, Germany) and analysis by a phosphorimager (Cyclone Storage Phosphor System, Canberra-Packard, Dreieich, Germany).



## 2.8 Transfection experiments

### 2.8.1 Rac1 mutants

The plasmids pcDNA3.1 (Invitrogen, Karlsruhe, Germany), pcDNA3RacN17-myc (containing an insert coding for myc-tagged RacN17, a dominant negative Rac1 mutant), and pcDNA3RacV12-myc (containing an insert coding for myc-tagged RacV12, a constitutively active Rac1 mutant) were kindly provided by Dr. Agnes Görlach (German Heart Center, Munich). HMEC were grown to 40-80 % confluence in 6- or 24-well plates and were transfected with the constructs by using SuperFect Transfection Reagent (Qiagen, Hilden, Germany). SuperFect is an activated dendrimer with a defined spherical structure with branches radiating from a central core and terminating at charged amino groups. The DNA is assembled by SuperFect into compact structures. DNA/SuperFect-complexes are positively charged which allows them to bind to negatively charged receptors (e.g. glycoproteins) on the eukaryotic cell surface. Following endocytosis, SuperFect buffers the lysosome after fusion with the endosome, leading to pH inhibition of lysosomal nucleases and stability of DNA/SuperFect-complexes. For 6-well plates 2 µg DNA and 10 µl SuperFect and for 24-well plates 1 µg DNA and 5 µl SuperFect were used. The DNA was incubated with SuperFect for 10 min at ambient temperature. Cells were treated with the DNA/SuperFect-complex for 2 h. To ensure a sufficient expression of the Rac1 mutant proteins, further treatments were started 48 h after transfection.

### 2.8.2 Antisense oligodesoxynucleotides

Transfection of antisense oligodesoxynucleotides (ODN) is used to silence the expression of a distinct gene. To prevent the transfected ODN from degradation, phosphorothioate-modified ODN are used. The antisense sequences were for MKP-1 5'-gggccCGAATGTGCTGagttc-3', for gp91<sup>phox</sup>/Nox2 5'-cctcatTCACAGCGcagtt-3',<sup>86</sup> and for Nox4 5'-ggacaCAGCCATGccgcc-3'.<sup>62</sup> Lower case letters represent phosphorothioate modifications. Control experiments were performed with the respective sense sequence. For transfection of the ODN, jetPEI transfection reagent (Polyplus-

Transfection/Biomol, Hamburg, Germany) was used. jetPEI is a linear polyethylenimine and compacts DNA into positively charged particles capable of interacting with anionic proteoglycans at the cell surface and entering cells by endocytosis. jetPEI buffers the endosomal pH and protects DNA from degradation. It also induces osmotic swelling and rupture of the endosome, which provides an escape mechanism for DNA particles to the cytoplasm. HUVEC were cultured until approx. 80 % confluence in 6- or 24-well plates. For 6-well plates 5 µg DNA and 10 µl jetPEI and for 24-well plates 3 µg DNA and 6 µl jetPEI were used. The DNA was incubated with jetPEI for 30 min at ambient temperature. Cells were treated with the DNA/jetPEI-complex for 4 h. To ensure a sufficient silencing of the targeted proteins, further experiments were started 24 h after transfection.

### **2.8.3 AP-1 decoy**

An AP-1 decoy is an oligonucleotide consisting of the consensus sequence of the transcription factor AP-1. Therefore, the decoy is capable of catching the activated transcription factor leading to an inactivation of the AP-1 response. The decoy sequences were as follows: AP-1 decoy 5'-cgctTGATGACTCAGCCggaa-3' and AP-1 scrambled decoy 5'-cgctTGATGACTTGCCggaa-3'.<sup>87</sup> Lower case letters represent phosphorothioate modifications. AP-1 decoys were transfected into HUVEC with SuperFect according to section 2.8.1. Experiments were performed 4 h after transfection.

## **2.9 Rac pull-down assay**

### **2.9.1 Principle of the assay**

The affinity precipitation assay detecting active Rac1 uses the p21-binding domain (PBD) of the Rac1 target p21-activated kinase 1 (PAK1) fused to glutathione S-transferase (GST) to isolate a complex containing GST-PBD bound to active Rac1 (Rac-GTP). The GST-PBD fusion protein is bound to glutathione sepharose beads, which allows the precipitation of the complex (figure 16).

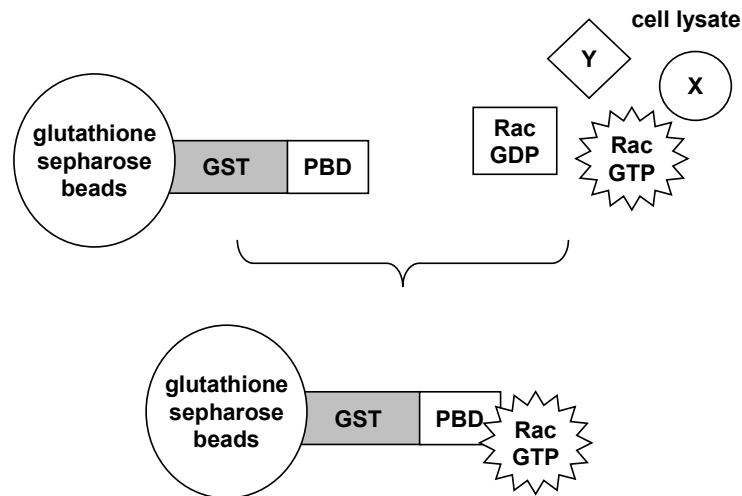


**Figure 16:** Schematic depiction of the Rac pull-down assay. The assay allows to specifically isolate active Rac (i.e. Rac-GTP) from cell lysates. Abbreviations: glutathione S-transferase (GST), p21-binding domain (PBD).

## 2.9.2 Preparation of the GST-PBD sepharose beads

GST-PBD sepharose beads were prepared according to Benard *et al.*<sup>88</sup> as follows: *E. coli* transformed with pGEX-4T-3 – a cloning vector for the inducible expression of genes (*lac* promoter) as GST fusion proteins – containing the information for PBD were kindly provided by Dr. Ulla Knaus (The Scripps Research Institute, La Jolla, USA). *E. coli* transformed with pGEX-4T-3PBD were cultured at 37°C overnight in 100 ml LB broth medium containing ampicillin (100 µg/ml) in a shaker for bacteria. The 100 ml-culture was added to 1,900 ml LB broth medium containing ampicillin and the bacteria were allowed to grow for 90 min at 37°C. The optical density (OD) at 600 nm was taken to check whether the bacteria expanded to a sufficient quantity (optimal OD<sub>600</sub>: 0.9). To induce the expression of the *lac* promoter-linked GST-PBD gene, isopropyl-β-D-thiogalactopyranoside (IPTG) was added to the culture to a final concentration of 0.3 mM. Bacteria were allowed to express the GST-PBD fusion protein for 3 h at 30°C. After centrifugation, the bacteria pellet was lysed in a buffer containing Tris pH 7.5 50 mM, NaCl 150 mM, MgCl<sub>2</sub> 5 mM, DTT 1 mM, PMSF 1 mM, EDTA 1 mM, leupeptin 1 µg/ml, and aprotinin 10 µg/ml. The lysate was homogenized by sonication and centrifuged. The supernatant was incubated with a glutathione sepharose bead suspension (Amersham, Freiburg, Germany) for 60 min at 4°C. Beads were washed five times with a buffer containing Tris pH 7.5 50 mM, NaCl 50 mM, MgCl<sub>2</sub> 5 mM, EDTA 1 mM, DTT 0.1 mM, and PMSF 0.1 mM. Different samples were taken during the purification

procedure and analyzed by Western blot analysis and Coomassie staining of the gel in order to judge the purity of the GST-PBD bead suspension and the degree of GST-PBD binding to the beads (figure 17).

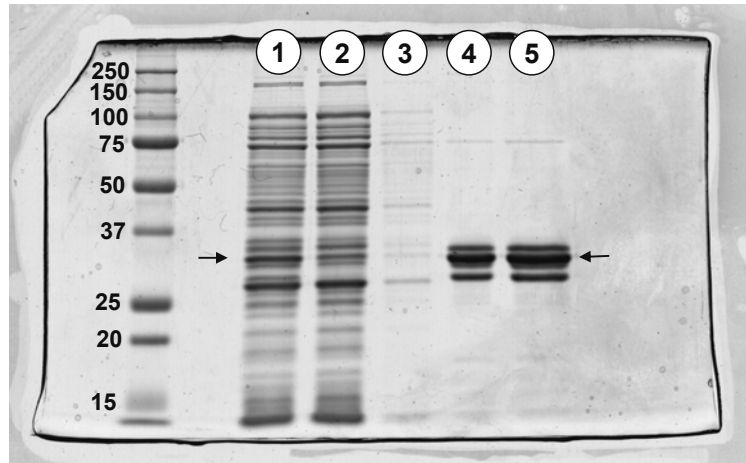


**Figure 17:** Coomassie-stained control gel. Lane 1: total bacterial lysate. Lane 2: lysate after bead incubation. Lane 3: supernatant after two bead washing steps. Lane 4: 5 µl beads. Lane 5: 10 µl beads. The arrows mark the GST-PBD band.

### 2.9.3 Pull-down assay

The Rac1 pulldown assay was performed according to Benard *et al.*<sup>88</sup> as follows: HUVEC were grown in 100 mm dishes until confluence and treated as indicated in the respective figure legend. Cells were washed once with ice-cold PBS and lysed either with PBD-buffer containing Tris pH 8.0 25 mM, DTT 1 mM, MgCl<sub>2</sub> 20 mM, NaCl 100 mM, EDTA 0.5 mM, and Triton X-100 1 % or with GTP $\gamma$ S-PBD-buffer containing Tris pH 8.0 25 mM, DTT 1 mM, MgCl<sub>2</sub> 5 mM, NaCl 100 mM, EDTA 1 mM, and Triton X-100 1 %. After scraping cells off with a rubber cell scraper, cells were incubated for complete lysis for 15 min at 4°C under vigorous shaking. The cell lysate was centrifuged and the supernatant was frozen at -80°C. Protein concentration was determined using the bicinchoninic assay method. 200 µg protein was used for the pull-down assay.

As a positive control specific samples were incubated for 10 min at 30°C with GTP $\gamma$ S (10 mM) and EDTA (100 mM), leading to an exchange of Rac-GDP to Rac-GTP. The exchange reaction was stopped by adding MgCl<sub>2</sub> (1 M).

The pull-down assay was performed by gently shaking the samples with the GST-PBD beads for 1 h at 4°C. After centrifugation, the bead-pellet was washed five times with PBD-buffer. The beads were resuspended in 1x Laemmli sample buffer (see section 2.3.1) and boiled for 5 min at 95°C. Western blot analysis was performed as described under 2.3.2.

## **2.10 Immunocytochemistry and confocal microscopy**

HUVEC were grown until confluence on collagen-coated (collagen 1 % in PBS) glass coverslips (Ø 12 mm) in 24-well plates. Cells were treated as indicated in the respective figure legend. After treatment cells were washed with PBS+ and fixed with a buffered formaldehyde solution (4 %) for 15 min. Cells were washed with PBS and permeabilized with Triton X-100 (0.2 %) for 2 min. After washing three times with PBS, unspecific binding was blocked by incubating cells with a bovine serum albumin (BSA) solution (0.2 %) for 15 min in order to minimize non-specific adsorption of antibodies. Cells were incubated with the primary antibody (1 µg/ml) for 1 h, washed three times with PBS, and subsequently incubated with the secondary antibody (5 µg/ml) for 30 min. Cells were again washed three times with PBS. The coverslips were embedded in fluorescent mounting medium (DakoCytomation, Hamburg, Germany) and put onto glass objective slides. Images were obtained using a Zeiss LSM 510 META (Zeiss, Oberkochen, Germany) confocal laser scanning microscope.

## **2.11 Flow cytometry (FACS)**

Cells were grown until confluence in 24-well plates and were treated as indicated in the respective figure legend. After treatment, cells were washed with PBS, detached by trypsinization as described under 2.2.3, and transferred into FACS tubes containing a buffered formaldehyde solution (4 %), which stopped trypsinization. Cells were incubated for 15 min in the formaldehyde solution for fixation. Subsequently, cells were washed with PBS and incubated with a fluorescent dye-labeled antibody in the dark for 20 min. After washing, cells were resuspended in PBS for flow cytometric analysis

(FACSCalibur, BD Biosciences, Heidelberg, Germany). The FACS buffer pH 7.37 consisted of NaCl 138.95 mM,  $\text{KH}_2\text{PO}_4$  1.91 mM,  $\text{Na}_2\text{HPO}_4$  16.55 mM, KCl 3.76 mM, LiCl 10.14 mM,  $\text{NaN}_3$  3.08 mM, and EDTA 0.967 mM.

## 2.12 Statistical analysis

All experiments were done from at least two to three different cell preparations ( $n \geq 2$ ). Each experiment was performed at least in duplicates. Data are expressed as mean  $\pm$  SEM. Statistical analysis was performed with GraphPad Prism 3.03. Unpaired t-test was used to compare two groups. To compare three or more groups, one-way ANOVA followed by Tukey's post test was used. Data gathered from ROS measurements in rat lungs were analyzed by Mann-Whitney U-test.

### **3 Results**





## 3.1 ANP and MKP-1

### 3.1.1 MKP-1 induction by ANP

#### 3.1.1.1 Time and concentration course of MKP-1 induction

The induction of MKP-1 by ANP in HUVEC has previously been shown by Dr. Nina Weber.<sup>14</sup> We confirmed these experiments both in HUVEC and in HMEC (figure 18A,C): ANP rapidly increased endothelial MKP-1 protein expression. This induction persists for approx. 90 min. Performing an ANP concentration course (figure 18B), we observed a slight protein induction already at 0.1 nM. For further experiments, 1  $\mu$ M was used as standard concentration for ANP.

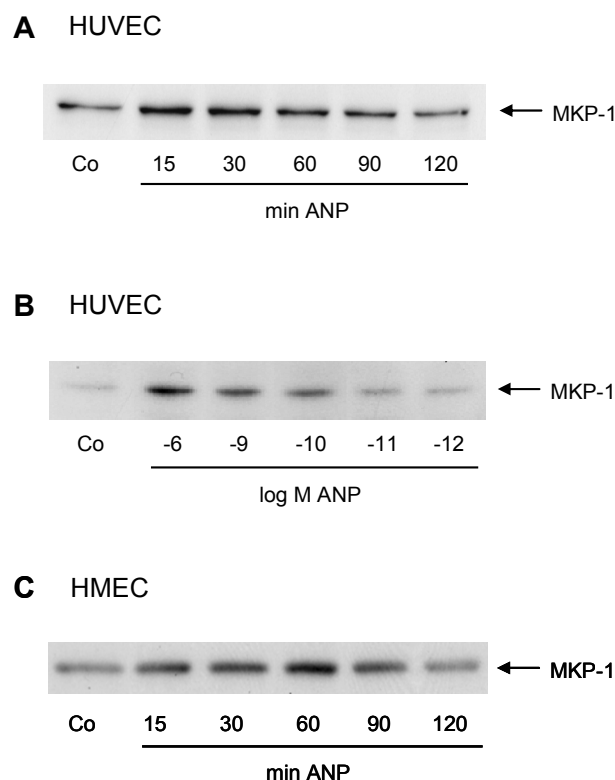


**Figure 18:** Time- and concentration-course of ANP-induced MKP-1 expression. Control (Co) cells were left untreated. **A:** HUVEC were treated with ANP (1  $\mu$ M) for the indicated times. **B:** HUVEC were treated with ANP for 60 min (concentration as indicated). **C:** HMEC were treated with ANP (1  $\mu$ M) for the indicated times. MKP-1 protein expression was determined by Western blot analysis as described in section 2.3.3.

### 3.1.1.2 Influence of cycloheximide on MKP-1 induction

To clarify whether the upregulation of MKP-1 by ANP depends on *de novo* protein biosynthesis, we used cycloheximide, an inhibitor of translation, and found that the ANP-induced MKP-1 induction was completely suppressed after 30 min (figure 19), whereas the early induction at 15 min was not affected by cycloheximide. These findings indicate that ANP activates MKP-1 protein *de novo* synthesis within 30 min and, moreover, suggest that the early effect of ANP might be independent from protein synthesis.

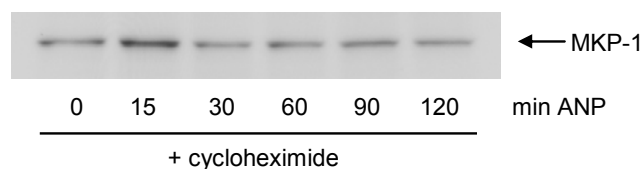


**Figure 19:** Effect of cycloheximide on ANP-induced MKP-1 expression. HUVEC were treated with ANP (1  $\mu$ M) for the indicated times in the presence of cycloheximide (10  $\mu$ g/ml, 30 min before ANP). MKP-1 protein expression was determined by Western blot analysis as described in section 2.3.3.

### 3.1.1.3 MKP-1 induction depends on cGMP/NPR-A

The effects of ANP can be mediated by two different receptors: NPR-A or NPR-C. We wanted to clarify which receptor participates in the induction of MKP-1 by ANP. Therefore, we treated HUVEC with 8-Br-cGMP, a cell-permeable analogue of the NPR-A-dependent second messenger of ANP. We observed that 8-Br-cGMP mimicked the effect of ANP on MKP-1 protein expression (figure 20), whereas cANF, a specific agonistic ligand of NPR-C, did not alter MKP-1 levels (figure 20). Our data indicate that MKP-1 upregulation by ANP is mediated *via* cGMP/NPR-A.

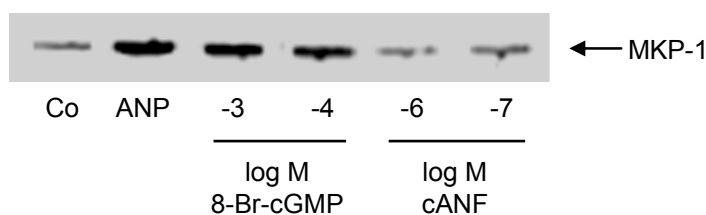


**Figure 20:** Receptor specificity of MKP-1 induction. HUVEC were treated with ANP (1  $\mu$ M), 8-Br-cGMP, and cANF (concentrations as indicated) for 60 min. MKP-1 protein expression was determined by Western blot analysis as described in section 2.3.3.

#### 3.1.1.4 PKG I is not expressed in HUVEC

Since we found that cGMP is the crucial mediator for the induction of MKP-1 by ANP, we wanted to check whether a central downstream target of cGMP, the cGMP-dependent protein kinase I (cGKI, PKG I), is a mediator of ANP's effect on MKP-1 expression. We used different HUVEC cell preparations (primary culture and passages no. 1-3) in order to investigate the expression of PKG I at the protein level. PKG I-transfected COS cells were used as positive control. Figure 21 indicates that HUVEC do not express PKG I protein.

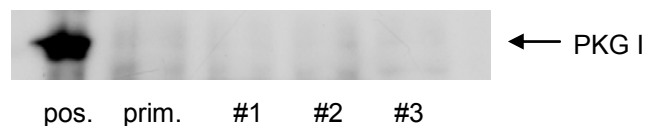


**Figure 21:** HUVEC do not express PKG I protein. 50 µg protein of HUVEC cell lysate obtained from primary culture (prim.) or passage no. 1-3 (#1-3) were analyzed by Western blot analysis as described in section 2.3.3. PKG I-transfected COS cells served as positive control (pos.).

### 3.1.2 ANP induces endothelial ROS production

#### 3.1.2.1 Time and concentration course of ROS generation

Since reactive oxygen species (ROS) have been described as inducers of MKP-1, we hypothesized that ROS generation could account for an induction of MKP-1 by ANP. However, nothing has as yet been known about the capability of ANP to induce the generation of ROS in endothelial cells. Therefore, we measured intracellular ROS formation by loading HUVEC with an ROS-sensitive fluorescent dye. Different control experiments were performed in order to ensure the validity of the used dye (see section 2.5). Treatment of HUVEC with ANP led to an increased ROS production with a maximum dye fluorescence at about 30 min (figure 22A). The concentration dependency of this effect is shown in figure 22B.

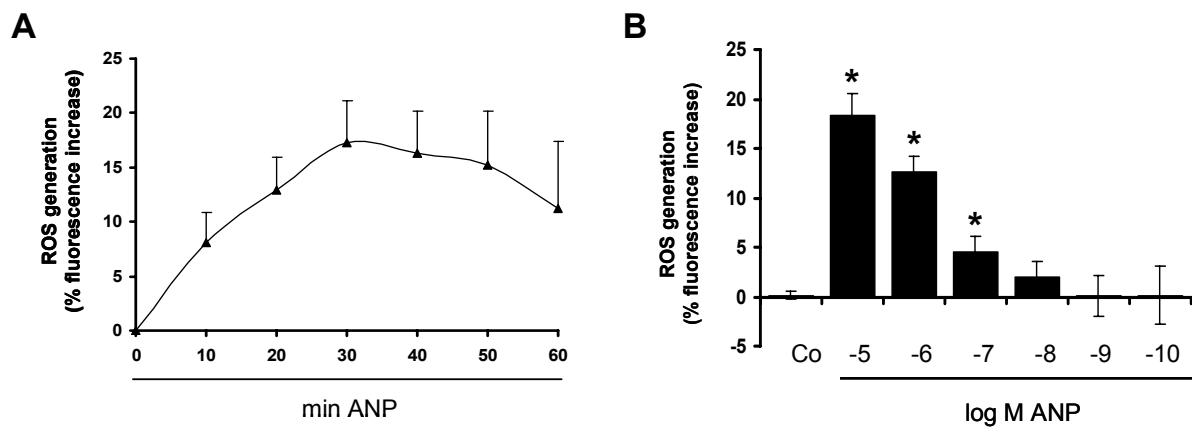


**Figure 22:** ROS generation induced by ANP. **A:** ANP time course. HUVEC were treated with ANP (1  $\mu$ M) for the indicated times. **B:** ANP concentration course. HUVEC were treated with the indicated concentrations of ANP. ROS generation was measured as described in section 2.5. \*  $P \leq 0.05$  vs. Co.

### 3.1.2.2 ROS generation depends on cGMP/NPR-A.

In analogy to the experiments regarding the induction of MKP-1 protein, we checked whether 8-Br-cGMP and cANF affect ROS generation in HUVEC. cANF did not significantly alter ROS levels, whereas 8-Br-cGMP clearly induced the production of ROS (figure 23). These data suggest that ANP induces endothelial ROS production *via* the cGMP/NPR-A-pathway.

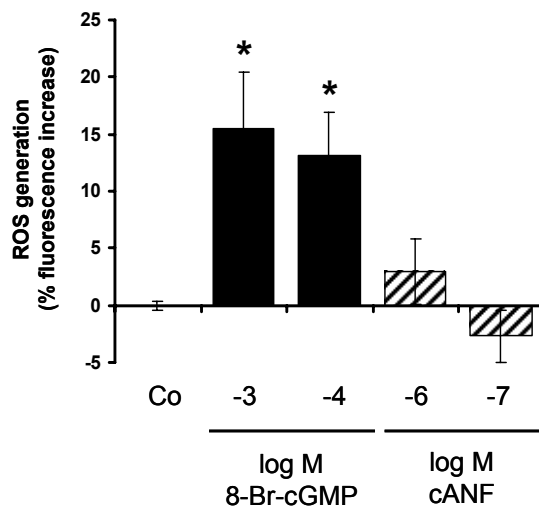


**Figure 23:** Effect of 8-Br-cGMP and cANF on ROS generation. HUVEC were treated with the indicated concentration of 8-Br-cGMP and cANF. ROS formation was measured as described in section 2.5. \*  $P \leq 0.05$  vs. Co.

### 3.1.3 ROS mediate the induction of MKP-1 by ANP

#### 3.1.3.1 Antioxidants abrogate ANP-induced MKP-1 expression

We aimed to causally link ANP-induced ROS generation and MKP-1 expression. Therefore, we treated HUVEC with different antioxidants: tiron (a scavenger of superoxide), ebselen (a scavenger of peroxynitrite and peroxides), and N-acetyl-L-cysteine (a thiol-based antioxidant). All used substances were able to abrogate the ANP-induced MKP-1 expression (figure 24), pointing to a pivotal role for ROS in the upregulation of MKP-1 by ANP.

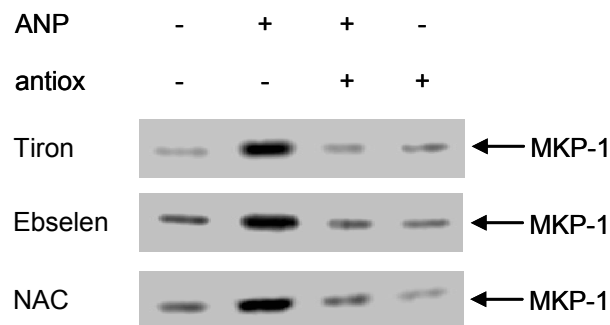


**Figure 24:** Antioxidants abolish the induction of MKP-1 by ANP. HUVEC were pre-incubated with the antioxidants tiron (10 mM), ebselen (40  $\mu$ M), and N-acetyl-L-cysteine (NAC, 10 mM) for 60 min before adding ANP (1  $\mu$ M, 60 min). MKP-1 protein expression was determined by Western blot analysis as described in section 2.3.3.

#### 3.1.3.2 Hydrogen peroxide induces MKP-1

We tested whether the exogenous administration of an oxidant is capable of augmenting MKP-1 levels in HUVEC. We added hydrogen peroxide ( $H_2O_2$ ) to the cells and found a clear increase of MKP-1 protein expression with a maximum at 60 min (figure 25).

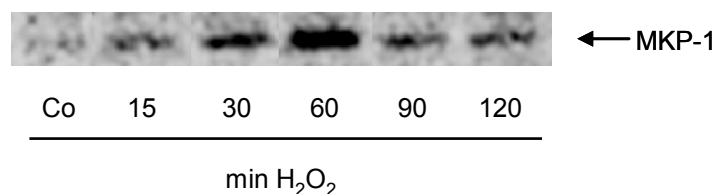


**Figure 25:** Hydrogen peroxide induces MKP-1 expression. HUVEC were either left untreated (Co) or were treated with hydrogen peroxide ( $H_2O_2$ , 50  $\mu$ M) for the indicated times. MKP-1 protein expression was determined by Western blot analysis as described in section 2.3.3.

### 3.1.4 Involvement of NAD(P)H oxidase

The superoxide-generating NAD(P)H oxidase (Nox) represents a major source of ROS production in endothelial cells. We intended to clarify whether NAD(P)H oxidase is involved in ANP-induced ROS formation and, moreover, which Nox isoforms are responsible for the observed effects, i.e. increased ROS formation and MKP-1 protein expression upon ANP-treatment.

#### 3.1.4.1 Influence of PEG-SOD and SOD on ANP-induced ROS generation

First, we aimed to specify which reactive oxygen species is generated in HUVEC upon ANP-treatment. We treated HUVEC with a pegylated superoxide dismutase (PEG-SOD), a stable and cell-permeable derivative of the superoxide-catabolizing enzyme SOD. As shown in figure 26A, PEG-SOD completely abrogated the ANP-induced fluorescence signal. Treatment with cell-impermeable SOD did not influence the ANP-induced generation of ROS (figure 26B). These findings suggest that intracellular superoxide is produced by HUVEC upon ANP-treatment.

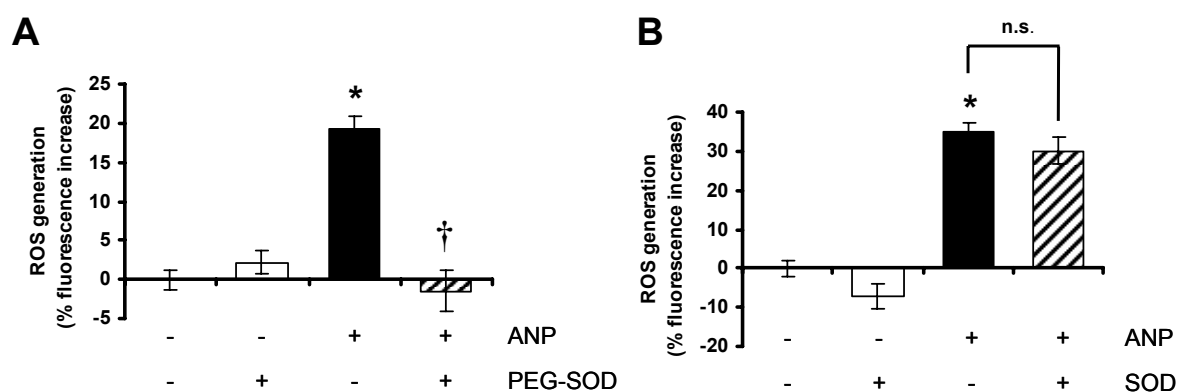


**Figure 26:** Influence of PEG-SOD and SOD on ANP-induced ROS generation. **A:** HUVEC were left untreated (Co), were treated with ANP (1  $\mu$ M) or pegylated superoxide dismutase (PEG-SOD, 300 U/ml, 60 min) alone, or were pre-treated with PEG-SOD (300 U/ml, 60 min) before ANP (1  $\mu$ M). **B:** HUVEC were left untreated (Co), were treated with ANP (1  $\mu$ M) or SOD (300 U/ml, 60 min) alone, or were pre-treated with SOD (300 U/ml, 60 min) before ANP (1  $\mu$ M). ROS generation was measured as described in section 2.5. \*  $P \leq 0.05$  vs. Co. †  $P \leq 0.05$  vs. ANP.

### 3.1.4.2 Influence of PEG-catalase and catalase on ANP-induced ROS generation

Intracellularly produced superoxide is rapidly degraded to hydrogen peroxide ( $H_2O_2$ ). Besides superoxide,  $H_2O_2$  is also able to oxidize the dye used for ROS measurements (see section 2.5). To investigate an involvement of  $H_2O_2$ , we treated HUVEC with catalase (degrades  $H_2O_2$ ) and PEG-catalase, the stable, cell-permeable modification of catalase. Figure 27 shows that neither PEG-catalase (A) nor catalase (B) altered the ANP-induced fluorescence signal, suggesting no involvement of hydrogen peroxide.

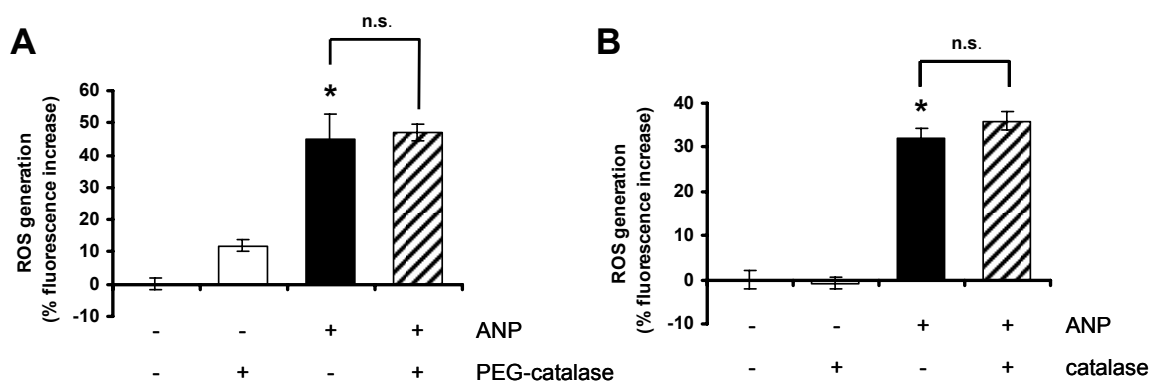


**Figure 27:** Influence of PEG-catalase and catalase on ANP-induced ROS generation. **A:** HUVEC were left untreated (Co), were treated with ANP (1  $\mu$ M) or pegylated (PEG)-catalase (3,000 U/ml, 60 min) alone, or were pre-treated with PEG-catalase (3,000 U/ml, 60 min) before ANP (1  $\mu$ M). **B:** HUVEC were left untreated (Co), were treated with ANP (1  $\mu$ M) or catalase (3,000 U/ml, 60 min) alone, or were pre-treated with catalase (3,000 U/ml, 60 min) before ANP (1  $\mu$ M). ROS generation was measured as described in section 2.5. \*  $P \leq 0.05$  vs. Co.

### 3.1.4.3 Influence of DPI and gp91ds-tat on ANP-induced ROS generation

We intended to figure out whether NAD(P)H oxidase is involved in the production of superoxide upon ANP-treatment by using Nox inhibitors: both the nonspecific inhibitor DPI (inhibitor of flavin-containing enzymes) (figure 28A) and the highly specific inhibitor peptide gp91ds-tat (prevents the activation of Nox by inhibiting the association of Nox1/2/4 and p47<sup>phox</sup>) (figure 28B) abolished the increase of ROS by ANP in HUVEC. These findings clearly point to NAD(P)H oxidase as the crucial ANP-activated ROS source.

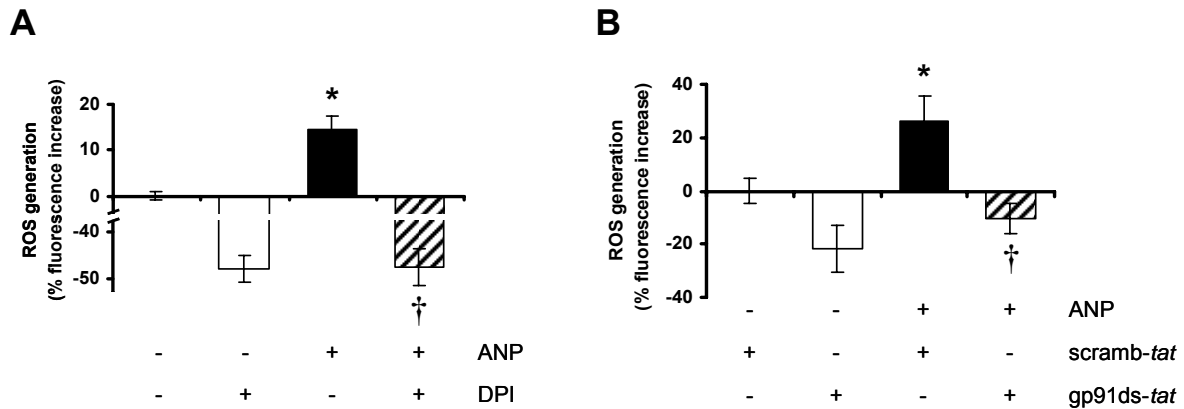


**Figure 28:** Influence of DPI and gp91ds-tat on ANP-induced ROS generation. **A:** HUVEC were left untreated (Co), were treated with ANP (1  $\mu$ M) or diphenyleneiodonium (DPI, 10  $\mu$ M, 60 min) alone, or were pre-treated with DPI (10  $\mu$ M, 60 min) before ANP (1  $\mu$ M). **B:** HUVEC were treated with the NAD(P)H oxidase inhibitor peptide gp91ds-tat (100  $\mu$ M, 30 min) or the scrambled peptide scramb-tat (100  $\mu$ M, 30 min) alone or in combination with ANP (1  $\mu$ M). ROS generation was measured as described in section 2.5. \*  $P \leq 0.05$  vs. Co. †  $P \leq 0.05$  vs. ANP.

#### 3.1.4.4 Influence of PEG-SOD and SOD on ANP-induced MKP-1 expression

In order to link superoxide generation to MKP-1 induction, we tested whether treatment of HUVEC with PEG-SOD or SOD influences the increase of MKP-1 protein expression by ANP. In line with the results obtained for ROS generation, the upregulation of MKP-1 by ANP was completely blocked in the presence of PEG-SOD, whereas SOD did not affect MKP-1 protein levels (figure 29). These data suggest that intracellular superoxide is crucial for the ANP-induced augmentation of MKP-1.

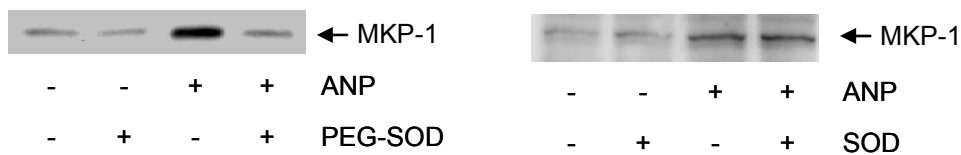


**Figure 29:** Influence of PEG-SOD and SOD on ANP-induced MKP-1 protein expression. **A:** HUVEC were pre-treated with pegylated superoxide dismutase (PEG-SOD, 300 U/ml, 60 min) before ANP (1  $\mu$ M, 60 min). **B:** HUVEC were pre-treated with SOD (300 U/ml, 60 min) before ANP (1  $\mu$ M, 60 min). MKP-1 protein expression was determined by Western blot analysis as described in section 2.3.3.



### 3.1.4.5 Influence of PEG-catalase and catalase on ANP-induced MKP-1 expression

Since we found that  $H_2O_2$  is not involved in the increase of ROS generation upon ANP-treatment, we wanted to investigate whether scavenging of  $H_2O_2$  alters ANP-induced MKP-1 expression. In analogy to the ROS measurements, we treated HUVEC with PEG-catalase and catalase. As figure 30 shows, neither PEG-catalase nor catalase did affect the increase of MKP-1 protein upon ANP-treatment.

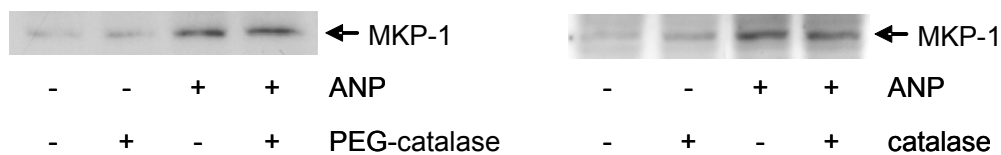


**Figure 30:** Influence of PEG-catalase and catalase on ANP-induced MKP-1 protein expression. **A:** HUVEC were pre-treated with pegylated (PEG)-catalase (3,000 U/ml, 60 min) before ANP (1  $\mu$ M, 60 min). **B:** HUVEC were pre-treated with catalase (3,000 U/ml, 60 min) before ANP (1  $\mu$ M, 60 min). MKP-1 protein expression was determined by Western blot analysis as described in section 2.3.3.

### 3.1.4.6 Influence of DPI and apocynin on ANP-induced MKP-1 expression

Furthermore, we examined the influence of the Nox inhibitors DPI and apocynin on ANP-induced MKP-1 expression. Both inhibitors clearly abrogated ANP's ability to increase MKP-1 protein levels in HUVEC (figure 31), suggesting a pivotal role for NAD(P)H oxidase in the upregulation of MKP-1 by ANP.

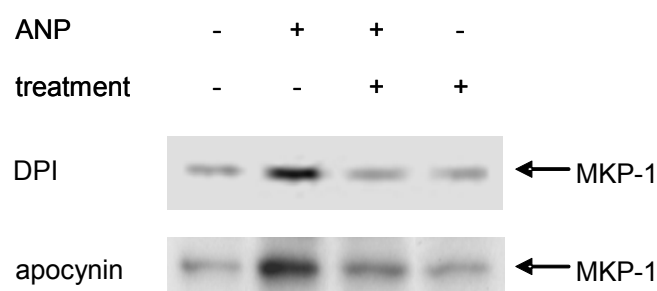


**Figure 31:** Influence of DPI and apocynin on ANP-induced MKP-1 expression. HUVEC were treated with DPI (10  $\mu$ M, 60 min) or apocynin (0.5 mM, 30 min) alone or in combination with ANP (1  $\mu$ M, 60 min). MKP-1 protein expression was determined by Western blot analysis as described in section 2.3.3.

### 3.1.4.7 Expression of Nox homologues' transcripts in HUVEC and HMEC

Different homologues of the proto-typical catalytic subunit gp91<sup>phox</sup>/Nox2 have been discovered in the recent years: Nox1-Nox5. The expression pattern of these Nox homologues seems to strongly depend on the examined cell-type. We wanted to check which Nox homologues are expressed both in HUVEC and HMEC. Therefore, we investigated Nox1-5 mRNA expression by RT-PCR and found that only Nox2 and Nox4 mRNA are expressed both in HUVEC and HMEC (figure 32).

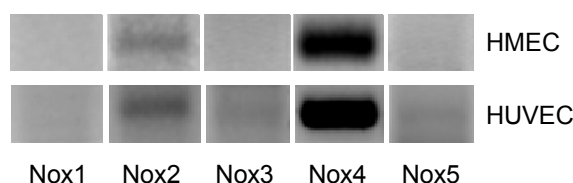


**Figure 32:** Expression of mRNA of Nox homologues in HUVEC and HMEC. RT-PCR was performed as described in section 2.4.

### 3.1.4.8 Influence of Nox2 and Nox4 antisense on ANP-induced ROS generation

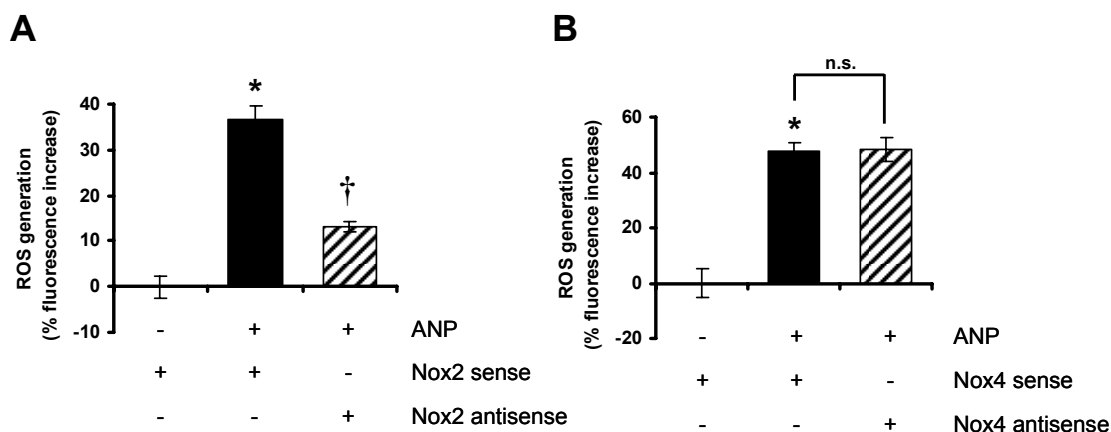


**Figure 33:** Influence of Nox2 and Nox4 antisense oligodesoxynucleotides (ODN) on ANP-induced ROS generation. **A:** HUVEC were either left untreated or were treated with ANP (1  $\mu$ M) in the presence of Nox2 sense or antisense ODN. **B:** HUVEC were either left untreated or were treated with ANP (1  $\mu$ M) in the presence of Nox4 sense or antisense ODN. Transfection with sense or antisense ODN was performed as described in section 2.8.2. ROS generation was measured as described in section 2.5. \*  $P \leq 0.05$  vs. Co. †  $P \leq 0.05$  vs. ANP.

Since we revealed that Nox2 and Nox4 are the only expressed Nox homologues, we aimed to clarify which isoform is involved in the generation of superoxide after ANP treatment. Therefore, we

transfected HUVEC with well-established Nox2 or Nox4 antisense oligodesoxynucleotides. Figure 33 shows that the ANP-induced increase of the fluorescence signal is strongly reduced in the presence of Nox2 antisense (A), whereas Nox4 antisense (B) did not alter ROS generation.

### 3.1.4.9 Influence of Nox2 and Nox4 antisense on ANP-induced MKP-1 expression

We then aimed to clarify whether Nox2/4 antisense does also influence the ANP-induced expression of MKP-1. Again, HUVEC were transfected with the antisense oligos. The functionality of the antisense oligos, i.e. the strong reduction of the Nox2/4 protein content, is shown in the upper panels of figure 34A,B. According to the results presented above, the upregulation of MKP-1 by ANP was completely abolished in the presence of Nox2 antisense, whereas Nox4 antisense oligos did not alter MKP-1 protein levels (figure 34A,B, lower panels)

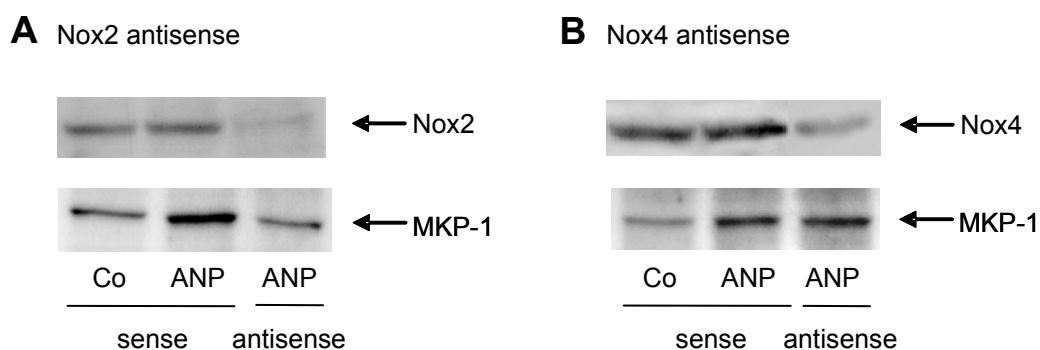


**Figure 34:** Influence of Nox2 and Nox4 antisense oligodesoxynucleotides (ODN) on ANP-induced MKP-1 expression. **A:** HUVEC were either left untreated (Co) or were treated with ANP (1  $\mu$ M, 60 min) in the presence of Nox2 sense or antisense ODN. **B:** HUVEC were either left untreated (Co) or were treated with ANP (1  $\mu$ M, 60 min) in the presence of Nox4 sense or antisense ODN. Transfection with sense or antisense ODN was performed as described in section 2.8.2. MKP-1 protein expression was determined as described in section 2.3.3.

## 3.1.5 Involvement of Rac1

### 3.1.5.1 ANP activates Rac1

The small Rho-GTPase Rac plays an important role in the activation of *phagocyte-type* NAD(P)H oxidase and might also be involved in the activation of *endothelial* Nox. Since ANP-treatment of HUVEC had led to an activation of Nox, the question arose whether ANP could influence the activity of

Rac1. In order to clarify this question, we performed Rac1 pull-down assays. This assay allows to specifically precipitate the activated form of Rac1, i.e. Rac1-GTP. HUVEC were treated with ANP and the amount of activated Rac1 was analyzed. As shown in figure 35 (upper panel) we found an increase of active Rac1 with a maximum at 2-5 min after ANP-treatment.

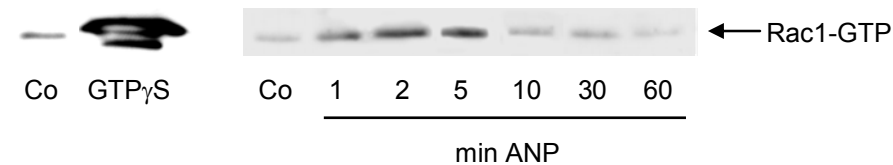


**Figure 35:** ANP leads to an activation of Rac1. HUVEC were either left untreated (Co) or were treated with ANP (1  $\mu$ M) for the indicated times. Activation of Rac1 by GTP $\gamma$ S serves as positive control. Rac pull-down assay was performed as described in section 2.9. The uniformity of the amount of total Rac1 is shown in the lower panel. The amounts of Rac1 protein were determined by Western blot analysis as described in section 2.3.3.

### 3.1.5.2 ANP induces Rac1 translocation

As a second marker for Rac1 activity we investigated Rac1 translocation by confocal microscopy, since Rac1 translocates to the plasma membrane upon activation. Figure 36 shows that ANP was able to mimic the Rac1 translocation observed by treating HUVEC with the known Rac1 activator phorbol-12-myristate-13-acetate (PMA).

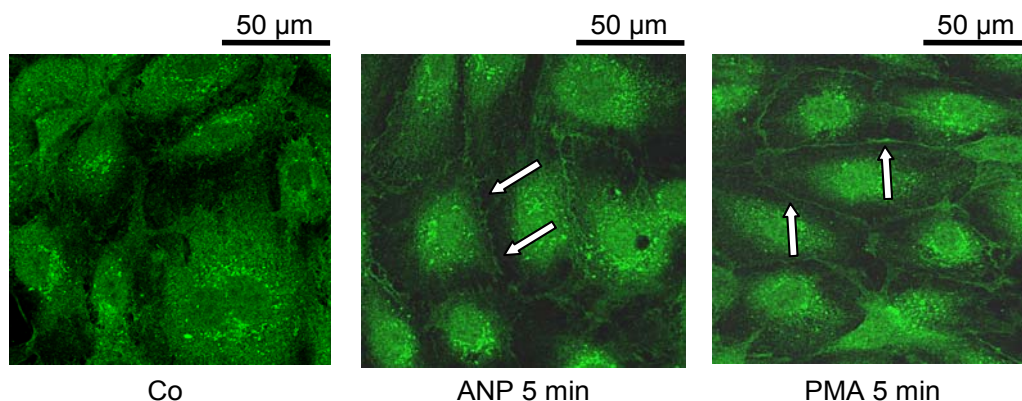


**Figure 36:** ANP leads to a translocation of Rac1. HUVEC were either left untreated (Co) or were treated with ANP (1  $\mu$ M) or phorbol-12-myristate-13-acetate (PMA, 1  $\mu$ M) for the indicated times. Rac1 translocation to the plasma membrane is indicated by arrows. Immunocytochemistry and confocal microscopy were performed as described in section 2.10.

### 3.1.5.3 Rac1 is crucially involved in ANP-induced ROS generation and MKP-1 expression

We then wanted to clarify whether the ANP-induced activation of Rac1 is causally related to the increase of ROS formation by ANP. Therefore, we transfected HMEC (due to difficulties with the transfection of plasmids into primary HUVEC)<sup>89</sup> with different Rac1 mutants: the dominant-negative RacN17 and the constitutively active RacV12 mutant. RacN17 clearly abrogated the fluorescence signal induced by ANP, whereas RacV12 mimicked the ANP-induced increase of ROS generation (figure 37, lower panel). The upregulation of MKP-1 protein by ANP was completely abolished by RacN17, whereas RacV12 mimicked the effect of ANP on MKP-1 expression (figure 37, upper panel). These data clearly point to a crucial involvement of Rac1 in both ANP-induced ROS generation and MKP-1 expression.

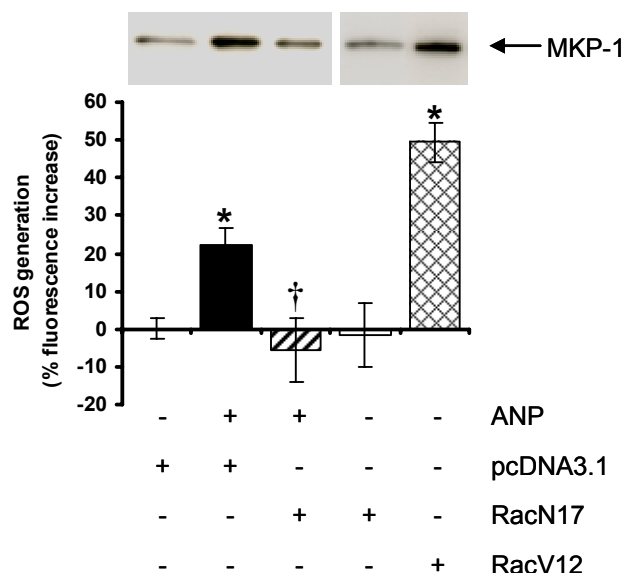


**Figure 37:** Influence of Rac1 mutants on ANP-induced ROS generation and MKP-1 expression. HMEC were transfected with the empty control plasmid pcDNA3.1, the dominant-negative (RacN17), or the constitutively active (RacV12) Rac1 mutant as described in section 2.8.1. Cells were treated with ANP 1  $\mu$ M. ROS generation was measured as described in section 2.5. MKP-1 protein expression (60 min ANP) was determined as described in section 2.3.3. \*  $P \leq 0.05$  vs. pcDNA3.1 alone. †  $P \leq 0.05$  vs. ANP+pcDNA3.1.

### 3.1.6 MKP-1 induction is not mediated by PKC, ERK, or p38 MAPK

Protein kinase C (PKC) and the MAP kinases ERK, p38, and JNK have been communicated to mediate the induction of MKP-1 after diverse stimuli. Since we intended to investigate which kinase is involved in the ANP-induced upregulation of MKP-1, we treated HUVEC with well-established pharmacological inhibitors of these kinases. The inhibitors calphostin C for PKC (figure 38A),

PD98059 for the ERK pathway (figure 38B), and SB203580 for p38 MAPK (figure 38C) did not affect ANP-induced MKP-1 protein expression, suggesting that PKC, ERK, and p38 MAPK do not mediate the induction of MKP-1 by ANP.

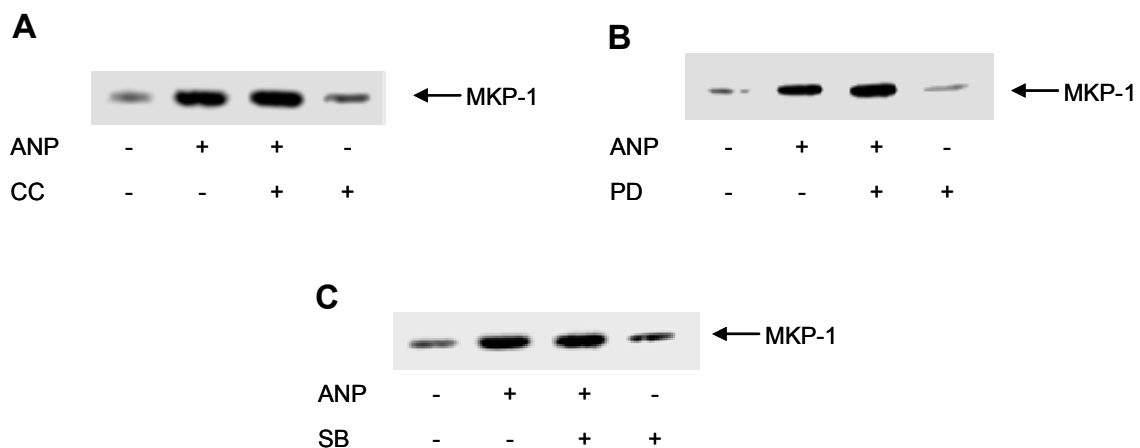


**Figure 38:** MKP-1 induction by ANP is not mediated by PKC, ERK, or p38 MAPK. HUVEC were either left untreated or were pre-treated with (A) the protein kinase C (PKC) inhibitor calphostin C (CC, 100 nM, 60 min), (B) the ERK pathway inhibitor PD98059 (PD, 10  $\mu$ M, 60 min), or (C) the p38 MAPK inhibitor SB203580 (SB, 5  $\mu$ M, 60 min). ANP was added to the cells for 60 min. MKP-1 protein expression was determined by Western blot analysis as described in section 2.3.3.

### 3.1.7 Role of JNK and AP-1

#### 3.1.7.1 JNK mediates the induction of MKP-1 by ANP

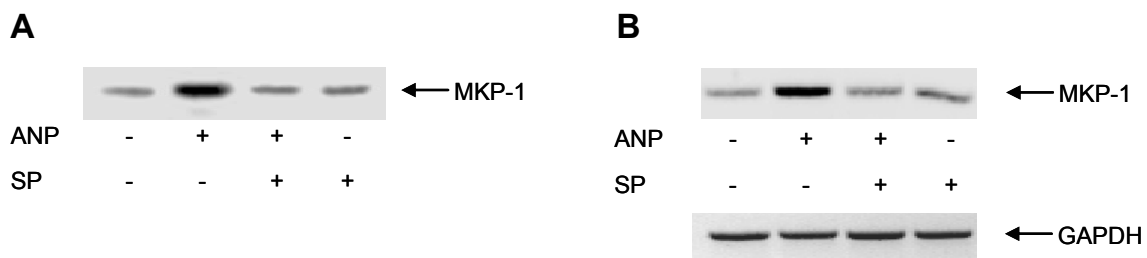


**Figure 39:** JNK mediated the induction of MKP-1 by ANP. **A:** HUVEC were either left untreated or were pre-treated with the JNK inhibitor SP600125 (SP, 10  $\mu$ M, 60 min). ANP was added to the cells for 60 min. MKP-1 protein expression was determined by Western blot analysis as described in section 2.3.3. **B:** HUVEC were either left untreated or were pre-treated with SP (10  $\mu$ M, 60 min). ANP was added for 30 min. MKP-1 and GAPDH mRNA expression was determined by RT-PCR and subsequent agarose gel electrophoresis as described in section 2.4.

The JNK inhibitor SP600125 abolished the ANP-induced expression of both MKP-1 protein (figure 39A) and mRNA expression (figure 39B) in HUVEC, suggesting a crucial involvement of JNK in the upregulation of MKP-1 by ANP.

### 3.1.7.2 ANP rapidly activates JNK

Since we found that JNK (p46/p54) is crucial for the induction of MKP-1 by ANP, the question arose whether ANP is in fact able to activate JNK. We revealed that ANP rapidly increases the activated form of JNK (phospho-p46/p54) with a maximum at about 5 min (figure 40, upper panel).

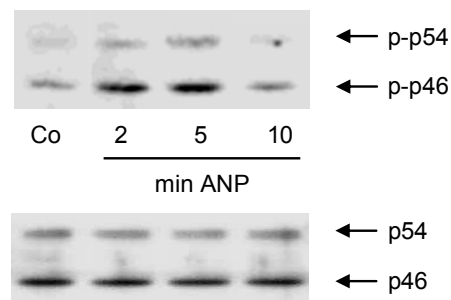


**Figure 40:** ANP rapidly activates JNK. HUVEC were either left untreated (Co) or were treated with ANP (1  $\mu$ M) for the indicated times. The amount of phospho-JNK (p-p46/54, upper panel) and total JNK (p46/54, lower panel, showing uniformity of total JNK content) was determined by Western blot analysis as described in section 2.3.3.

### 3.1.7.3 Superoxide is involved in the activation of JNK by ANP

Since we found that ANP induces the intracellular formation of superoxide, we investigated the role of superoxide in the activation of JNK by ANP. HUVEC were treated with the superoxide scavengers tiron and PEG-SOD. Figure 41 shows that both tiron (figure 41A) and PEG-SOD (figure 41B) decreased ANP-induced JNK phosphorylation. This indicates that superoxide is crucial for the activation of JNK by ANP.

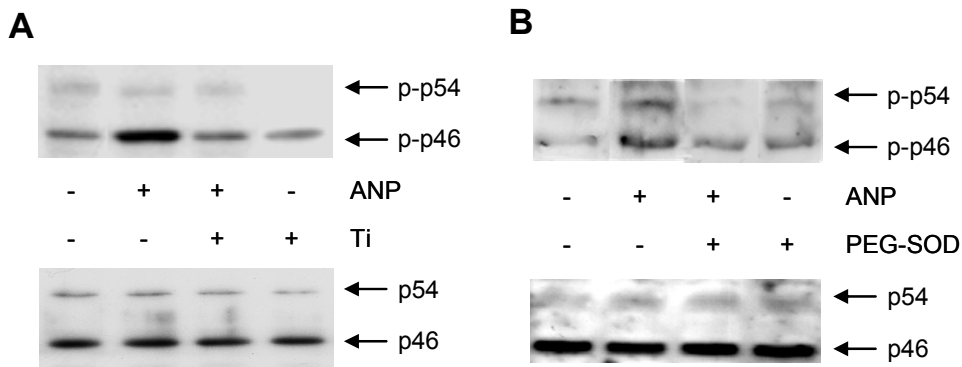


**Figure 41:** Superoxide is involved in the activation of JNK by ANP. HUVEC were either left untreated or were pre-treated with the superoxide scavengers **(A)** tiron (Ti, 10 mM, 60 min) or **(B)** PEG-SOD (300 U/ml, 60 min). ANP (1  $\mu$ M) was added to the cells for 5 min. The amount of phospho-JNK (upper panels) and total JNK (lower panels, showing uniformity of total JNK content) was determined by Western blot analysis as described in section 2.3.3.

#### 3.1.7.4 ANP activates AP-1 via JNK

The transcription factor activator protein-1 (AP-1) is an important target of JNK. Therefore, we assessed DNA-binding of AP-1 after treatment of HUVEC with ANP and the JNK inhibitor SP600125. The inhibition of JNK completely blocked the ANP-induced activity of AP-1 (figure 42).

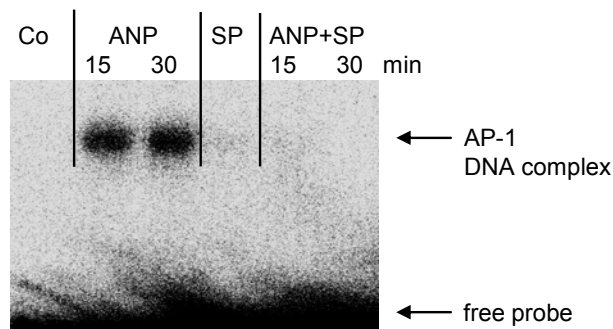


**Figure 42:** ANP activates AP-1 via JNK. HUVEC were either left untreated (Co) or were pre-treated with the JNK inhibitor SP600125 (10  $\mu$ M, 60 min). ANP (1  $\mu$ M) was added to the cells for the indicated times. AP-1 DNA-binding activity was determined by electrophoretic mobility shift assay (EMSA) as described in section 2.7.

#### 3.1.7.5 AP-1 is crucially involved in the upregulation of MKP-1 by ANP

To causally link AP-1 to the induction of MKP-1, we used a well-established AP-1 decoy approach. The functionality of this approach, i.e. ability of the decoys to inhibit the activation of AP-1 by ANP, is demonstrated in figure 43.



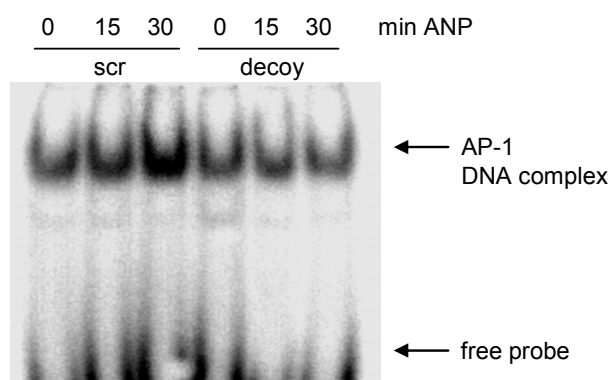


**Figure 43:** Prove of functionality of the used AP-1 decoy. HUVEC were transfected with AP-1 decoy or scrambled decoy (scr) as described in section 2.8.3. Cells were treated with ANP (1  $\mu$ M) for the indicated times. DNA-binding activity of AP-1 was determined by electrophoretic mobility shift assay (EMSA) as described in section 2.7.

HUVEC were transfected with the AP-1 decoy and treated with ANP. The decoy completely abrogated the increase of MKP-1 expression by ANP (figure 44), suggesting that AP-1 is crucial for the ANP-induced upregulation of MKP-1.

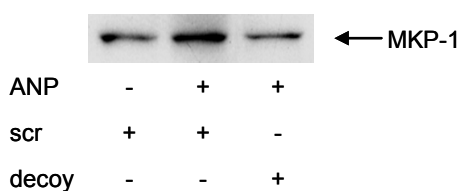


**Figure 44:** AP-1 is crucially involved in the upregulation of MKP-1 by ANP. HUVEC were transfected with AP-1 decoy or scrambled decoy (scr) as described in section 2.8.3. Cells were treated with ANP (1  $\mu$ M) for 60 min. MKP-1 protein expression was determined by Western blot analysis as described in section 2.3.3.

### 3.1.8 ROS generation in intact blood vessels

We aimed to clarify whether the ANP-induced ROS generation measured in cultured endothelial cells is also relevant *in vivo*, i.e. in intact blood vessels. Therefore, we loaded rat lung endothelial cells in isolated perfused organs with an ROS-sensitive fluorescent dye. Intracellular ROS generation was measured by *in situ* fluorescence microscopy. Resting endothelial cells showed no alteration of dye fluorescence over 2 h (figure 45A), but ANP-treatment increased endothelial ROS formation (figure 45B). This increase was abolished by addition of the Nox inhibitor DPI (figure 45C, figure 46).

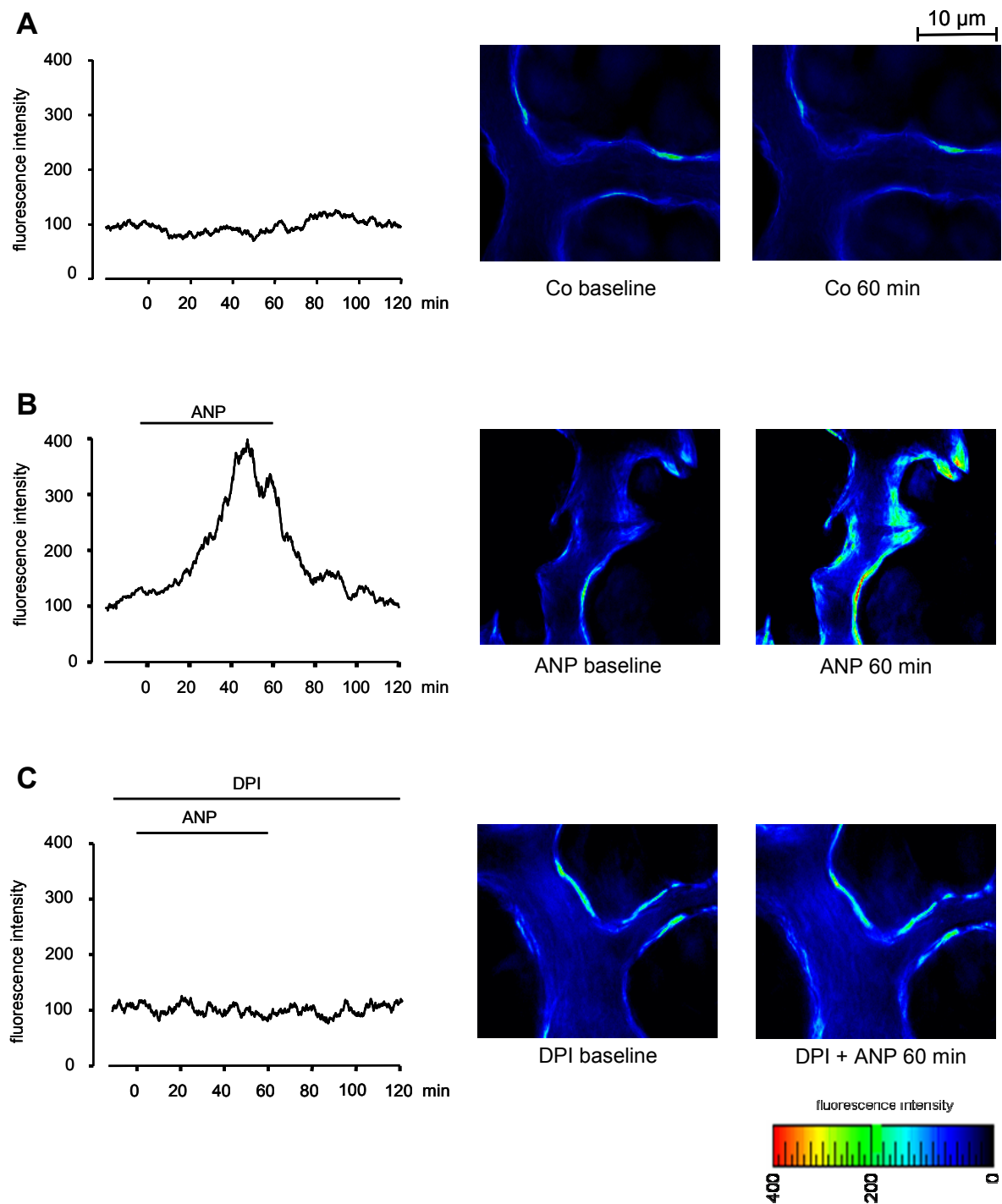


**Figure 45:** ROS generation in the endothelium of intact blood vessels. Baseline fluorescence is shown in each panel. **A:** Regular HEPES buffer was continuously infused over 120 min. **B:** ANP ( $1 \mu\text{M}$ ) was infused for 60 min, followed by 60 min of buffer perfusion. **C:** Vessels were pre-treated with the Nox inhibitor diphenyleneiodonium (DPI,  $20 \mu\text{M}$ ) for 20 min, followed by 60 min ANP and 60 min buffer perfusion. One representative graph and image out of 5 independent experiments is shown. ROS generation in the endothelium of isolated-perfused rat lungs was determined as described in section 2.6.

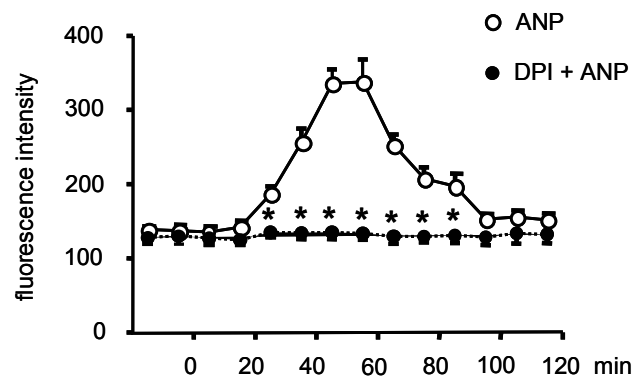


**Figure 46:** ROS generation in the endothelium of intact blood vessels. Data of ANP-treated versus ANP- and DPI-treated cells of all 5 experiments are shown as means  $\pm$  SEM. \*  $P \leq 0.05$  vs. data from lungs treated with ANP alone. ROS generation in the endothelium of isolated-perfused rat lung vessels was determined as described in section 2.6.

Moreover, we aimed to check whether ANP is able to increase MKP-1 not only in cultured endothelial cells, but also in the rat lung. Importantly, as shown in figure 47, ANP induces MKP-1 protein expression also *in vivo*.

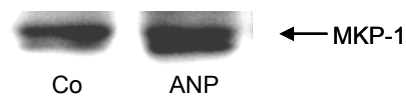


**Figure 47:** ANP induces MKP-1 in the endothelium of intact blood vessels. Rats were anesthetized and a NaCl-solution (Co) or ANP (approx. 1  $\mu$ M plasma concentration) was parenterally applied. After 1 h, lungs were excised. Rat lung lysates were investigated for MKP-1 protein expression by Western blot analysis as described in section 2.3.2.

## 3.2 Dexamethasone and MKP-1

### 3.2.1 Dex reduces TNF- $\alpha$ -induced E-selectin expression

Dex is known to reduce TNF- $\alpha$ -induced E-selectin expression in endothelial cells. We aimed to confirm this fact in our cell system. Pre-treating HUVEC with Dex concentration-dependently reduced the expression of E-selectin (figure 48). Importantly, we found that even low concentrations of Dex (1-100 nM) lead to a highly significant reduction of E-selectin expression.

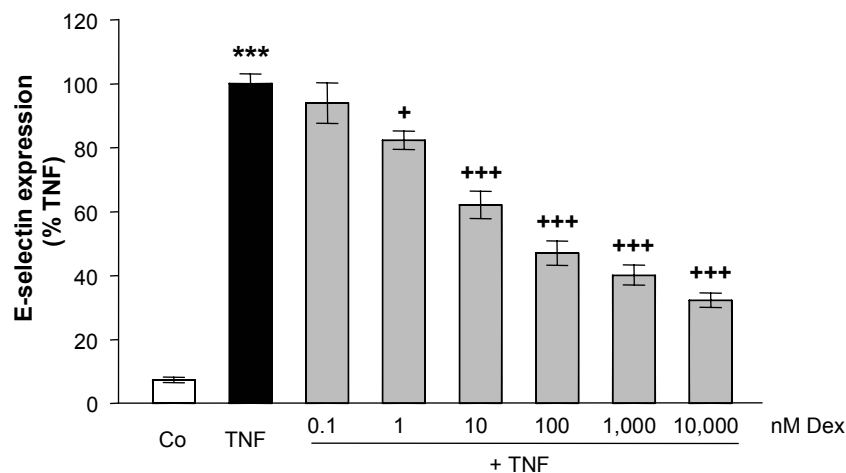


**Figure 48:** Dex reduces TNF- $\alpha$ -induced E-selectin expression. HUVEC were either left untreated (Co) or were pre-treated with dexamethasone (Dex, 60 min, concentrations as indicated). Where indicated, cells were treated with TNF- $\alpha$  (10 ng/ml) for 4 h. E-selectin expression was analyzed by flow cytometry as described in section 2.11. \*\*\*  $P \leq 0.001$  vs. Co. +  $P \leq 0.05$  vs. TNF. \*\*\*  $P \leq 0.001$  vs. TNF.

### 3.2.2 Dex at low concentrations does not influence NF- $\kappa$ B

The transcription factor NF- $\kappa$ B is thought to play a key role in the upregulation of E-selectin upon TNF- $\alpha$  treatment and Dex is known to inhibit NF- $\kappa$ B. Interestingly, we found that in our system TNF- $\alpha$ -activated NF- $\kappa$ B is not influenced by Dex at low concentrations. Figure 49 shows that Dex neither alters the TNF- $\alpha$ -induced increase of NF- $\kappa$ B DNA-binding activity (figure 49B) nor the TNF- $\alpha$ -induced p65 translocation (figure 49A). To ensure the functionality of our EMSA system, we used the well-

established NF- $\kappa$ B inhibitors pyrrolidine dithiocarbamate (PDTC) and parthenolide. Both were able to abolish the TNF- $\alpha$ -induced NF- $\kappa$ B DNA-binding activity.

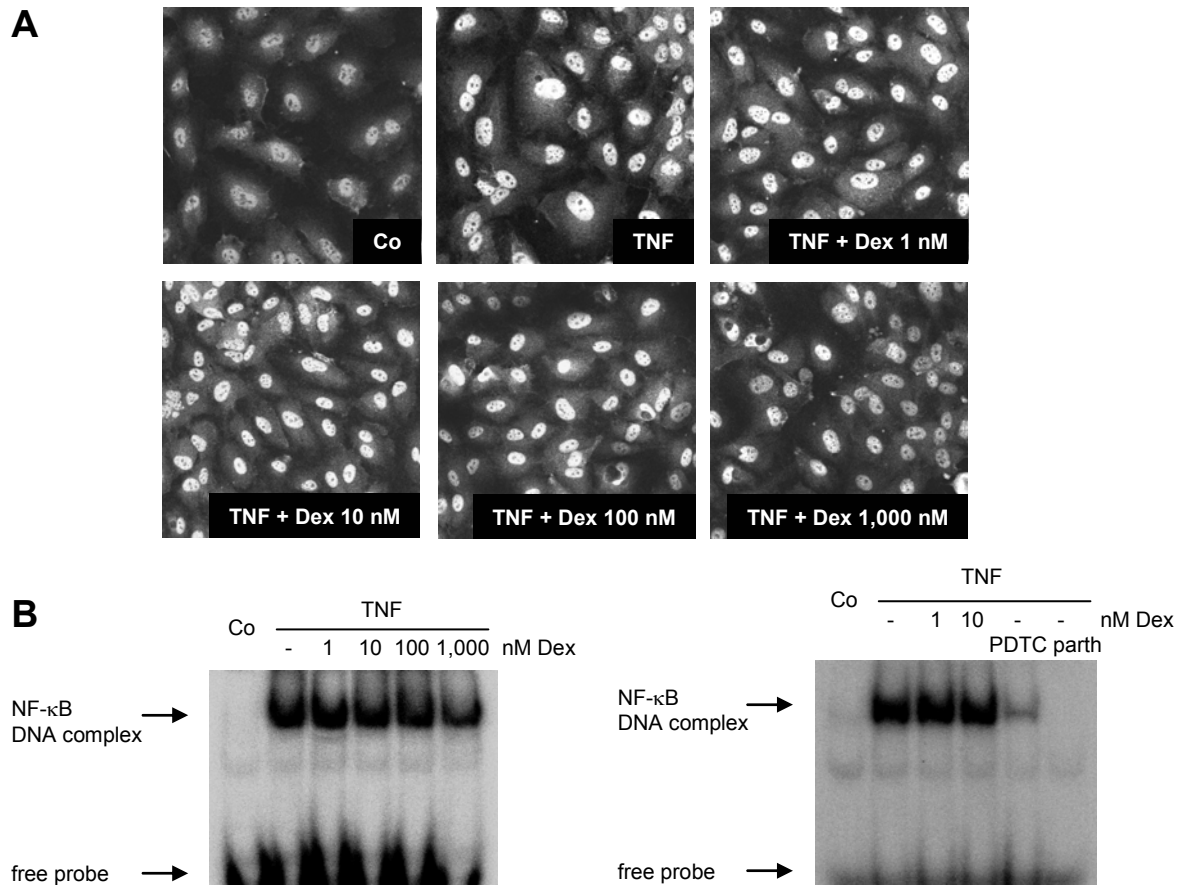


**Figure 49:** Dex at low concentrations does not influence NF- $\kappa$ B. **A:** HUVEC were left untreated (Co) or were pre-treated with Dex for 60 min (concentrations as indicated). TNF- $\alpha$  (10 ng/ml) was added for 60 min. Immunocytochemistry and confocal microscopy were performed as described in section 2.10. **B:** HUVEC were left untreated (Co) or were pre-treated with Dex for 60 min (concentrations as indicated). The NF- $\kappa$ B inhibitors PDTC (50  $\mu$ M, 60 min) and parthenolide (parth, 5  $\mu$ M, 60 min) served as positive control. TNF- $\alpha$  (10 ng/ml) was added for 60 min. NF- $\kappa$ B DNA-binding activity was judged by electrophoretic mobility shift assay (EMSA) as described in section 2.7.

### 3.2.3 p38 MAPK is involved in TNF- $\alpha$ -induced E-selectin expression

Since we revealed that Dex at low concentrations does not influence NF- $\kappa$ B, we checked whether p38 MAPK could be involved in the inhibitory action on E-selectin. Inhibition of p38 MAPK by a pharmacological inhibitor (SB203580) resulted in a strong decrease of TNF- $\alpha$ -evoked E-selectin expression (figure 50) pointing to a crucial involvement of p38 MAPK in E-selectin expression induced by TNF- $\alpha$ .

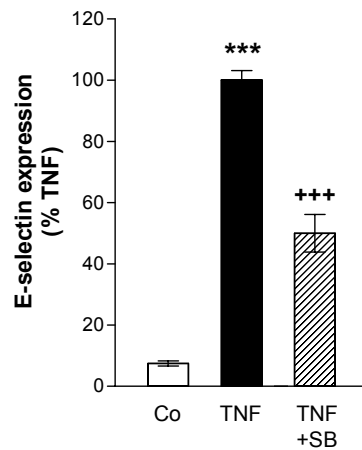


**Figure 50:** p38 MAPK is involved in E-selectin expression induced by TNF- $\alpha$ . HUVEC were either left untreated (Co) or were pre-treated with SB203580 (SB, 10  $\mu$ M, 60 min). TNF- $\alpha$  (10 ng/ml) was added for 4 h. E-selectin expression was analyzed by flow cytometry as described in section 2.11. \*\*\*  $P \leq 0.001$  vs. Co. +++  $P \leq 0.001$  vs. TNF.

### 3.2.4 Influence of Dex on TNF- $\alpha$ -activated p38 MAPK

Since we could show that p38 MAPK is crucially involved in TNF- $\alpha$ -induced E-selectin expression, we wanted to clarify whether p38 MAPK activity is influenced by Dex at a low concentration (1 nM). First, we performed a TNF- $\alpha$  time course and found a very rapid (within 5 min) and transient activation of p38 MAPK (figure 51).

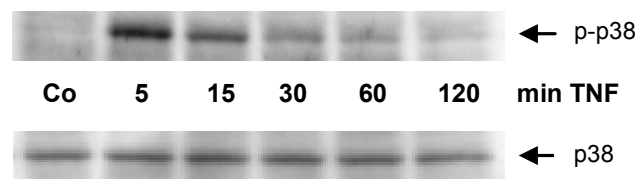


**Figure 51:** TNF- $\alpha$  time-dependently activates p38 MAPK. HUVEC were either left untreated (Co) or were treated with TNF- $\alpha$  (10 ng/ml) for the indicated times. Amounts of phospho-p38 MAPK (p-p38) and p38 MAPK were judged by Western blot analysis as described in section 2.3.3.

We then checked whether pre-incubation of HUVEC with Dex (1 nM) alters the activation status of p38 MAPK and revealed that Dex abrogates the activation of p38 MAPK by TNF- $\alpha$  (figure 52).

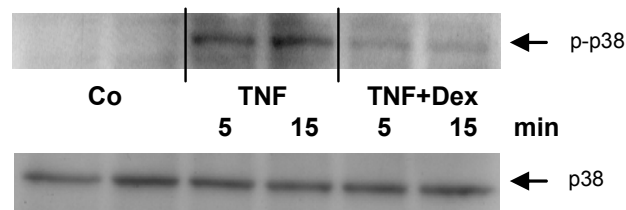


**Figure 52:** Dex abrogates TNF- $\alpha$ -induced p38 MAPK activation. HUVEC were either left untreated (Co) or were pre-treated with Dex (60 min, 1 nM). TNF- $\alpha$  (10 ng/ml) was added for the indicated times. Amounts of phospho-p38 MAPK (p-p38) and p38 MAPK were judged by Western blot analysis as described in section 2.3.3.

### 3.2.5 Vanadate abrogates the influence of Dex on p38 MAPK

We wanted to clarify the underlying mechanism of p38 MAPK deactivation. We assumed an involvement of phosphatases, which could be activated or induced by Dex. Therefore, we treated HUVEC with sodium orthovanadate, a known inhibitor of protein tyrosine phosphatases. As shown in figure 53, we found that sodium orthovanadate strongly diminished the influence of Dex on TNF- $\alpha$ -induced p38 MAPK activation. These results suggested that protein tyrosine phosphatases are involved in the deactivation of p38 MAPK by Dex.

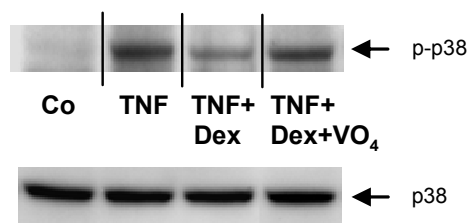


**Figure 53:** Vanadate abrogates the influence of Dex on p38 MAPK activation induced by TNF- $\alpha$ . HUVEC were either left untreated (Co) or were pre-treated with the protein tyrosine phosphatase inhibitor sodium orthovanadate (VO<sub>4</sub>, 100  $\mu$ M, 30 min). Cells were treated with Dex (1 nM) for 60 min. TNF- $\alpha$  (10 ng/ml) was added for 15 min. Amounts of phospho-p38 MAPK (p-p38) and p38 MAPK were judged by Western blot analysis as described in section 2.3.3.

### 3.2.6 MKP-1 induction by Dex

Since tyrosine phosphatases seem to be involved in the deactivation of p38 MAPK by Dex, we checked whether MKP-1 is upregulated by Dex. In fact, treatment of HUVEC with different Dex concentrations lead to an increased expression of MKP-1 protein (figure 54A). A maximal MKP-1

induction occurred at 1 nM Dex. The upregulation was found to be time-dependent with a maximum at 60 min (figure 54B).

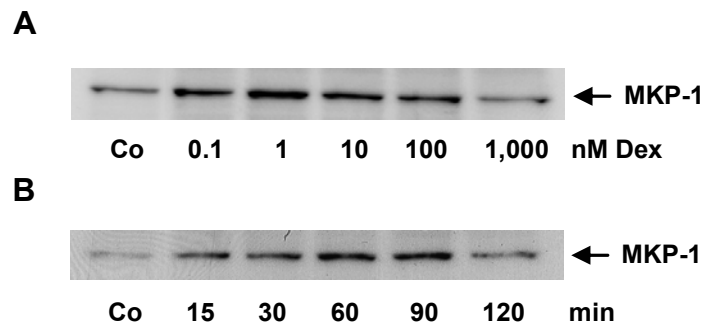


**Figure 54:** Dex induces MKP-1 in endothelial cells. **A:** HUVEC were either left untreated (Co) or were treated with Dex (60 min) at the indicated concentrations. **B:** HUVEC were either left untreated (Co) or were treated with Dex (1 nM) for the indicated times. MKP-1 protein expression was determined by Western blot analysis as described in section 2.3.3.

### 3.2.7 Dex induces MKP-1 *via* glucocorticoid receptor

We wanted to investigate whether the observed upregulation of MKP-1 depends on the activation of the glucocorticoid receptor (GR). Therefore, we used the well-established GR antagonist RU486/mifepristone. Figure 55 shows that RU486 completely blocks the induction of MKP-1 protein by Dex pointing to a crucial involvement of the glucocorticoid receptor.

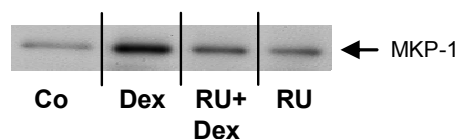


**Figure 55:** Dex induces MKP-1 *via* the glucocorticoid receptor. HUVEC were either left untreated (Co) or were pre-treated with the glucocorticoid receptor antagonist RU486/mifepristone (RU, 10 nM, 15 min). Dex (1 nM) was added for 60 min. MKP-1 protein expression was determined by Western blot analysis as described in section 2.3.3.

### 3.2.8 MKP-1 antisense restores p38 MAPK activation

We aimed to clarify whether MKP-1 in fact plays a causal role in the reduction of TNF- $\alpha$ -induced p38 MAPK activation. Therefore, we used an MKP-1 antisense approach. First, we checked the



functionality of the MKP-1 antisense oligonucleotides. As shown in figure 56, transfection of HUVEC with MKP-1 antisense but not sense strongly diminished the Dex-induced increase of MKP-1 protein.

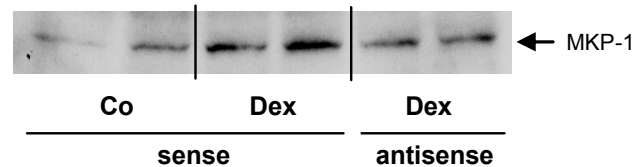


**Figure 56:** Functionality of MKP-1 antisense oligonucleotides. HUVEC were either left untreated (Co) or were treated with Dex (1 nM) for 60 min in the presence of MKP-1 sense or antisense oligonucleotides (4 h). The transfection with the oligonucleotides was performed as described in section 2.8.2. MKP-1 protein expression was determined by Western blot analysis as described in section 2.3.3.

After confirming the functionality of our antisense approach, we treated HUVEC with Dex and TNF- $\alpha$  in the presence of MKP-1 antisense and found that the capability of Dex to diminish the TNF- $\alpha$ -induced activation of p38 MAPK was completely reversed (figure 57). This result shows that MKP-1 is crucially involved in the deactivation of p38 MAPK by Dex.

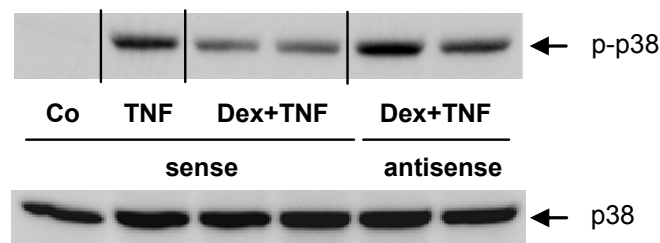


**Figure 57:** MKP-1 antisense reverses the ability of Dex to diminish the TNF- $\alpha$ -induced p38 MAPK activation. HUVEC were either left untreated (Co) or were pre-treated with Dex (1 nM) for 60 min in the presence of MKP-1 sense or antisense oligonucleotides (4 h). TNF- $\alpha$  (10 ng/ml) was added for 15 min. The transfection with the oligonucleotides was performed as described in section 2.8.2. Amounts of phospho-p38 MAPK (p-p38) and p38 MAPK were judged by Western blot analysis as described in section 2.3.3.

### 3.2.9 MKP-1 antisense restores E-selectin expression

Furthermore, we wanted to causally relate the Dex-induced increase of MKP-1 to the reduction of TNF- $\alpha$ -induced E-selectin expression. We again used MKP-1 antisense oligonucleotides and found that the reduction of E-selectin expression by Dex was significantly reversed in the presence of MKP-1 antisense oligonucleotides (figure 58), pointing to a crucial involvement of MKP-1 in the pathway by which Dex diminishes TNF- $\alpha$ -induced E-selectin expression.

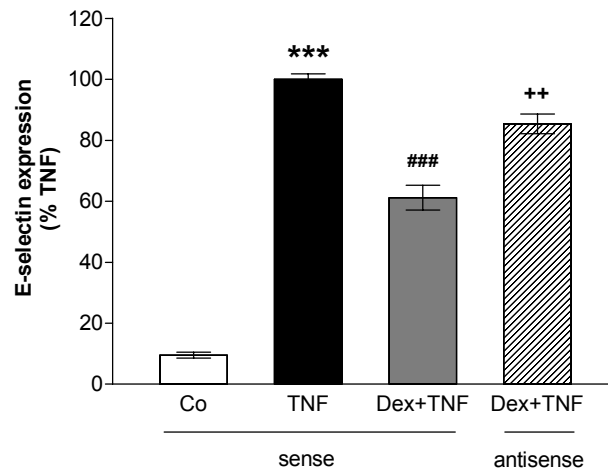


**Figure 58:** MKP-1 antisense restores E-selectin expression. HUVEC were either left untreated (Co) or were pre-treated with Dex (1 nM) for 60 min in the presence of MKP-1 sense or antisense oligonucleotides (4 h). TNF- $\alpha$  (10 ng/ml) was added for 4 h. The transfection with the oligonucleotides was performed as described in section 2.8.2. E-selectin expression was analyzed by flow cytometry as described in section 2.11. \*\*\*  $P \leq 0.001$  vs. Co (sense). \*\*  $P \leq 0.01$  vs. Dex+TNF (sense). ###  $P \leq 0.001$  vs. TNF (sense).

## **4 Discussion**



## 4.1 ANP and MKP-1

### 4.1.1 Beneficial actions of MKP-1

In the recent years the MAPK phosphatase MKP-1 emerged as an important mediator of beneficial actions in cardiovascular and renal diseases. These properties were demonstrated in diverse cell culture and *in vivo* models:

(i) MKP-1 seems to play an important role in the proliferation of vascular smooth muscle cells (VSMCs). The uncontrolled growth of VSMCs is commonly regarded as a key event in the pathogenesis of different vascular disorders, such as atherosclerosis. Li *et al.* revealed that overexpression of MKP-1 in VSMCs leads to an inhibition of DNA-synthesis, i.e. an attenuated VSMC proliferation.<sup>90</sup> Jacob *et al.* showed that the inhibiting effect of insulin on platelet-derived growth factor (PDGF)-evoked VSMC migration is mediated *via* NO/cGMP-induced MKP-1.<sup>91</sup> A defective induction of MKP-1 in spontaneous hypertensive rats was found to promote the proliferation and hypertrophy of VSMCs.<sup>92</sup> Moreover, a disturbed MKP-1 expression in these rats was revealed to be due to defects of the NO/cGMP signaling pathway.<sup>93</sup> In diabetic rats, an enhanced VSMC migration was shown to be crucially related to a failure of insulin-stimulated MKP-1 expression.<sup>94</sup>

(ii) The induction of MKP-1 protects against cardiac dysfunctions. Cardiomyocyte hypertrophy, i.e. an increased ventricular mass, is a risk factor for cardiac morbidity and mortality. The ANP-induced inhibition of cardiomyocyte hypertrophy evoked by angiotensin II or endothelin-1 was found to be mediated *via* an increased MKP-1 expression.<sup>95</sup> Moreover, a recent study communicated that mice overexpressing MKP-1 are protected against cardiac ischemia-reperfusion injury, while MKP-1 gene-targeted mice showed greater injury.<sup>96</sup>

(iii) MKP-1 has been reported to mediate cytoprotective effects in renal cells. Tubular hypertrophy is an early morphological feature of chronic renal diseases. In this context, ANP was shown to reduce

angiotensin II-evoked hypertrophy of renal tubular cells *via* an induction of MKP-1.<sup>27</sup> In mechanical strain-activated glomerular mesangial cells, an increased MKP-1 induction by estradiol was found to reduce the activity of MAPKs. MKP-1 induction by estradiol was assumed to be the cause for the protective effect of female gender on renal disease progression.<sup>97</sup>

Taken together, these data clearly point to a pivotal role for MKP-1 in different signaling pathways transducing anti-atherogenic and cytoprotective actions.

#### 4.1.2 ANP induces MKP-1

In accordance with the above described cytoprotective potential of MKP-1, we have recently found that ANP exerts its beneficial actions on TNF- $\alpha$ -activated endothelial cells *via* an induction of MKP-1.<sup>14,15</sup> Therefore, it seemed of special interest to clarify the underlying signaling pathway leading to an upregulation of MKP-1 by ANP since mechanisms involved in MKP-1 induction by ANP in endothelial cells have as yet been completely unknown. As previously shown by ourselves,<sup>14</sup> a rapid expression of MKP-1 occurs upon treatment of HUVEC with ANP. MKP-1 is an immediate early gene product and therefore well known to be rapidly expressed (for review see<sup>98</sup>). ANP has as yet been described to induce MKP-1 in the tubular<sup>27</sup> and glomerular mesangial cells<sup>99</sup>, and in cardiomyocytes<sup>95</sup>.

The induction of MKP-1 in HUVEC was found to depend on the NPR-A/cGMP-pathway, whereas an involvement of NPR-C was excluded. Supporting this result, a cGMP-dependent MKP-1 upregulation was described in VSMC<sup>91,93</sup> and renal cells.<sup>27,99</sup> Data regarding the mechanism of cGMP-mediated MKP-1 induction, however, have as yet been lacking.

Blockade of protein biosynthesis did not inhibit the early increase of MKP-1 at 15 min, suggesting that other effects than an increase of MKP-1 protein *de novo* synthesis are responsible for this early induction. MKP-1 is known to be rapidly degraded by the ubiquitin/proteasome-pathway.<sup>25</sup> It might be speculated that ANP interferes with MKP-1 catabolism accounting for the early increase of MKP-1.

The augmented MKP-1 protein levels at later time points, however, definitely represent newly synthesized protein.

Treatment of HUVEC with ANP leads to an increase of intracellular cGMP *via* activation of NPR-A (data not shown). Since we have shown that MKP-1 induction by ANP is mediated by the NPR-A/cGMP-pathway, we aimed to elucidate an involvement of protein kinase G I (PKG I), an important cGMP effector system. Controversial data exist regarding the presence of PKG I in endothelial cells. MacMillan-Crow et al. were the first who described the presence of PKG I in primary bovine endothelial cells.<sup>100</sup> By using inhibitors and activators of PKG I, two groups found an involvement of PKG I in the ANP-induced proliferation of HUVEC.<sup>101,102</sup> In contrast, the group of van Hinsbergh showed that PKG I is absent in endothelial cells derived from umbilical veins.<sup>103</sup> Our data confirm the latter: PKG I is not expressed in HUVEC and, therefore, not involved as an cGMP effector system. Consistently, our group also observed that the cGMP-mediated induction of heme oxygenase-1 by ANP in HUVEC was not influenced by an inhibitor of PKG I<sup>104</sup>. The controversy about an involvement of PKG I in cGMP-mediated signaling pathways might be explained by the findings that the expression of PKG in endothelial cells might depend on their origin and that PKG I might be down-regulated during cell culture passaging.<sup>105</sup> However, we have found that PKG I is not even expressed in primary HUVECs.

#### 4.1.3 Generation of ROS by ANP

Exogenously supplied hydrogen peroxide (H<sub>2</sub>O<sub>2</sub>) led to augmented endothelial MKP-1 protein levels. This is in line with two studies showing that H<sub>2</sub>O<sub>2</sub> is able to upregulate MKP-1 expression in epithelial<sup>28</sup> and smooth muscle cells.<sup>106</sup> This potency of exogenous ROS to induce MKP raised the question whether ANP possesses the ability to increase endothelial ROS generation. ANP has been shown to induce the production of ROS in macrophages<sup>107</sup> and in renal cells,<sup>27</sup> but nothing has as yet been reported about its potency to induce ROS in the endothelium. We for the first time provide evidence that ANP concentration-dependently augments the formation of ROS. In analogy to the induction of MKP-1, this increase was shown to be mediated *via* NPR-A/cGMP, which is in consistence with a

recent study reporting that cGMP is able to induce ROS in cardiomyocytes.<sup>108</sup> Importantly, we could establish a causal link between ROS generation in EC and MKP-1 induction by using several antioxidants.

It seemed of special interest to clarify whether these results obtained from cell culture experiments could be confirmed *in vivo*, i.e. by *in situ* measurement of ROS in the endothelium of lung vessels. In fact, we provide clear evidence that ANP induces endothelial ROS generation in intact vessels. Similar to our cell culture model, we confirmed that ANP induces MKP-1 also in the isolated perfused rat lung. This strongly suggests an *in vivo* relevance of our findings obtained from cultured endothelial cells.

Reactive oxidants in the pulmonary vascular wall are mainly mentioned in the context of pathophysiological events,<sup>109</sup> but also appear as signaling molecules.<sup>48</sup> Studies concerning a connection between ANP and ROS formation in the lung are as yet not available. ANP has been shown to reduce a TNF- $\alpha$ -evoked increase of endothelial permeability<sup>14</sup> and ANP-induced pulmonary ROS generation was found to be connected to ANP's ability to counteract a thrombin- and oxidant-induced increase in permeability of pulmonary endothelial cells.<sup>110,111</sup> Therefore, it might be speculated that an ANP-evoked ROS augmentation in pulmonary ECs could contribute to ANP's protective effect. This important issue needs to be examined in detail in future studies.

Summarizing, we have shown that ANP enhances ROS production in endothelial cells both in cell culture as well as in intact blood vessels. ROS emerged as a critical signaling step in ANP-induced MKP-1 induction.

#### **4.1.4 Involvement of NAD(P)H oxidase**

A great variety of sources involved in endothelial ROS generation exists including the mitochondrial respiratory chain, and peroxisomal, cytosolic, and membrane-bound oxidases.<sup>48</sup> In the recent years the superoxide-producing NAD(P)H oxidase (Nox) enzyme complex has emerged as the major source



of ROS in the endothelium.<sup>57</sup> Importantly, we identified Nox as the crucial ANP-induced ROS source responsible for MKP-1 induction by using different inhibitors.

Experiments with catalase and superoxide dismutase (SOD) corroborated that superoxide, but not H<sub>2</sub>O<sub>2</sub>, is the crucially involved oxidant species mediating the effects of ANP. SOD converts superoxide to H<sub>2</sub>O<sub>2</sub>. Interestingly, we did not observe an augmented MKP-1 induction upon ANP/SOD-treatment, although exogenously supplied H<sub>2</sub>O<sub>2</sub> leads to an upregulation of MKP-1. This might be due to the fact that endothelial Nox produces only low amounts of superoxide, which may consequently lead to SOD-converted H<sub>2</sub>O<sub>2</sub> levels unable to increase MKP-1 expression. In contrast, the exogenously supplied amounts of hydrogen peroxide are incomparably higher.

The phagocyte-type NAD(P)H oxidase contains a transmembrane electron transport chain. Oxygen is reduced to superoxide in the extracellular space or in phagocytic vacuoles.<sup>112</sup> However, neither the precise structure nor the exact localization of functionally active endothelial NAD(P)H oxidase have as yet been clarified. The question arises whether endothelial Nox releases superoxide intra- or extracellularly. Our data suggest an intracellular superoxide release, since the cell-permeable PEG-SOD completely blocked the fluorescence signal, whereas SOD present only extracellularly did not alter the signal.

In order to clarify which Nox isoform is responsible for superoxide generation, we characterized the Nox homologue spectrum expressed in HUVEC and HMEC and found Nox2 and Nox4 mRNA and protein to be present. Ago *et al.* communicated similar findings for HUVEC and rat aortic endothelial cells,<sup>62</sup> but they also described an extremely low expression of Nox1, which we could not confirm and which might be due to different cell culture conditions and experimental settings. We used a well-established Nox2/4 antisense approach<sup>62,113</sup> and found that only Nox2 is responsible for the ANP-induced superoxide generation and subsequent MKP-1 induction. Interestingly, the two Nox inhibitors DPI and gp91ds-*tat* both reduced superoxide production below control levels. This suggests a constitutive production of superoxide in resting cells. DPI is known to inhibit several other ROS sources (flavin-containing enzymes), which could in part account for basal ROS/superoxide

production. The fact that the inhibitor peptide gp91ds-*tat* targets both Nox2 and Nox4 suggests that Nox4 might be a constitutively active Nox isoform responsible for basal levels of superoxide formation, since Nox2 but not Nox4 antisense reverses the effect of ANP. In summary, we found that ANP-induced superoxide generation and MKP-1 expression are mediated *via* a Nox2-containing NAD(P)H oxidase.

#### 4.1.5 The role of Rac1

Rac1, a well-known activating component of the phagocyte-type NAD(P)H oxidase, was revealed to be rapidly activated by ANP. The precise role of Rac1 in endothelial Nox assembly and activation is as yet not completely understood and only few studies suggest a role for Rac1 in Nox-derived endothelial ROS generation.<sup>114-116</sup> Therefore, it might be of special interest that our results show for the first time that Rac1 plays a pivotal role both in the generation of superoxide as well as in the upregulation of MKP-1. We observed that Rac1 translocates to the plasma membrane, which represents another indicator for its activation.<sup>65</sup> Whether endothelial Nox assembles at the membrane, as it does in phagocytes, as well as the question about the direction of superoxide release (cytosolic vs. extracellular), however, remains to be clarified.

A number of studies report that an activation of Rac1 and a subsequent superoxide formation is connected to different pro-inflammatory effects in the endothelium. For instance, Rac1 and superoxide were shown to regulate the expression of different endothelial cellular adhesion molecules (CAMs).<sup>117</sup> Besides the upregulation of CAMs as a typical marker of endothelial cell activation, also the expression and release of monocyte chemoattractant protein-1 (MCP-1) has recently been revealed to be mediated *via* Rac1 and superoxide.<sup>118</sup> In this context, it is worth mentioning that in our system the activation of Rac1 by ANP exerts cytoprotective effects due to the upregulation of MKP-1. Our findings are supported by a study showing that Rac1-dependent generation of ROS leads to a protection of HUVEC against TNF- $\alpha$ -induced cell death.<sup>119</sup> It seems that Rac1 possesses the ability to participate in divergent signaling pathways mediating either pro- or anti-inflammatory effects. Further studies are required to investigate the mechanistic basis for this variable role of Rac1 in different settings.

#### 4.1.6 Involvement of the JNK/AP-1 pathway

The downstream signaling of MKP-1, i.e. the control of MAPK activity, is quite well investigated compared to the upstream pathways leading to an induction of MKP-1. Referring to the latter, we aimed to elucidate the role of different protein kinases, which could potentially be involved in the induction of MKP-1 (PKC, ERK, JNK, and p38 MAPK).<sup>29-32</sup> The data from the literature suggest that the signaling pathway responsible for an induction of MKP-1 highly depends on both the used stimulus and the cell-type. By using well-established pharmacological inhibitors, we could causally link JNK to the ANP-induced expression of MKP-1 in HUVEC. A role for PKC, ERK, and p38 MAPK was excluded. Accordingly, we investigated the influence of ANP on JNK activation and found a rapid and transient activation of JNK with a maximum at about 5 min. ANP is also known to induce JNK activity at later time points, suggesting a biphasic process evoked by ANP.<sup>104</sup> Since ANP induces MKP-1 protein biosynthesis within 30 min, the very rapid JNK activation by ANP supports the crucial role for JNK in MKP-1 induction. Taken together, we revealed for the first time that ANP-induced MKP-1 protein expression in the endothelium is mediated *via* JNK, but excluded a role for PKC, ERK, or p38 MAPK.

The transcription factor AP-1 is a central target of JNK and the promoter of MKP-1 possesses an AP-1 binding domain.<sup>120</sup> Therefore, a role for AP-1 in mediating the signal from activated JNK to MKP-1 expression seemed plausible. As previously shown by ourselves<sup>104</sup> and confirmed in the present study, ANP is able to induce AP-1 activity. A study showing cGMP, the second messenger of ANP, as inducer of AP-1 activity<sup>121</sup> supports our finding of ANP as an activator of AP-1. Considering that ANP activates JNK within 2 min and that MKP-1 *de novo* protein synthesis starts at about 30 min, the activation of AP-1 within 15 min could be responsible for the induction of MKP-1. In fact, we proved the crucial involvement of AP-1 in the signaling pathway leading to an upregulation of MKP-1 by using an AP-1 decoy approach.<sup>122</sup>

Since numerous studies demonstrate that JNK is regulated by ROS,<sup>45,123</sup> we checked for a participation of superoxide in its activation. In fact, we were able to causally link the ANP-induced formation of superoxide to the activation of JNK by using different superoxide scavengers.

In conclusion, our data suggest that JNK, activated by superoxide, mediates the activation of AP-1. JNK and AP-1 are crucially involved in the induction of MKP-1 by ANP.

#### 4.1.7 General comments

The potential of ANP to induce an increase in ROS formation might be regarded as a form of preconditioning leading to a protection of endothelial cells against an inflammatory response, since ANP induces MKP-1, the crucial mediator of ANP's cytoprotective effects on the endothelium.<sup>14,15</sup> This consideration is supported by a similar observation in HUVEC, which were treated for a short time with hydrogen peroxide: the cells showed a strongly reduced inflammatory response<sup>124</sup> upon activation by TNF- $\alpha$ .

A huge number of studies suggest that activation of Nox leads to oxidant stress, which is thought to be involved in the pathogenesis of many cardiovascular diseases, such as hypertension, atherosclerosis, diabetes, or heart failure.<sup>125</sup> The activity of NAD(P)H oxidase is regulated by cytokines, growth factors, and mechanical forces. Endothelial dysfunction caused by the inactivation of nitric oxide (NO) by Nox-derived superoxide seems to play an important role in the above mentioned disorders.<sup>125</sup> Moreover, Nox activators like thrombin, angiotensin II, or TNF- $\alpha$ <sup>55</sup> are typically pro-inflammatory agents. Therefore, it seems of special interest that the functional outcome of Nox activation by ANP is the induction of MKP-1, a protein which exerts profound cytoprotective effects on endothelial cells.<sup>14,15</sup> This is in consistence with a growing number of studies showing that ROS are not only deleterious molecules involved in a plethora of pathologies, but also important physiological signal transducers.<sup>126</sup>

## 4.2 Dexamethasone and MKP-1

### 4.2.1 Dex reduces E-selectin expression independent of NF- $\kappa$ B

Dex is well-known to decrease LPS-, IL-1-, and TNF- $\alpha$ -induced endothelial E-selectin expression.<sup>127-</sup>  
<sup>131</sup> We confirmed this in our experimental setting and, importantly, found that even low Dex concentrations (1-100 nM) lead to a significant reduction of E-selectin induced by TNF- $\alpha$ . It is commonly accepted that the upregulation of E-selectin in activated endothelial cells is an NF- $\kappa$ B-regulated event<sup>132</sup> and that Dex interferes with the NF- $\kappa$ B-pathway.<sup>68</sup> This interference is thought to be one of the major mechanisms of action of Dex responsible for its anti-inflammatory properties. Therefore, it was very interesting to find that Dex at low concentrations (1-100 nM) readily decreases TNF- $\alpha$ -evoked E-selectin expression, whereas it does not influence TNF- $\alpha$ -activated NF- $\kappa$ B. Higher Dex concentrations ( $\geq$  1,000 nM) lead to a decrease of NF- $\kappa$ B activity. The finding that Dex exerts a concentration-dependent influence on the activity of NF- $\kappa$ B is supported by studies performed in human lung epithelial cells,<sup>129</sup> human peripheral blood mononuclear cells,<sup>133</sup> human astrocytoma and neuroblastoma cells,<sup>134</sup> and fibroblast-like rheumatoid synoviocytes.<sup>135</sup> However, to the best of our knowledge, this effect has as yet been unknown for endothelial cells.

### 4.2.2 The role of p38 MAPK in TNF- $\alpha$ -induced E-selectin expression

Besides the well-known NF- $\kappa$ B-dependent upregulation of E-selectin by TNF- $\alpha$ , an additional pathway has been described that occurs simultaneously with the NF- $\kappa$ B-pathway: TNF- $\alpha$  activates both p38 MAPK and JNK, resulting in the phosphorylation of the transcription factors activating transcription factor-2 (ATF-2) and c-Jun, respectively. The NF- $\kappa$ B- and the ATF-2/c-Jun-pathway converge on the E-selectin promoter. Both pathways are required for full activation of E-selectin gene transcription in response to TNF- $\alpha$ .<sup>136</sup> Moreover, a study by Reimold *et al.* stressed the importance of an ATF-2 activation for E-selectin expression since ATF-2-deficient mice showed an attenuated E-selectin

expression.<sup>137</sup> This highlights the important role of p38 MAPK in the upregulation of E-selectin by TNF- $\alpha$ . In accordance with these findings, we found that a pharmacological inhibitor of p38 MAPK activity was able to significantly decrease E-selectin expression (50% reduction) in HUVEC.

### 4.2.3 Dex reduces p38 MAPK activity *via* induction of MKP-1

In the recent years an influence of glucocorticoids on different members of the MAPK family has been increasingly recognized as a mechanism involved in glucocorticoid action.<sup>73</sup> In this context, a study by Pelaia *et al.* reported that Dex (100 nM) is very effective in preventing the TNF- $\alpha$ -induced activation of p38 MAPK in human pulmonary endothelial cells.<sup>138</sup> This is in consistence with our finding that pre-treatment of Dex abrogates TNF- $\alpha$ -induced p38 MAPK activity in primary human endothelial cells derived from umbilical veins. The question arose how Dex is able to decrease the activity of p38 MAPK. We hypothesized that a phosphatase accounts for this decrease. In fact, a phosphatase inhibitor reversed the effect of Dex on p38 MAPK. MKP-1 has been shown by ourselves to be crucially involved in the deactivation of TNF- $\alpha$ -induced p38 MAPK in endothelial cells.<sup>14,15</sup> Additionally, Lasa *et al.* reported that MKP-1 is the only p38 MAPK-inhibiting phosphatase induced by Dex in epithelial cells.<sup>139</sup> Therefore, we hypothesized an induction of MKP-1 by Dex in HUVEC and, in fact, found a time- and concentration-dependent upregulation of MKP-1. MKP-1 expression is known to be induced by Dex in mast cells,<sup>140,141</sup> epithelial cells,<sup>139,142</sup> macrophages,<sup>143</sup> osteoblasts,<sup>144</sup> adipocytes,<sup>145</sup> and breast cancer cells.<sup>146</sup> However, nothing has as yet been reported about the ability of Dex to increase MKP-1 protein levels in human endothelial cells. It has to be mentioned that in most studies Dex is used at concentrations of about 100 nM, whereas in our cell system Dex concentrations as low as 1 nM lead to a strong upregulation of MKP-1 and an effective deactivation of p38 MAPK. Interestingly, higher Dex concentrations ( $\geq 1,000$  nM) do not lead to an induction of MKP-1, but reduce NF- $\kappa$ B activity. This suggests that the pathways Dex uses for the transduction of its anti-inflammatory properties depend on the applied concentration. It might be speculated that low (reflecting endogenous) glucocorticoid concentrations exert their anti-inflammatory properties rather *via* MKP-1 than *via* NF- $\kappa$ B. Employing an inhibitor of the glucocorticoid receptor (GR), we proved an involvement of this receptor in the induction of MKP-1 by Dex.

#### **4.2.4 MKP-1 is critical for the inhibition of p38 MAPK activity and E-selectin induction**

An involvement of MKP-1 in the action of glucocorticoids in endothelial cells has as yet been completely unknown. By using an MKP-1 antisense approach, we were able to show that Dex-induced MKP-1 plays a pivotal role both in the reduction of p38 MAPK and, importantly, E-selectin expression induced by TNF- $\alpha$ . It has to be stressed that we for the first time provide evidence that MKP-1 is a crucial mediator of the anti-inflammatory actions of glucocorticoids in the endothelium, since we discovered a functional impact of the upregulation of MKP-1 by Dex.

#### **4.2.5 The functional role of MKP-1 induction by Dex**

Besides its above discussed function as a mediator of profound cytoprotective effects (chapter 4.1.1), MKP-1 can also be regarded as an important transducer of anti-inflammatory actions.

(i) MKP-1 was found to act as a negative regulator of the inflammatory response of macrophages, since MKP-1 is critically involved in the termination of LPS-induced signals responsible for the biosynthesis of the pro-inflammatory cytokines TNF- $\alpha$  and IL-6.<sup>143</sup> In response to peptidoglycan, MKP-1-overexpressing macrophages were shown to produce substantially lower amounts of the pro-inflammatory cytokines TNF- $\alpha$  and IL-1 $\beta$ .<sup>147</sup>

(ii) In the context of resolution of inflammatory processes, MKP-1 participates in a negative feedback loop responsible for the limitation of inflammatory effects. A TNF- $\alpha$ -induced upregulation of MKP-1 reduces p38 MAPK activity and E-selectin promoter activity evoked by TNF- $\alpha$  in the endothelium.<sup>148</sup> Moreover, in glomerular mesangial cells MKP-1 was found to limit the expression of the prominent pro-inflammatory mediator cyclooxygenase-2 (COX-2) induced by endothelin-1 (ET-1),<sup>149</sup> a potent vasoconstrictor, which is thought to contribute to renal inflammatory diseases, such as glomerulonephritis.

(iii) Most importantly, MKP-1 has recently been assumed to be a novel regulatory mechanism for the action of glucocorticoids in different cell-types:<sup>74</sup> in HeLa cells Dex was shown to destabilize the mRNA of COX-2 by inhibiting p38 MAPK function *via* an induction of MKP-1.<sup>139,150</sup> Moreover, in rheumatoid arthritis synoviocytes MKP-1 was induced by Dex leading to a deactivation of different MAPK, which are known to be involved in the pathogenesis of rheumatoid arthritis.<sup>151</sup>

It has to be noted that two studies by the group of Fogelman also deal with a pro-inflammatory role of MKP-1: they revealed a role for MKP-1 in oxidized low density lipoproteins (LDL)-induced signaling pathways leading to an expression of the pro-inflammatory cytokine monocyte chemoattractant protein-1 (MCP-1) in human aortic endothelial cells.<sup>152</sup> Recently, they found that MKP-1 is expressed in atherosclerotic lesions of mice and that mice treated with the protein tyrosine phosphatase inhibitor sodium orthovanadate have smaller atherosclerotic lesions compared to the control group.<sup>153</sup> Further studies are required in order to confirm these findings, since the simple appearance of MKP-1 in atherosclerotic lesions and the application of orthovanadate – an inhibitor of all tyrosine phosphatases – do not properly prove a critical involvement of MKP-1. Furthermore, it seems likely that MKP-1 is able to mediate conflicting effects in one single cell-type, since Chandrasekharan *et al.* reported that thrombin-induced MKP-1 differentially regulates thrombin-evoked effects: MKP-1 was found to increase platelet derived growth factor (PDGF), but to decrease VCAM-1 and E-selectin expression in thrombin-activated endothelial cells.<sup>154</sup> MKP-1 seems to be able to mediate both pro- or anti-inflammatory effects. Further investigations are necessary to elucidate the precise underlying mechanisms, which may depend on the experimental settings, the stimulus, or the activation status of the used cells.



## **5 Summary**



## 5.1 MKP-1 and ANP

The cardiovascular hormone atrial natriuretic peptide (ANP) protects endothelial cells against TNF- $\alpha$ -induced activation by inducing MKP-1. In the present work we unraveled the underlying signaling pathway leading to an induction of MKP-1 by ANP (figure 59). An activation of the small Rho-GTPase Rac1 and, subsequently, of a Nox2-containing NAD(P)H oxidase were shown to initiate the signaling cascade. The resulting increase in the generation of superoxide, in turn, led to the activation of the JNK/AP-1 pathway, which was found to be crucial for the transcriptional upregulation of MKP-1 by ANP. Most importantly, we revealed that Rac1 and ROS take part in an ANP-activated transduction mechanism resulting in the increase of a cytoprotective mediator.

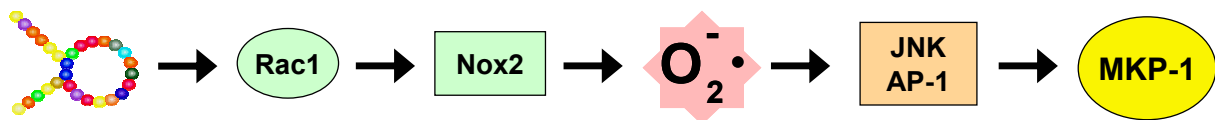


**Figure 59:** Signal transduction pathway of ANP leading to an induction of MKP-1

## 5.2 MKP-1 and Dex

Glucocorticoids are the most common group of drugs used for the treatment of inflammatory diseases. Their anti-inflammatory potential is generally ascribed to their ability to inhibit pro-inflammatory transcription factors, predominantly NF- $\kappa$ B. In the present study we discovered that dexamethasone (Dex), a synthetic glucocorticoid, is able to induce endothelial MKP-1 *via* the glucocorticoid receptor. This induction leads to a deactivation of p38 MAPK and, subsequently, to an inhibition of TNF- $\alpha$ -activated endothelial E-selectin expression (figure 60). Interestingly, the upregulation of MKP-1 was achieved by Dex at very low concentrations (1-100 nM), at which an influence of Dex on the NF- $\kappa$ B pathway was excluded. Most importantly, we describe MKP-1 as a novel mediator of the anti-inflammatory actions of glucocorticoids on endothelial cells. The induction of MKP-1 by Dex was for the first time linked to a functional effect in endothelial cells, i.e. the reduction of TNF- $\alpha$ -evoked E-

selectin expression. In summary, we defined a new anti-inflammatory signal transduction mechanism for glucocorticoids in endothelial cells. This opens up new insights which may help to defeat two major problems in glucocorticoids therapy: resistance and side effects.

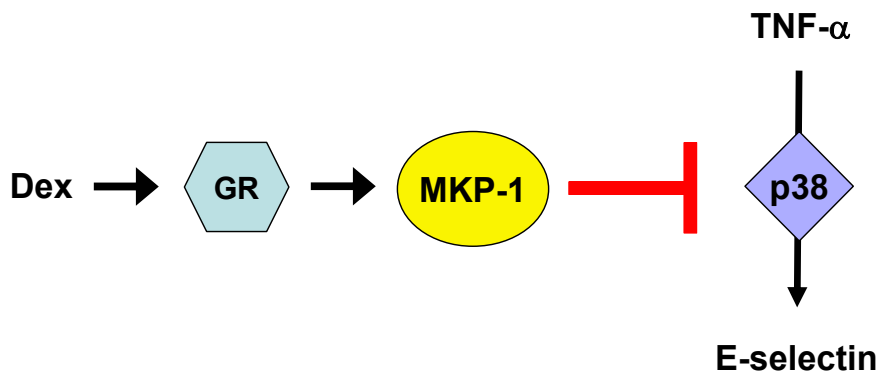


**Figure 60:** The glucocorticoid receptor (GR)-mediated induction of MKP-1 by dexamethasone (Dex) leads to an inhibition of the TNF- $\alpha$ -induced activation of p38 MAPK and, subsequently, E-selectin expression.

### 5.3 MKP-1 as a central protective mediator of the endothelium

In the recent years, the MAPK phosphatase MKP-1 emerged as an important cytoprotective mediator in different cell-types. The role of MKP-1 in the endothelium has as yet been widely unknown. In the present study we characterized the role of MKP-1 in mediating the anti-inflammatory and cytoprotective properties of the Atrial Natriuretic Peptide (ANP) and dexamethasone (figure 61). Pro-inflammatory stimuli, such as TNF- $\alpha$ , lead to an activation of endothelial cells, i.e. the expression of different adhesion molecules (e.g. E-selectin), cytokines (MCP-1), or the reorganization of cytoskeletal elements resulting in stress fiber formation or increase of permeability. p38 MAPK is crucially involved in the signaling leading to the TNF- $\alpha$  induced deterioration of endothelial functionality. MKP-1, induced by ANP and Dex, exerts its effects by inhibiting p38 MAPK activity. The findings of the present study provide a further insight into both the functions and the mechanisms of induction of MKP-1. This highlights the potential of this phosphatase as a useful and valuable drug target.

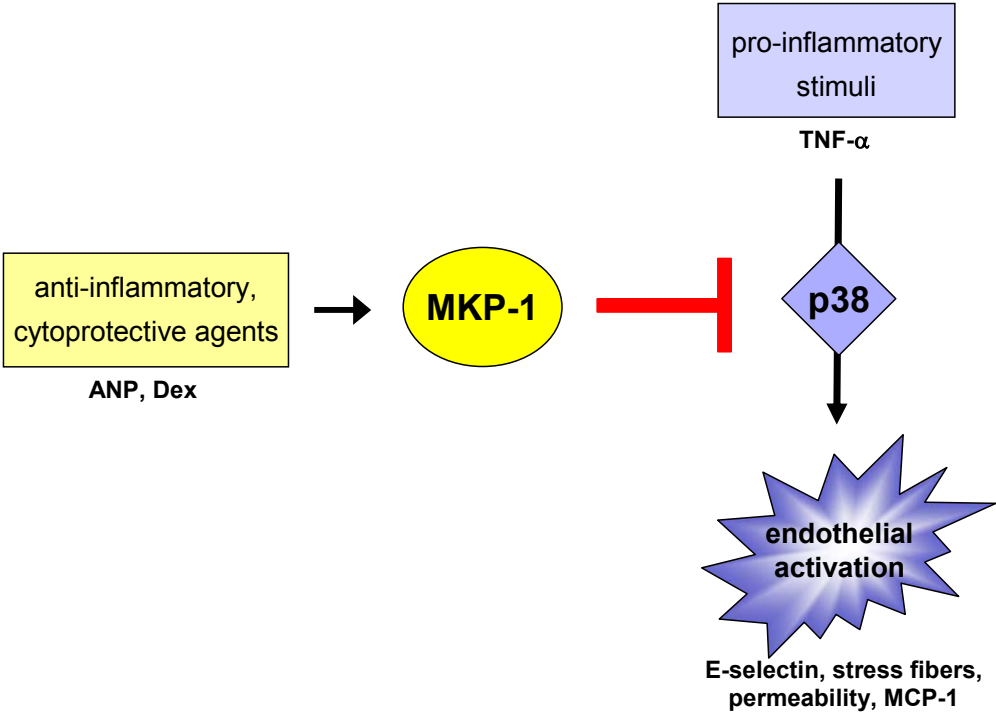


Figure 61: MKP-1 as a central protective mediator of the endothelium.



## **6 References**





- (1) Cines DB, Pollak ES, Buck CA et al. Endothelial cells in physiology and in the pathophysiology of vascular disorders. *Blood*. 1998;91:3527-3561.
- (2) Galley HF, Webster NR. Physiology of the endothelium. *Br J Anaesth*. 2004;93:105-113.
- (3) Szmítko PE, Wang CH, Weisel RD et al. New markers of inflammation and endothelial cell activation: Part I. *Circulation*. 2003;108:1917-1923.
- (4) Gonzalez MA, Selwyn AP. Endothelial function, inflammation, and prognosis in cardiovascular disease. *Am J Med*. 2003;115 Suppl 8A:99S-106S.
- (5) Ross R. Atherosclerosis - an inflammatory disease. *N Engl J Med*. 1999;340:115-126.
- (6) Libby P. Inflammation in atherosclerosis. *Nature*. 2002;420:868-874.
- (7) Greaves DR, Channon KM. Inflammation and immune responses in atherosclerosis. *Trends Immunol*. 2002;23:535-541.
- (8) Pober JS. Endothelial activation: intracellular signaling pathways. *Arthritis Res*. 2002;4 Suppl 3:S109-S116.
- (9) Endemann DH, Schiffrin EL. Endothelial dysfunction. *J Am Soc Nephrol*. 2004;15:1983-1992.
- (10) Libby P. Vascular biology of atherosclerosis: overview and state of the art. *Am J Cardiol*. 2003;91:3A-6A.
- (11) Plutzky J. The vascular biology of atherosclerosis. *Am J Med*. 2003;115 Suppl 8A:55S-61S.
- (12) Lentsch AB, Ward PA. Activation and regulation of NF $\kappa$ B during acute inflammation. *Clin Chem Lab Med*. 1999;37:205-208.
- (13) De Martin R, Hoeth M, Hofer-Warbinek R, Schmid JA. The transcription factor NF- $\kappa$ B and the regulation of vascular cell function. *Arterioscler Thromb Vasc Biol*. 2000;20:E83-E88.

- (14) Kiemer AK, Weber NC, Fürst R et al. Inhibition of p38 MAPK activation via induction of MKP-1: atrial natriuretic peptide reduces TNF- $\alpha$ -induced actin polymerization and endothelial permeability. *Circ Res.* 2002;90:874-881.
- (15) Weber NC, Blumenthal SB, Hartung T, Vollmar AM, Kiemer AK. ANP inhibits TNF- $\alpha$ -induced endothelial MCP-1 expression - involvement of p38 MAPK and MKP-1. *J Leukoc Biol.* 2003;74:932-941.
- (16) Pearson G, Robinson F, Beers GT et al. Mitogen-activated protein (MAP) kinase pathways: regulation and physiological functions. *Endocr Rev.* 2001;22:153-183.
- (17) Chang L, Karin M. Mammalian MAP kinase signalling cascades. *Nature.* 2001;410:37-40.
- (18) Herlaar E, Brown Z. p38 MAPK signalling cascades in inflammatory disease. *Mol Med Today.* 1999;5:439-447.
- (19) Chen Z, Gibson TB, Robinson F et al. MAP kinases. *Chem Rev.* 2001;101:2449-2476.
- (20) Obata T, Brown GE, Yaffe MB. MAP kinase pathways activated by stress: the p38 MAPK pathway. *Crit Care Med.* 2000;28:N67-N77.
- (21) Tibbles LA, Woodgett JR. The stress-activated protein kinase pathways. *Cell Mol Life Sci.* 1999;55:1230-1254.
- (22) Keyse SM. Protein phosphatases and the regulation of mitogen-activated protein kinase signalling. *Curr Opin Cell Biol.* 2000;12:186-192.
- (23) Camps M, Nichols A, Arkinstall S. Dual specificity phosphatases: a gene family for control of MAP kinase function. *FASEB J.* 2000;14:6-16.
- (24) Theodosiou A, Ashworth A. MAP kinase phosphatases. *Genome Biol.* 2002;3:reviews3009.1-3009.10.

- (25) Brondello JM, Pouyssegur J, McKenzie FR. Reduced MAP kinase phosphatase-1 degradation after p42/p44MAPK-dependent phosphorylation. *Science*. 1999;286:2514-2517.
- (26) Sun H, Charles CH, Lau LF, Tonks NK. MKP-1 (3CH134), an immediate early gene product, is a dual specificity phosphatase that dephosphorylates MAP kinase in vivo. *Cell*. 1993;75:487-493.
- (27) Hannken T, Schroeder R, Stahl RA, Wolf G. Atrial natriuretic peptide attenuates ANG II-induced hypertrophy of renal tubular cells. *Am J Physiol Renal Physiol*. 2001;281:F81-F90.
- (28) Yoneda K, Peck K, Chang MM et al. Development of high-density DNA microarray membrane for profiling smoke- and hydrogen peroxide-induced genes in a human bronchial epithelial cell line. *Am J Respir Crit Care Med*. 2001;164:S85-S89.
- (29) Bokemeyer D, Sorokin A, Yan M et al. Induction of mitogen-activated protein kinase phosphatase 1 by the stress-activated protein kinase signaling pathway but not by extracellular signal-regulated kinase in fibroblasts. *J Biol Chem*. 1996;271:639-642.
- (30) Bokemeyer D, Lindemann M, Kramer HJ. Regulation of mitogen-activated protein kinase phosphatase-1 in vascular smooth muscle cells. *Hypertension*. 1998;32:661-667.
- (31) Kim F, Corson MA. Adhesion to fibronectin enhances MKP-1 activation in human endothelial cells. *Biochem Biophys Res Commun*. 2000;273:539-545.
- (32) Valledor AF, Xaus J, Marques L, Celada A. Macrophage colony-stimulating factor induces the expression of mitogen-activated protein kinase phosphatase-1 through a protein kinase C-dependent pathway. *J Immunol*. 1999;163:2452-2462.
- (33) de Bold AJ, Borenstein HB, Veress AT, Sonnenberg H. A rapid and potent natriuretic response to intravenous injection of atrial myocardial extract in rats. *Life Sci*. 1981;28:89-94.
- (34) Levin ER, Gardner DG, Samson WK. Natriuretic peptides. *N Engl J Med*. 1998;339:321-328.

- (35) Richards AM, Lainchbury JG, Nicholls MG, Cameron AV, Yandle TG. Dendroaspis natriuretic peptide: endogenous or dubious? *Lancet*. 2002;359:5-6.
- (36) Suttner SW, Boldt J. Natriuretic peptide system: physiology and clinical utility. *Curr Opin Crit Care*. 2004;10:336-341.
- (37) Kiemer AK, Fürst R, Vollmar AM. Vasoprotective actions of the atrial natriuretic peptide. *Curr Med Chem Cardiovasc Hematol Agents*. 2005;3:in press.
- (38) Kuhn M. Structure, regulation, and function of mammalian membrane guanylyl cyclase receptors, with a focus on guanylyl cyclase-A. *Circ Res*. 2003;93:700-709.
- (39) Misono KS. Natriuretic peptide receptor: structure and signaling. *Mol Cell Biochem*. 2002;230:49-60.
- (40) Tremblay J, Desjardins R, Hum D, Gutkowska J, Hamet P. Biochemistry and physiology of the natriuretic peptide receptor guanylyl cyclases. *Mol Cell Biochem*. 2002;230:31-47.
- (41) Murthy KS, Teng BQ, Zhou H et al.  $G_{i1}/G_{i2}$ -dependent signaling by single-transmembrane natriuretic peptide clearance receptor. *Am J Physiol Gastrointest Liver Physiol*. 2000;278:G974-G980.
- (42) Richards AM. The natriuretic peptides in heart failure. *Basic Res Cardiol*. 2004;99:94-100.
- (43) Brunner-La Rocca HP, Kiowski W, Ramsay D, Sutsch G. Therapeutic benefits of increasing natriuretic peptide levels. *Cardiovasc Res*. 2001;51:510-520.
- (44) Commoner B, Townsend J, Pake GE. Free radicals in biological materials. *Nature*. 1954;174:689-691.
- (45) Dröge W. Free radicals in the physiological control of cell function. *Physiol Rev*. 2002;82:47-95.
- (46) Scandalios JG. The rise of ROS. *Trends Biochem Sci*. 2002;27:483-486.

- (47) Taniyama Y, Griendling KK. Reactive oxygen species in the vasculature: molecular and cellular mechanisms. *Hypertension*. 2003;42:1075-1081.
- (48) Thannickal VJ, Fanburg BL. Reactive oxygen species in cell signaling. *Am J Physiol Lung Cell Mol Physiol*. 2000;279:L1005-L1028.
- (49) Herrlich P, Böhmer FD. Redox regulation of signal transduction in mammalian cells. *Biochem Pharmacol*. 2000;59:35-41.
- (50) Forman HJ, Torres M, Fukuto J. Redox signaling. *Mol Cell Biochem*. 2002;234-235:49-62.
- (51) Wolin MS. Interactions of oxidants with vascular signaling systems. *Arterioscler Thromb Vasc Biol*. 2000;20:1430-1442.
- (52) Babior BM. NADPH oxidase: an update. *Blood*. 1999;93:1464-1476.
- (53) Babior BM. The leukocyte NADPH oxidase. *Isr Med Assoc J*. 2002;4:1023-1024.
- (54) Babior BM. NADPH oxidase. *Curr Opin Immunol*. 2004;16:42-47.
- (55) Lassegue B, Clempus RE. Vascular NAD(P)H oxidases: specific features, expression, and regulation. *Am J Physiol Regul Integr Comp Physiol*. 2003;285:R277-R297.
- (56) Frey RS, Rahman A, Kefer JC, Minshall RD, Malik AB. PKC $\zeta$  regulates TNF- $\alpha$ -induced activation of NADPH oxidase in endothelial cells. *Circ Res*. 2002;90:1012-1019.
- (57) Görlach A, Brandes RP, Nguyen K et al. A gp91<sup>phox</sup> containing NADPH oxidase selectively expressed in endothelial cells is a major source of oxygen radical generation in the arterial wall. *Circ Res*. 2000;87:26-32.
- (58) Li JM, Shah AM. Differential NADPH- versus NADH-dependent superoxide production by phagocyte-type endothelial cell NADPH oxidase. *Cardiovasc Res*. 2001;52:477-486.
- (59) Li JM, Shah AM. Intracellular localization and preassembly of the NADPH oxidase complex in cultured endothelial cells. *J Biol Chem*. 2002;277:19952-19960.

- (60) Li JM, Shah AM. Mechanism of endothelial cell NADPH oxidase activation by angiotensin II. Role of the p47<sup>phox</sup> subunit. *J Biol Chem*. 2003;278:12094-12100.
- (61) Meyer JW, Holland JA, Ziegler LM et al. Identification of a functional leukocyte-type NADPH oxidase in human endothelial cells :a potential atherogenic source of reactive oxygen species. *Endothelium*. 1999;7:11-22.
- (62) Ago T, Kitazono T, Ooboshi H et al. Nox4 as the major catalytic component of an endothelial NAD(P)H oxidase. *Circulation*. 2004;109:227-233.
- (63) Bishop AL, Hall A. Rho GTPases and their effector proteins. *Biochem J*. 2000;348 Pt 2:241-255.
- (64) Takai Y, Sasaki T, Matozaki T. Small GTP-binding proteins. *Physiol Rev*. 2001;81:153-208.
- (65) Gregg D, Rauscher FM, Goldschmidt-Clermont PJ. Rac regulates cardiovascular superoxide through diverse molecular interactions: more than a binary GTP switch. *Am J Physiol Cell Physiol*. 2003;285:C723-C734.
- (66) Lundberg IE, Grundtman C, Larsson E, Klareskog L. Corticosteroids - from an idea to clinical use. *Best Pract Res Clin Rheumatol*. 2004;18:7-19.
- (67) Hatz HJ. Glucocorticoide: immunologische Grundlagen, Pharmakologie und Therapierichtlinien. Stuttgart: Wissenschaftliche Verlagsgesellschaft; 1998.
- (68) De Bosscher K, Vanden Berghe W, Haegeman G. The interplay between the glucocorticoid receptor and nuclear factor- $\kappa$ B or activator protein-1: molecular mechanisms for gene repression. *Endocr Rev*. 2003;24:488-522.
- (69) Leung DY, Bloom JW. Update on glucocorticoid action and resistance. *J Allergy Clin Immunol*. 2003;111:3-22.
- (70) Schaaf MJ, Cidlowski JA. Molecular mechanisms of glucocorticoid action and resistance. *J Steroid Biochem Mol Biol*. 2002;83:37-48.

- (71) Schäcke H, Döcke WD, Asadullah K. Mechanisms involved in the side effects of glucocorticoids. *Pharmacol Ther.* 2002;96:23-43.
- (72) Limbourg FP, Liao JK. Nontranscriptional actions of the glucocorticoid receptor. *J Mol Med.* 2003;81:168-174.
- (73) Clark AR, Lasa M. Crosstalk between glucocorticoids and mitogen-activated protein kinase signalling pathways. *Curr Opin Pharmacol.* 2003;3:404-411.
- (74) Clark AR. MAP kinase phosphatase 1: a novel mediator of biological effects of glucocorticoids? *J Endocrinol.* 2003;178:5-12.
- (75) Jaffe EA, Nachman RL, Becker CG, Minick CR. Culture of human endothelial cells derived from umbilical veins. Identification by morphologic and immunologic criteria. *J Clin Invest.* 1973;52:2745-2756.
- (76) Ades EW, Candal FJ, Swerlick RA et al. HMEC-1: establishment of an immortalized human microvascular endothelial cell line. *J Invest Dermatol.* 1992;99:683-690.
- (77) Diehl KH, Hull R, Morton D et al. A good practice guide to the administration of substances and removal of blood, including routes and volumes. *J Appl Toxicol.* 2001;21:15-23.
- (78) Bradford MM. A rapid and sensitive method for the quantitation of microgram quantities of protein utilizing the principle of protein-dye binding. *Anal Biochem.* 1976;72:248-254.
- (79) Hempel SL, Buettner GR, O'Malley YQ, Wessels DA, Flaherty DM. Dihydrofluorescein diacetate is superior for detecting intracellular oxidants: comparison with 2',7'-dichlorodihydrofluorescein diacetate, 5-(and 6)-carboxy-2',7'-dichlorodihydrofluorescein diacetate, and dihydrorhodamine 123. *Free Radic Biol Med.* 1999;27:146-159.
- (80) Kuebler WM, Ying X, Singh B, Issekutz AC, Bhattacharya J. Pressure is proinflammatory in lung venular capillaries. *J Clin Invest.* 1999;104:495-502.

- (81) Kuebler WM, Parthasarathi K, Wang PM, Bhattacharya J. A novel signaling mechanism between gas and blood compartments of the lung. *J Clin Invest.* 2000;105:905-913.
- (82) Parthasarathi K, Ichimura H, Quadri S, Issekutz A, Bhattacharya J. Mitochondrial reactive oxygen species regulate spatial profile of proinflammatory responses in lung venular capillaries. *J Immunol.* 2002;169:7078-7086.
- (83) Ying X, Minamiya Y, Fu C, Bhattacharya J.  $Ca^{2+}$  waves in lung capillary endothelium. *Circ Res.* 1996;79:898-908.
- (84) Tsukada H, Ying X, Fu C et al. Ligation of endothelial  $\alpha_v\beta_3$  integrin increases capillary hydraulic conductivity of rat lung. *Circ Res.* 1995;77:651-659.
- (85) Schreiber E, Matthias P, Muller MM, Schaffner W. Rapid detection of octamer binding proteins with 'mini-extracts', prepared from a small number of cells. *Nucleic Acids Res.* 1989;17:6419.
- (86) Wagner AH, Schroeter MR, Hecker M.  $17\beta$ -estradiol inhibition of NADPH oxidase expression in human endothelial cells. *FASEB J.* 2001;15:2121-2130.
- (87) Lauth M, Wagner AH, Cattaruzza M et al. Transcriptional control of deformation-induced preproendothelin-1 gene expression in endothelial cells. *J Mol Med.* 2000;78:441-450.
- (88) Benard V, Bohl BP, Bokoch GM. Characterization of rac and cdc42 activation in chemoattractant-stimulated human neutrophils using a novel assay for active GTPases. *J Biol Chem.* 1999;274:13198-13204.
- (89) Teifel M, Heine LT, Milbredt S, Friedl P. Optimization of transfection of human endothelial cells. *Endothelium.* 1997;5:21-35.
- (90) Li C, Hu Y, Mayr M, Xu Q. Cyclic strain stress-induced mitogen-activated protein kinase (MAPK) phosphatase 1 expression in vascular smooth muscle cells is regulated by Ras/Rac-MAPK pathways. *J Biol Chem.* 1999;274:25273-25280.



- (91) Jacob A, Molkenin JD, Smolenski A, Lohmann SM, Begum N. Insulin inhibits PDGF-directed VSMC migration via NO/ cGMP increase of MKP-1 and its inactivation of MAPKs. *Am J Physiol Cell Physiol.* 2002;283:C704-C713.
- (92) Begum N, Song Y, Rienzie J, Ragolia L. Vascular smooth muscle cell growth and insulin regulation of mitogen-activated protein kinase in hypertension. *Am J Physiol.* 1998;275:C42-C49.
- (93) Begum N, Ragolia L, Rienzie J, McCarthy M, Duddy N. Regulation of mitogen-activated protein kinase phosphatase-1 induction by insulin in vascular smooth muscle cells. Evaluation of the role of the nitric oxide signaling pathway and potential defects in hypertension. *J Biol Chem.* 1998;273:25164-25170.
- (94) Jacob A, Smolenski A, Lohmann SM, Begum N. MKP-1 expression and stabilization and cGK I $\alpha$  prevent diabetes-associated abnormalities in VSMC migration. *Am J Physiol Cell Physiol.* 2004;287:C1077-C1086.
- (95) Hayashi D, Kudoh S, Shiojima I et al. Atrial natriuretic peptide inhibits cardiomyocyte hypertrophy through mitogen-activated protein kinase phosphatase-1. *Biochem Biophys Res Commun.* 2004;322:310-319.
- (96) Kaiser RA, Bueno OF, Lips DJ et al. Targeted inhibition of p38 mitogen-activated protein kinase antagonizes cardiac injury and cell death following ischemia-reperfusion in vivo. *J Biol Chem.* 2004;279:15524-15530.
- (97) Krepinsky J, Ingram AJ, James L et al. 17 $\beta$ -Estradiol modulates mechanical strain-induced MAPK activation in mesangial cells. *J Biol Chem.* 2002;277:9387-9394.
- (98) Haneda M, Sugimoto T, Kikkawa R. Mitogen-activated protein kinase phosphatase: a negative regulator of the mitogen-activated protein kinase cascade. *Eur J Pharmacol.* 1999;365:1-7.

- (99) Sugimoto T, Haneda M, Togawa M et al. Atrial natriuretic peptide induces the expression of MKP-1, a mitogen-activated protein kinase phosphatase, in glomerular mesangial cells. *J Biol Chem.* 1996;271:544-547.
- (100) MacMillan-Crow LA, Murphy-Ullrich JE, Lincoln TM. Identification and possible localization of cGMP-dependent protein kinase in bovine aortic endothelial cells. *Biochem Biophys Res Commun.* 1994;201:531-537.
- (101) Kook H, Itoh H, Choi BS et al. Physiological concentration of atrial natriuretic peptide induces endothelial regeneration in vitro. *Am J Physiol Heart Circ Physiol.* 2003;284:H1388-H1397.
- (102) Yamahara K, Itoh H, Chun TH et al. Significance and therapeutic potential of the natriuretic peptides/cGMP/cGMP-dependent protein kinase pathway in vascular regeneration. *Proc Natl Acad Sci U S A.* 2003;100:3404-3409.
- (103) Draijer R, Vaandrager AB, Nolte C et al. Expression of cGMP-dependent protein kinase I and phosphorylation of its substrate, vasodilator-stimulated phosphoprotein, in human endothelial cells of different origin. *Circ Res.* 1995;77:897-905.
- (104) Kiemer AK, Bildner N, Weber NC, Vollmar AM. Characterization of heme oxygenase 1 (heat shock protein 32) induction by atrial natriuretic peptide in human endothelial cells. *Endocrinology.* 2003;144:802-812.
- (105) Cornwell TL, Lincoln TM. Regulation of intracellular Ca<sup>2+</sup> levels in cultured vascular smooth muscle cells. Reduction of Ca<sup>2+</sup> by atriopeptin and 8-bromo-cyclic GMP is mediated by cyclic GMP-dependent protein kinase. *J Biol Chem.* 1989;264:1146-1155.
- (106) Baas AS, Berk BC. Differential activation of mitogen-activated protein kinases by H<sub>2</sub>O<sub>2</sub> and O<sub>2</sub><sup>-</sup> in vascular smooth muscle cells. *Circ Res.* 1995;77:29-36.
- (107) Vollmar AM, Förster R, Schulz R. Effects of atrial natriuretic peptide on phagocytosis and respiratory burst in murine macrophages. *Eur J Pharmacol.* 1997;319:279-285.

- (108) Xu Z, Ji X, Boysen PG. Exogenous nitric oxide generates ROS and induces cardioprotection: involvement of PKG, mitochondrial  $K_{ATP}$  channels, and ERK. *Am J Physiol Heart Circ Physiol*. 2004;286:H1433-H1440.
- (109) Haddad JJ. Science review: redox and oxygen-sensitive transcription factors in the regulation of oxidant-mediated lung injury: role for hypoxia-inducible factor-1 $\alpha$ . *Crit Care*. 2003;7:47-54.
- (110) Lofton CE, Baron DA, Heffner JE, Currie MG, Newman WH. Atrial natriuretic peptide inhibits oxidant-induced increases in endothelial permeability. *J Mol Cell Cardiol*. 1991;23:919-927.
- (111) Westendorp RG, Draijer R, Meinders AE, van Hinsbergh VW. Cyclic-GMP-mediated decrease in permeability of human umbilical and pulmonary artery endothelial cell monolayers. *J Vasc Res*. 1994;31:42-51.
- (112) Cross AR, Segal AW. The NADPH oxidase of professional phagocytes - prototype of the NOX electron transport chain systems. *Biochim Biophys Acta*. 2004;1657:1-22.
- (113) Touyz RM, Chen X, Tabet F et al. Expression of a functionally active gp91<sup>phox</sup>-containing neutrophil-type NAD(P)H oxidase in smooth muscle cells from human resistance arteries: regulation by angiotensin II. *Circ Res*. 2002;90:1205-1213.
- (114) Sohn HY, Keller M, Gloe T et al. The small G-protein Rac mediates depolarization-induced superoxide formation in human endothelial cells. *J Biol Chem*. 2000;275:18745-18750.
- (115) Lopes NH, Vasudevan SS, Gregg D et al. Rac-dependent monocyte chemoattractant protein-1 production is induced by nutrient deprivation. *Circ Res*. 2002;91:798-805.
- (116) Wung BS, Cheng JJ, Shyue SK, Wang DL. NO modulates monocyte chemotactic protein-1 expression in endothelial cells under cyclic strain. *Arterioscler Thromb Vasc Biol*. 2001;21:1941-1947.

- (117) Chen XL, Zhang Q, Zhao R et al. Rac1 and superoxide are required for the expression of cell adhesion molecules induced by tumor necrosis factor- $\alpha$  in endothelial cells. *J Pharmacol Exp Ther.* 2003;305:573-580.
- (118) Chen XL, Zhang Q, Zhao R, Medford RM. Superoxide, H<sub>2</sub>O<sub>2</sub>, and iron are required for TNF- $\alpha$ -induced MCP-1 gene expression in endothelial cells: role of Rac1 and NADPH oxidase. *Am J Physiol Heart Circ Physiol.* 2004;286:H1001-H1007.
- (119) Deshpande SS, Angkeow P, Huang J, Ozaki M, Irani K. Rac1 inhibits TNF- $\alpha$ -induced endothelial cell apoptosis: dual regulation by reactive oxygen species. *FASEB J.* 2000;14:1705-1714.
- (120) Kwak SP, Hakes DJ, Martell KJ, Dixon JE. Isolation and characterization of a human dual specificity protein-tyrosine phosphatase gene. *J Biol Chem.* 1994;269:3596-3604.
- (121) Sciorati C, Nistico G, Meldolesi J, Clementi E. Nitric oxide effects on cell growth: GMP-dependent stimulation of the AP-1 transcription complex and cyclic GMP-independent slowing of cell cycling. *Br J Pharmacol.* 1997;122:687-697.
- (122) Park SK, Yang WS, Han NJ et al. Dexamethasone regulates AP-1 to repress TNF- $\alpha$ -induced MCP-1 production in human glomerular endothelial cells. *Nephrol Dial Transplant.* 2004;19:312-319.
- (123) Adler V, Yin Z, Tew KD, Ronai Z. Role of redox potential and reactive oxygen species in stress signaling. *Oncogene.* 1999;18:6104-6111.
- (124) Zahler S, Kupatt C, Becker BF. Endothelial preconditioning by transient oxidative stress reduces inflammatory responses of cultured endothelial cells to TNF- $\alpha$ . *FASEB J.* 2000;14:555-564.
- (125) Cai H, Harrison DG. Endothelial dysfunction in cardiovascular diseases: the role of oxidant stress. *Circ Res.* 2000;87:840-844.

- (126) Sorg O. Oxidative stress: a theoretical model or a biological reality? *C R Biol.* 2004;327:649-662.
- (127) Cronstein BN, Kimmel SC, Levin RI, Martiniuk F, Weissmann G. A mechanism for the antiinflammatory effects of corticosteroids: the glucocorticoid receptor regulates leukocyte adhesion to endothelial cells and expression of endothelial-leukocyte adhesion molecule 1 and intercellular adhesion molecule 1. *Proc Natl Acad Sci U S A.* 1992;89:9991-9995.
- (128) Aziz KE, Wakefield D. Modulation of endothelial cell expression of ICAM-1, E-selectin, and VCAM-1 by  $\beta$ -estradiol, progesterone, and dexamethasone. *Cell Immunol.* 1996;167:79-85.
- (129) Ray KP, Farrow S, Daly M, Talabot F, Searle N. Induction of the E-selectin promoter by interleukin 1 and tumour necrosis factor  $\alpha$ , and inhibition by glucocorticoids. *Biochem J.* 1997;328 (Pt 2):707-715.
- (130) Ray KP, Searle N. Glucocorticoid inhibition of cytokine-induced E-selectin promoter activation. *Biochem Soc Trans.* 1997;25:189S.
- (131) Brostjan C, Anrather J, Csizmadia V, Natarajan G, Winkler H. Glucocorticoids inhibit E-selectin expression by targeting NF- $\kappa$ B and not ATF/c-Jun. *J Immunol.* 1997;158:3836-3844.
- (132) Chen CC, Manning AM. Transcriptional regulation of endothelial cell adhesion molecules: a dominant role for NF- $\kappa$ B. *Agents Actions Suppl.* 1995;47:135-141.
- (133) Rowland TL, McHugh SM, Deighton J et al. Differential effect of thalidomide and dexamethasone on the transcription factor NF- $\kappa$ B. *Int Immunopharmacol.* 2001;1:49-61.
- (134) Bourke E, Moynagh PN. Antiinflammatory effects of glucocorticoids in brain cells, independent of NF- $\kappa$ B. *J Immunol.* 1999;163:2113-2119.
- (135) Han CW, Choi JH, Kim JM et al. Glucocorticoid-mediated repression of inflammatory cytokine production in fibroblast-like rheumatoid synoviocytes is independent of nuclear factor- $\kappa$ B activation induced by tumour necrosis factor  $\alpha$ . *Rheumatology (Oxford).* 2001;40:267-273.

- (136) Read MA, Whitley MZ, Gupta S et al. Tumor necrosis factor  $\alpha$ -induced E-selectin expression is activated by the nuclear factor- $\kappa$ B and c-JUN N-terminal kinase/p38 mitogen-activated protein kinase pathways. *J Biol Chem.* 1997;272:2753-2761.
- (137) Reimold AM, Grusby MJ, Kosaras B et al. Chondrodysplasia and neurological abnormalities in ATF-2-deficient mice. *Nature.* 1996;379:262-265.
- (138) Pelaia G, Cuda G, Vatrella A et al. Effects of glucocorticoids on activation of c-jun N-terminal, extracellular signal-regulated, and p38 MAP kinases in human pulmonary endothelial cells. *Biochem Pharmacol.* 2001;62:1719-1724.
- (139) Lasa M, Abraham SM, Boucheron C, Saklatvala J, Clark AR. Dexamethasone causes sustained expression of mitogen-activated protein kinase (MAPK) phosphatase 1 and phosphatase-mediated inhibition of MAPK p38. *Mol Cell Biol.* 2002;22:7802-7811.
- (140) Jeong HJ, Na HJ, Hong SH, Kim HM. Inhibition of the stem cell factor-induced migration of mast cells by dexamethasone. *Endocrinology.* 2003;144:4080-4086.
- (141) Kassel O, Sancono A, Krätzschar J et al. Glucocorticoids inhibit MAP kinase via increased expression and decreased degradation of MKP-1. *EMBO J.* 2001;20:7108-7116.
- (142) Imasato A, Desbois-Mouthon C, Han J et al. Inhibition of p38 MAPK by glucocorticoids via induction of MAPK phosphatase-1 enhances nontypeable *Haemophilus influenzae*-induced expression of toll-like receptor 2. *J Biol Chem.* 2002;277:47444-47450.
- (143) Chen P, Li J, Barnes J et al. Restraint of proinflammatory cytokine biosynthesis by mitogen-activated protein kinase phosphatase-1 in lipopolysaccharide-stimulated macrophages. *J Immunol.* 2002;169:6408-6416.
- (144) Engelbrecht Y, de Wet H, Horsch K et al. Glucocorticoids induce rapid up-regulation of mitogen-activated protein kinase phosphatase-1 and dephosphorylation of extracellular signal-regulated kinase and impair proliferation in human and mouse osteoblast cell lines. *Endocrinology.* 2003;144:412-422.

- (145) Bazuine M, Carlotti F, Tafrechi RS, Hoeben RC, Maassen JA. Mitogen-activated protein kinase (MAPK) phosphatase-1 and -4 attenuate p38 MAPK during dexamethasone-induced insulin resistance in 3T3-L1 adipocytes. *Mol Endocrinol*. 2004;18:1697-1707.
- (146) Wu W, Chaudhuri S, Brickley DR et al. Microarray analysis reveals glucocorticoid-regulated survival genes that are associated with inhibition of apoptosis in breast epithelial cells. *Cancer Res*. 2004;64:1757-1764.
- (147) Shepherd EG, Zhao Q, Welty SE et al. The function of mitogen-activated protein kinase phosphatase-1 in peptidoglycan-stimulated macrophages. *J Biol Chem*. 2004;in press.
- (148) Wadgaonkar R, Pierce JW, Somnay K et al. Regulation of c-Jun N-terminal kinase and p38 kinase pathways in endothelial cells. *Am J Respir Cell Mol Biol*. 2004;31:423-431.
- (149) Pratt PF, Bokemeyer D, Foschi M, Sorokin A, Dunn MJ. Alterations in subcellular localization of p38 MAPK potentiates endothelin-stimulated COX-2 expression in glomerular mesangial cells. *J Biol Chem*. 2003;278:51928-51936.
- (150) Lasa M, Brook M, Saklatvala J, Clark AR. Dexamethasone destabilizes cyclooxygenase 2 mRNA by inhibiting mitogen-activated protein kinase p38. *Mol Cell Biol*. 2001;21:771-780.
- (151) Toh ML, Yang Y, Leech M, Santos L, Morand EF. Expression of mitogen-activated protein kinase phosphatase 1, a negative regulator of the mitogen-activated protein kinases, in rheumatoid arthritis: Up-regulation by interleukin-1 $\beta$  and glucocorticoids. *Arthritis Rheum*. 2004;50:3118-3128.
- (152) Reddy S, Hama S, Grijalva V et al. Mitogen-activated protein kinase phosphatase 1 activity is necessary for oxidized phospholipids to induce monocyte chemotactic activity in human aortic endothelial cells. *J Biol Chem*. 2001;276:17030-17035.
- (153) Reddy ST, Nguyen JT, Grijalva V et al. Potential role for mitogen-activated protein kinase phosphatase-1 in the development of atherosclerotic lesions in mouse models. *Arterioscler Thromb Vasc Biol*. 2004;24:1676-1681.

- (154) Chandrasekharan UM, Yang L, Walters A, Howe P, Dicorleto PE. Role of CL-100, a dual specificity phosphatase, in thrombin-induced endothelial cell activation. *J Biol Chem.* 2004;279:46678-46685.



## **7 Appendix**



## 7.1 Abbreviations

A	Ampere
ANP	atrial natriuretic peptide
AP-1	activator protein-1
BNP	brain natriuretic peptide
°C	degrees Celsius
CAM	cell adhesion molecule
cGMP	cyclic guanosin-5'-monophosphate
cpm	counts per minute
CNP	C-type natriuretic peptide
Co	control
Dex	dexamethasone
DNA	desoxyribonucleic acid
EC	endothelial cell
EMSA	electrophoretic mobility shift assay
ERK	extracellular-regulated kinase
g	gram
GC	glucocorticoid
GDP	guanosine-5'-diphosphate
GR	glucocorticoid receptor
GTP	guanosine-5'-triphosphate
h	hour
HMEC	human microvascular endothelial cell
HUVEC	human umbilical vein endothelial cell
ICAM-1	intercellular adhesion molecule-1
JNK	c-Jun N-terminal kinase
l	liter
m	meter

---

m	milli ( $10^{-3}$ )
M	molar
$\mu$	micro ( $10^{-6}$ )
min	minute
MAPK	mitogen-activated protein kinase
MCP-1	monocyte chemoattractant protein-1
MKP	mitogen-activated protein kinase phosphatase
mRNA	messenger ribonucleic acid
n	nano ( $10^{-9}$ )
NADPH	nicotinamide dinucleotide phosphate
NF- $\kappa$ B	nuclear factor- $\kappa$ B
NO	nitric oxide
Nox	NAD(P)H oxidase
NP	natriuretic peptide
NPR	natriuretic peptide receptor
PCR	polymerase chain reaction
PKC	protein kinase C
PKG	protein kinase G (cGMP-dependent protein kinase)
RNA	ribonucleic acid
ROS	reactive oxygen species
rpm	rotations per minute
s	second
SEM	standard error of the mean value
SOD	superoxide dismutase
TNF- $\alpha$	tumor necrosis factor- $\alpha$
VCAM-1	vascular cell adhesion molecule-1
VSMC	vascular smooth muscle cell

## 7.2 Alphabetical list of companies

Alexis	Grünberg, Germany
AGFA	Cologne, Germany
Amersham	Freiburg, Germany
Bachem	Heidelberg, Germany
BD Biosciences	Heidelberg, Germany
Biochrom	Berlin, Germany
biomers.net	Ulm, Germany
Biomol	Hamburg, Germany
Bio-Rad	Munich, Germany
BioWhittaker	Rockland, USA
Biozol	Eching, Germany
Calbiochem	Schwalbach, Germany
Cambrex	Verviers, Belgium
Canberra-Packard	Dreieich, Germany
Cell Signaling/New England Biolabs	Frankfurt/Main, Germany
Chiron Diagnostics	Fernwald, Germany
DakoCytomation	Hamburg, Germany
Dianova	Hamburg, Germany
Fuji	Düsseldorf, Germany
Gibco/Invitrogen	Karlsruhe, Germany
Hellige	Erlangen, Germany
Interdim	Montluçon, France
Kodak	Rochester, USA
Leinco/Biotrend	Cologne, Germany
Merck	Darmstadt, Germany
Millipore	Schwalbach, Germany
Minerva Biolabs	Berlin, Germany

---

Molecular Probes/Invitrogen	Karlsruhe, Germany
MWG	Ebersberg, Germany
Olympus Optical	Hamburg, Germany
Owl Separation Systems	Portsmouth, USA
PAN Biotech	Aidenbach, Germany
PerkinElmer	Überlingen, Germany
Polyplus Transfection/Biomol	Hamburg, Germany
Promega	Heidelberg, Germany
Promocell	Heidelberg, Germany
Qiagen	Hilden, Germany
Roche	Mannheim, Germany
Roth	Karlsruhe, Germany
Santa Cruz	Heidelberg, Germany
Saxon	Hannover, Germany
Siemens	Erlangen, Germany
Sigma-Aldrich	Taufkirchen, Germany
SIMS Portex	Kent, UK
Stratagene	La Jolla, USA
TILL Photonics	Martinsried, Germany
TPP	Trasadingen, Switzerland
Upstate/Biomol	Hamburg, Germany
USB	Cleveland, USA
Zeiss	Oberkochen, Germany

## 7.3 Publications

### 7.3.1 Original publications

Fürst R, Zahler S, Vollmar AM, Kiemer AK. MKP-1 as mediator of the anti-inflammatory effects of dexamethasone in endothelial cells. In preparation.

Fürst R, Brueckl C, Kuebler WM, Zahler S, Krötz F, Görlach A, Vollmar AM, Kiemer AK. Atrial natriuretic peptide induces mitogen-activated protein kinase phosphatases-1 in human endothelial cells *via* Rac1 and NAD(P)H oxidase-2 activation.

Circ Res. 2005;96:43-53.

Kiemer AK, Weber NC, Fürst R, Bildner N, Kulhanek-Heinze S, Vollmar AM. Inhibition of p38 MAPK activation *via* induction of MKP-1: atrial natriuretic peptide reduces TNF- $\alpha$ -induced actin polymerization and endothelial permeability.

Circ Res. 2002;90:874-881.

### 7.3.2 Reviews

Kiemer AK, Fürst R, Vollmar AM. Vasoprotective actions of the atrial natriuretic peptide.

Curr Med Chem Cardiovasc Hematol Agents. 2005;3:11-21.

### 7.3.3 Oral presentations

Fürst R, Brueckl C, Kuebler WM, Vollmar AM, Kiemer AK. NAD(P)H oxidase-generated ROS mediate the induction of MKP-1 by ANP in human endothelial cells.

45<sup>th</sup> Spring Meeting of the Deutsche Gesellschaft für experimentelle und klinische Pharmakologie und Toxikologie, March 9-11, 2004, Mainz, Germany.

Naunyn Schmiedeberg Arch Pharmacol. 2004;369Suppl1:R75

Fürst R, Brueckl C, Kuebler WM, Vollmar AM, Kiemer AK. ROS generation *via* NAD(P)H oxidase is crucial for the induction of MKP-1 by ANP in human endothelial cells.

10. Workshop Mechanismen der Zell- und Gewebeschädigung, Dezember 11-13, 2003, Xanten, Germany

Fürst R, Brueckl C, Kuebler WM, Vollmar AM, Kiemer AK. ROS generation *via* NAD(P)H oxidase is crucial for the induction of MKP-1 by ANP in human endothelial cells.

Young Investigator Award Session of the Annual Meeting of the Gesellschaft für Mikrozirkulation und Vaskuläre Biologie, October 16-18, 2003, Munich, Germany.

J Vasc Res. 2004;41:100-101

Weber NC, Fürst R, Vollmar AM, Kiemer AK. Das Atriale Natriuretische Peptid hemmt die TNF- $\alpha$ -induzierte Permeabilitätssteigerung und Aktinpolymerisation in human Nabelschnurendothelzellen.

8. Workshop Mechanismen der Zell- und Gewebeschädigung, November 22-24, 2001, Halle, Germany



### 7.3.4 Poster presentations

Fürst R, Zahler S, Vollmar AM, Kiemer AK. MKP-1 mediates anti-inflammatory effects of glucocorticoids in endothelial cells.

Experimental Biology 2005 Annual Meeting and the XXXV. International Congress of Physiological Sciences, March 31 - April 6, 2005, San Diego, USA.

Accepted.

Fürst R, Zahler S, Vollmar AM, Kiemer AK. Anti-inflammatory action of dexamethasone in human endothelial cells by induction of MKP-1.

Annual Meeting of the Gesellschaft für Mikrozirkulation und Vaskuläre Biologie, October 7-9, 2004, Berlin, Germany.

J Vasc Res. 2004;41:467

Fürst R, Vollmar AM, Kiemer AK. Induction of MKP-1 by atrial natriuretic peptide is mediated *via* reactive oxygen species and JNK in human endothelial cells.

44<sup>th</sup> Spring Meeting of the Deutsche Gesellschaft für experimentelle und klinische Pharmakologie und Toxikologie, March 17-20, 2003, Mainz, Germany.

Naunyn Schmiedebergs Arch Pharmacol. 2003;367Suppl1:R80

### 7.3.5 Awards

Sanofi-Aventis [i]lab award (travel grant), November 2004.

## 7.4 Curriculum vitae

### Persönliche Daten

Name:	Robert Fürst
Geburtstag und -ort:	1. März 1975, Temeschburg
Staatsangehörigkeit:	deutsch
Familienstand:	ledig

### Hochschule

seit 01/2002	Dissertation zum Dr. rer. nat. in der Arbeitsgruppe von Frau PD Dr. Alexandra K. Kiemer am Lehrstuhl Pharmazeutische Biologie von Frau Prof. Dr. Angelika M. Vollmar, Department Pharmazie, Ludwig-Maximilians-Universität München
1996-2000	Studium der Pharmazie an der Ludwig-Maximilians-Universität München
10/2000	2. Teil der Pharmazeutischen Prüfung
08/1998	1. Teil der Pharmazeutischen Prüfung
1994-1996	Studium der Physik an der Technischen Universität München
11/1995	Physik Diplomvorprüfung Teil I

### Schule

1985-1994	Hans-Leinberger-Gymnasium, Landshut
1981-1985	Grundschule St. Wolfgang, Landshut

### Berufsausbildung und Tätigkeiten

seit 04/2002	nebenberuflich als Apotheker in der Löwen-Apotheke, München
12/2001	Approbation als Apotheker
12/2001	3. Teil der Pharmazeutischen Prüfung

---

05/2001-11/2001	Pharmaziepraktikum am Lehrstuhl für Pharmazeutische Biologie von Frau Prof. Dr. Angelika M. Vollmar, Department für Pharmazie, Ludwig-Maximilians-Universität München
11/2000-04/2001	Pharmaziepraktikum bei Herrn Pharmazierat Dr. Ulrich Krötsch, Johannes-Apotheke, Gröbenzell
02-04/2000	Forschungspraktikum am Centro de investigacion biomedical de occidente, Guadalajara, Mexiko

## 7.5 Acknowledgements

At first I would like to express my deepest gratitude to Prof. Dr. Angelika M. Vollmar for giving me the opportunity to perform this extremely interesting work in her laboratories. Her encouragement and her continuous and generous support were exceedingly helpful to me. I am also very thankful to her for caring for such a motivating, pleasant, and relaxed atmosphere in her group.

I also want to thank the thesis committee, notably Prof. Dr. Ernst Wagner for his time and effort to be coreferee of this work.

I am deeply grateful to PD Dr. Alexandra K. Kiemer for her highly experienced advice, for the kind support, and for her success-oriented and extremely pleasant guidance throughout this work. I am also deeply grateful for the numerous helpful discussions and especially for always being open for questions and ready for proof-readings. I am also very thankful to her for the great time in her PBII-team.

Special thanks go to PD Dr. Stefan Zahler for his very friendly help and profound support, for the always stimulating talks, and for proof-reading of this work.

Moreover, I am indebted to Prof. Dr. Wolfgang Kübler (Charité, Berlin) and Corinna Brückl (University of Munich) for kindly performing the *in situ* ROS measurements, and to Dr. Florian Krötz (University of

Munich) for the convenient cooperation. I also thank PD Dr. Agnes Görlach (German Heart Center, Munich) and Prof. Dr. Ulla Knaus (The Scripps Research Institute, La Jolla) for their material support.

My warm, sincere, and dearest thanks go to my “Hasi” Signe Blumenthal for the great, fascinating, and amusing time in the lab. I am deeply grateful for her close friendship and for the numerous wonderful leisure time activities. Thanks a lot to Dr. Nina Weber, Dr. Anke Förnges, and Dr. Nicole Mohaupt for their warmhearted reception in this working group, for the introduction in different research techniques, and for the great “cooking & ratsching” sessions. My dearest thanks also go to Dr. Stefanie Kulhanek-Heinze, Melanie Keller, and Florian Hoffmann for their friendship, for the numerous amusing breaks, for laughing, joking, and kidding, and for the wonderful time I could spend with them. Thanks to the former PBII-team Dr. Ursula Haider, Dr. Irina Müller, and Dr. Hans-Peter Keiss, and to the current PBIII/1-team Kathrin Ladetzki-Baehs, Elke Koch, Anja Koltermann, Dr. Guido Jürgenliemk, Dr. Rainer Samtleben, and Uschi Kollmannsberger for so many successful practical courses for the students and for the great fun and teamwork during this time. I am also very grateful to the team of the B 4.074 lab Elisabeth Grieblinger and Sylvia Bächer for the pleasant time we spent together, and especially to Dr. Rainer Samtleben for the motivating talks and for sharing his wisdom with me in all circumstances. I would also like to express my gratitude to the technical staff Brigitte Weiss, Cornelia Niemann, and Hanna Stöckl for their continuous kind support in cell culture and HUVEC preparation. Many thanks also to the staff of the numerous hospitals for providing umbilical cords. Thanks to Thomas Roos for his support in all IT issues, to Anita Rudy for her help with the FACS, and to Thomas Räthel for the NO measurements. Of course I want to thank all members of the research group of Prof. Dr. Vollmar which I have not mentioned above for their contribution to the pleasant and relaxing working climate.

Last but not least I have to express my deepest and innermost gratitude to my family and friends. Without their love and constant support this work would not exist. Thank you so much!